MITOCHONDRIAL DYSFUNCTION AS A LINK BETWEEN CARTILAGE INJURY AND OSTEOARTHRITIS

A Dissertation

Presented to the Faculty of the Graduate School

of Cornell University

in Partial Fulfillment of the Requirements for the Degree of

Doctor of Philosophy

by

Michelle Lee Delco

January 2017

MITOCHONDRIAL DYSFUNCTION AS A LINK BETWEEN CARTILAGE INJURY AND OSTEOARTHRITIS

Michelle Lee Delco, Ph.D.

Cornell University 2017

The overall goal of this thesis project was to investigate the role of mitochondria (MT) in the very early pathogenesis of posttraumatic osteoarthritis (PTOA) and to test mitoprotection as a strategy to prevent chondrocyte death and cartilage degeneration after cartilage injury.

Ankle sprain is the most common athletic injury, and the most common cause of end-stage ankle osteoarthritis (OA). Evidence suggests that the magnitude of the initial cartilage/subchondral bone injury is the most important factor in the development of sprain-associated PTOA. However, most PTOA models utilize the knee and rely on joint destabilization or intraarticular fracture to initiate disease. These models cause rapid progression of cartilage pathology with severe synovitis and do not reflect the likely etiology of ankle PTOA resulting from a high-speed impact injury. Therefore, the first aim of this dissertation research was to develop a clinically relevant large animal model of impact-induced talocrural (ankle) PTOA. A minimally invasive surgical approach was used to apply rapid impact injuries to the equine talus. Twelve weeks after injury, the severity of cartilage lesions was positively correlated to peak impact stress. The significance of this work is that it allows us to directly link *in vitro* mechanistic studies to *in vivo* longitudinal studies of disease development, using the same impact system. This model will also allow preclinical testing of disease modifying OA drugs.

The second aim of this thesis was to study MT function of chondrocytes within their native extracellular matrix immediately following a single, rapid impact, which simulates an injury expected to initiate PTOA *in vivo*. Fresh cartilage explants were subjected to injury at varying stress rates. MT respiratory rate and control were assessed by microrespirometry. Functional integrity of the inner MT membrane was investigated using polarity-sensitive fluorescent probes on confocal microscopy. We found that injury resulted in decreased basal and maximal chondrocyte respiration as well as MT depolarization within hours of cartilage impact, indicating that MT dysfunction is an acute response of articular cartilage to injury. The response of chondrocytes differed between two areas of the same joint; chondrocytes from a non-weight bearing articular surface (the distal patellofemoral groove) were more sensitive to MT dysfunction and chondrocyte death than the main weight-bearing surface of the knee (the medial femoral condyle), indicating regional differences in mechanotransduction. These findings suggest that MT may represent an early therapeutic target in the prevention of PTOA.

The third aim of this thesis work was therefore to investigate mitoprotection as a strategy to prevent chondrocyte death and cartilage degeneration *in vitro*. SS-31 is a highly targeted peptide antioxidant that prevents MT respiratory dysfunction, MT-mediated apoptosis, and ROS production by stabilizing the MT-specific phospholipid cardiolipin. Cartilage was injured, then treated with SS-31 at 0, 1, or 6 hours after injury, and cultured for 1 week. We found that SS-31 prevented impact induced chondrocyte death, apoptosis, and cartilage matrix degradation at 1 day and 1 week after injury. Our findings indicate that mitoprotective therapy within 6 hours after joint injury may be a useful strategy to prevent PTOA.

BIOGRAPHICAL SKETCH

Michelle Lee Delco was born in Tarrytown, New York on March 11, 1976 to Jeryl Dene Lee Viscum Delco and Thomas Albert Delco. Michelle attended Cornell University College of Agriculture and Life Sciences and received her Bachelor of Science degree in Animal Science in 1998. After receiving her Doctor of Veterinary Medicine Degree from Cornell University College of Veterinary Medicine in 2002, she completed an internship at Rood and Riddle Equine Hospital in Lexington, KY. Michelle went on to advanced clinical training, completing a residency in equine surgery at the University of California, Davis from 2003-2006 and attained diplomate status in the American College of Veterinary Surgeons in 2007. Following her residency, Michelle served as Assistant Clinical Professor of Equine Surgery at Kansas State University College of Veterinary Medicine from 2006-2008. She then practiced equine surgery and lameness as an associate at Pilchuck Veterinary Hospital's Equine Referral Hospital in Snohomish, WA. In 2012, Michelle was awarded a National Institutes of Health Institutional National Research Service Award from Cornell University and returned to pursue her Ph.D. degree in the Graduate Field of Comparative Biomedical Sciences, with minor fields of study in Biomedical Engineering and Biochemistry, Molecular & Cell Biology. In 2016 she was awarded a 5-year National Institutes of Health Mentored Clinical Scientist Career Development Award (K08).

This thesis is dedicated to my parents,

Thomas Albert Delco
&
Jeryl Dene Lee Viscum Delco

who taught me that with determination, imagination, and love, anything is possible.

Thank you, David Jones.

ACKNOWLEDGEMENTS

I would like to acknowledge and sincerely thank my Special Committee Chair and advisor, Dr. Lisa Fortier for her support and for allowing me the opportunity to pursue this line of investigation. I would also like to thank my minor advisor, Dr. Lawrence Bonassar for generously sharing his knowledge and perspective. I thank all the members of my Special Committee, including Drs. Carolyn Sevier, Rory Todhunter and Mary Goldring for their time and invaluable guidance.

I thank my collaborators and colleagues who made these studies possible. I would especially like to thank Dr. Hazel Szeto for encouraging me to pursue this area of interest, contributing her expertise in mitochondrial pharmacology and providing essential research materials. I thank the past and present members of the Fortier laboratory, including Dr. Lauren Schnabel for her encouragement and advice, Meg Goodale for her help executing these experiments and tireless logistical support and Dr. Jennifer Cassano for her camaraderie. I would like to thank the veterinary students and undergraduates who contributed to these studies including Rebecca Hicks, Lauren DeGenero, Shannon Walsh, Alexis Gale, Miriam Asher, and Sarah Hanif.

I would like to thank all the members of the Bonassar group for including me in their discussions and their research, most especially Edward Bonnevie for contributing work and considerable expertise in area of cartilage mechanics. I would like to thank Dr. Itai Cohen and his graduate student, Lena Bartell for their thoughtful input and work on imaging techniques and analysis. I thank Dr. Alan Nixon and his laboratory group

including Dr. Heidi Reesink, Leila Begum, and Ryan Peterson for sharing knowledge and equipment. I thank members of the Cornell Imaging Core for their imaging expertise including Drs. Rebecca Williams, Warren Zipfel, and Johanna Dela Cruz. I also thank MaryLou Norman for her work on histology and Walt Iddings for technical support and training on the confocal microscope and Seahorse XF analyzer.

I would like to acknowledge and sincerely thank Dr. Susan Fubini who has been an important mentor, role model, and advocate throughout my career. I thank the many clinical mentors who have shaped the way I think and practice, including Dr. Jorge Nieto, Dr. Larry Bramledge, Dr. Alan Ruggles, Dr. Wayne McIlwraith, Dr. Larry Galuppo, and Dr. Norm Ducharme.

Finally, I would like to acknowledge the funding sources that have made this work possible. Stipend support was provided by a National Institutes of Health Comparative Medicine Training Grant (5T320D0011000-20; PI: Dr. John Parker, 2012-2015) and the Department of Clinical Sciences/Dr. Margaret McEntee (2015-2016). Research was funded by the Harry M. Zweig Memorial Fund for Equine Research, the Dante and Sharon Ferrini Award for Veterinary Thoroughbred Racing Studies, and a Clinical and Translational Science Center/Weill Cornell Medical College Seed Grant.

TABLE OF CONTENTS

LIST OF FIGURES

LIST OF TABLES

LIST OF ABBREVIATIONS

ATP	Adenosine triphosphate
Ca^{2+}	Calcium (ionic)
CL	Cardiolipin
CytC	Cytochrome C
ECM	Extracellular matrix (of articular cartilage)
ETC	Electron transport chain
GAG	Glycosaminoglycan
IMM	Inner mitochondrial membrane
LDH	Lactose dehydrogenase
MT	Mitochondria/mitochondrial
OA	Osteoarthritis
O_2	Oxygen
OMM	Outer mitochondrial membrane
OxPhos	Oxidative phosphorylation
PTOA	Posttraumatic osteoarthritis
ROS	Reactive oxygen species
TC	Talocrural/tarsocrural (joint)

CHAPTER 1

GENERAL INTRODUCTION

Goals of the dissertation research and thesis overview

The overall goal of this thesis project was to investigate the role of mitochondria (MT) in the early pathogenesis of posttraumatic osteoarthritis (PTOA). This introductory chapter provides relevant background related to cartilage pathobiology, clinical PTOA, MT function in health and disease, and rationale to support the clinical concept of targeted MT therapy (i.e. mitoprotection) to prevent osteoarthritis.

The first aim of this dissertation research was to develop a clinically relevant large animal model of talocrural (ankle) PTOA. Chapter 2 presents the rationale for this aim in detail, Chapter 3 describes *ex vivo* model development and *in vivo* validation studies. The significance of this work is that it allows us to directly link *in vitro* mechanistic studies to *in vivo* longitudinal studies of disease development, using the same impact system.

The second aim of this thesis, presented in Chapter 4, was to determine the effects of cartilage impact injury on chondrocyte MT function *in situ*. Specifically, the goal was to study MT function of chondrocytes within their native extracellular matrix immediately following a single, rapid impact, which simulates an injury expected to initiate PTOA *in vivo*. We found that MT respiratory function declined, and MT depolarization occurred within hours of cartilage impact, indicating that MT dysfunction is an acute response of articular cartilage to mechanical injury. The response of chondrocytes differed between two areas of the same joint; chondrocytes from a non-

weight bearing articular surface (the distal patellofemoral groove) were more sensitive to MT dysfunction and chondrocyte death than the main weight-bearing surface of the knee (the medial femoral condyle), indicating regional differences in mechanotransduction. These findings suggest that MT may represent an early therapeutic target in the prevention of PTOA.

The third aim, presented in chapter 5, was to investigate mitoprotection as a strategy to prevent early PTOA changes *in vitro*. SS-31, a highly targeted mitoprotective drug, provided cellular and structural protection 1 day and 1 week after cartilage injury. Treatment with SS-31 at 0, 1, or 6 hours after injury prevented impact-induced cell membrane damage, chondrocyte death, apoptosis, and cartilage extracellular matrix degeneration. Our findings indicate that mitoprotective therapy within 6 hours after joint injury may be a useful strategy to prevent PTOA.

The final chapter of this thesis presents a discussion of the significance of our findings in the context of the current state of PTOA research and therapy. Future research directions are explored.

Background and significance

Osteoarthritis

Osteoarthritis (OA) is the leading cause of chronic disability in the United States.[1,2] The estimated total annual cost exceeded $160 billion in 2014.[1,3] OA can generally be described as degenerative disease of articular cartilage, however all joint tissues are affected including subchondral bone, synovium, and joint capsule. In most

clinical cases, the etiopathogenesis of OA is multifactorial, with age, weight, disease, and genetics all likely playing a role.

Posttraumatic osteoarthritis

In addition to biological factors, OA is a disease of mechanics.[2,4-6] Post-traumatic osteoarthritis (PTOA) develops secondary to joint trauma with clinical signs of pain and dysfunction often lagging years or decades behind the initiating injury.[7,8] Currently, no effective therapy exists to prevent or slow progression of PTOA,[9] and mounting evidence suggests that interventions must occur in the acute time frame after injury to modify the disease course.[6] Therefore, understanding the immediate events following joint impact injury is critical for developing effective preventative therapies.[10] Some of the earliest known pathomechanisms of OA, such as oxidative stress and chondrocyte apoptosis, are regulated by mitochondria.[11,12]

Mitochondria

Mitochondria (MT) sustain eukaryotic cellular life and dictate cell fate. The natural history of this semi-autonomous organelle might explain many peculiar features of MT, including their double membrane structure, distinct genome of circular DNA (mtDNA), autonomous replication and translation machinery, and strict maternal mode of inheritance.[13] MT evolved from rickettsia-like, endosymbiotic bacteria roughly 1.5 billion years ago.[14] Over 150 human diseases arise from point-mutations affecting one of the roughly 1,100 proteins comprising the MT proteome.[13]

Mitochondrial function and structure

The most important functions of MT within the context of this thesis are: 1) energy production, 2) production and neutralization of reactive oxygen species (ROS), 3) regulation of apoptosis, and 4) calcium buffering.

Energy Production. MT produce ATP by oxidative phosphorylation, providing the energy required for cells to survive, maintain cell membranes and electrochemical gradients, reproduce, and perform tissue-specific biological functions such as synthesize and export proteins, maintain the extracellular matrix, etc. Oxidative phosphorylation is carried out by the electron transport chain, a series of protein complexes that reside within the inner MT membrane (**Figure 1.1**). The high-energy molecules NAD and $FADH_2$ derived from non-MT respiration (glycolysis) and the Krebs cycle, donate electrons to complexes I and III of the electron transport chain. Through a series of oxidation-reduction (redox) reactions, electrons are passed along the electron transport chain, causing protons to be pumped across the inner MT membrane into the intermembrane space. This creates potential energy in the form of an electrochemical gradient. Oxygen (O_2) acts as the final electron acceptor, and is converted to H_2O and H+. Protons flow down their gradient through the enzyme ATP synthase, causing the A_0 subunit to rotate and phosphorylate ADP to generate ATP.

ROS production and neutralization. ROS is a term used to describe molecules and free radicals, including superoxide ($^{\bullet}O_2^-$), nitric oxide ($^{\bullet}NO$) and hydrogen peroxide (H_20_2), which are derived from oxygen. The main intracellular source of ROS is the MT,

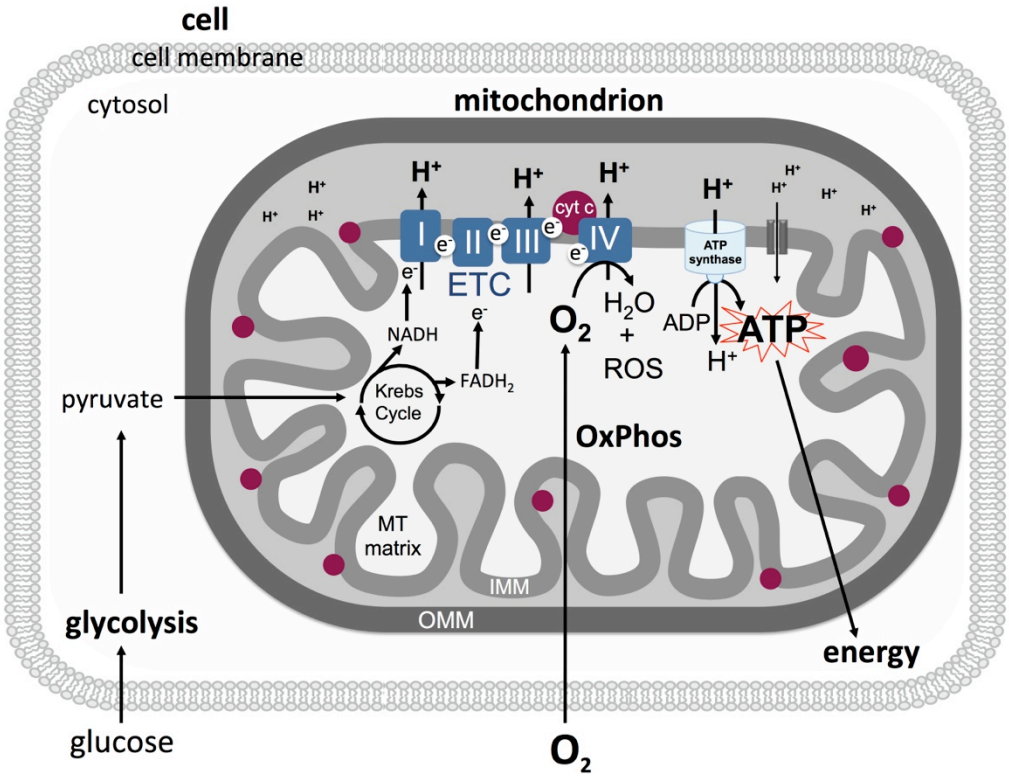

Figure 1.1. Mitochondrial respiration. Nutrients such as glucose enter the cell and are metabolized through anaerobic, non-mitochondrial respiration (glycolysis) in the cytosol. In the presence of oxygen (O_2), pyruvate enters the Krebs cycle in MT to produce NADH and $FADH_2$, which donate electrons (e^-) to the electron transport chain (ETC.) The transfer of e^- between complexes I-IV drive protons across the inner MT membrane (IMM), establishing an electrochemical gradient. Cytochrome C (Cyt C) catalyzes the rate-limiting step and O_2 acts as the final electron acceptor. When protons flow down their gradient through ATP synthase, ADP is converted to ATP, the molecular unit of cellular energy. This process of MT respiration or oxidative phosphorylation (OxPhos) generates reactive oxygen species (ROS) as a byproduct.

where they are produced as a byproduct of oxidative phosphorylation.[15] Approximately 0.2-2% of O_2 consumed by oxidative phosphorylation is converted to superoxide in the electron transport chain, mainly by complexes I and III.[16] ROS play diverse roles in cell signaling and homeostasis.[17-19] For example, in cartilage, ROS are critical in ion homeostasis and cartilage differentiation.[16] However, by virtue of their unstable bonding structure, which often includes an unpaired electron, they can act as potent oxidizing agents, resulting in damage to lipid membranes and DNA. Therefore, redox balance is tightly regulated by multiple antioxidant systems, the most notable of which is the superoxide dismutase (SOD) family of antioxidants. Members of the SOD family convert superoxide to H_20_2, and occur in the cytoplasm (SOD_1), within MT (SOD_2, aka MnSOD) and extracellularly (SOD_3).

Calcium buffering. Calcium signaling governs many basic cell functions. Intracellular calcium concentrations are primarily controlled by flux across the plasma membrane,[20] while transient cytosolic Ca^{+2} concentration is determined by Ca^{+2} distribution between three intracellular compartments; the cytosol, the endoplasmic reticulum, and the MT.[21] MT contribute to intracellular Ca^{+2} homeostasis during episodes of cellular stress and intracellular hypercalcemia. MT can rapidly take up cytoplasmic Ca^{+2} into the matrix through the calcium uniporter on the inner MT membrane, increasing MT Ca^{+2} up to 1,000-fold, transiently store it, then release it back into the cytosol.[22] During MT dysfunction, increased intra-MT Ca^{+2} is pro-apoptotic by contributing to opening of the MT transition pore.[23]

Apoptosis. The basic pathway of MT-mediated controlled cell death by apoptosis is initiated when cytochrome C (CytC) dissociates from the inner MT membrane, and

members of the Bcl-2 family of proteins cause permeabilization of the outer MT membrane, allowing Cyt C and other MT proteins to leak into the cytosol (**Figure 1.2**). CytC initiates oligomerization of APAF-1, recruitment and dimerization of caspase-9 and formation of the apoptosome. Caspase-9 is activated, which in turn cleaves caspase-3 and -7. Activation of these 'executioner' caspases commits the cell to death by apoptosis.[24]

Cardiolipin. Cardiolipin (CL) is a phospholipid exclusively expressed on the inner MT membrane, and comprises ~10% of its content.[25] CL is a dimer, with small acidic head groups and four diverging hydrophobic acyl chain tails, resulting in a conical shape. This shape promotes curvature of the inner MT membrane and formation of cristae structure (**Figure 1.2**). CL rafts allow electron transport chain proteins to form supercomplexes, which optimizes the efficiency of electron transport chain, increasing ATP production and reducing ROS generation.[26]

Cytochrome C. CytC has contrasting functions; one promoting cell survival, one promoting cell death. It is a soluble protein and is the only non-integral component of the electron transport chain. CytC acts as an electron carrier from complex III to complex IV, the rate-limiting step in the respiratory chain. Under certain circumstances, CytC can bind to CL, which prevents its own ability to participate in electron transfer. This binding converts CytC to a peroxidase that oxidizes CL, which in turn causes CytC to dissociate from the inner MT membrane. Oxidized CL synergizes with Ca^{2+} to cause opening of the MT permeability transition pore,[26,27] resulting in MT depolarization, uncoupling of oxidative phosphorylation and release of CytC into the cytosol, triggering the caspase cascade and apoptosis (**Figure 1.2**).

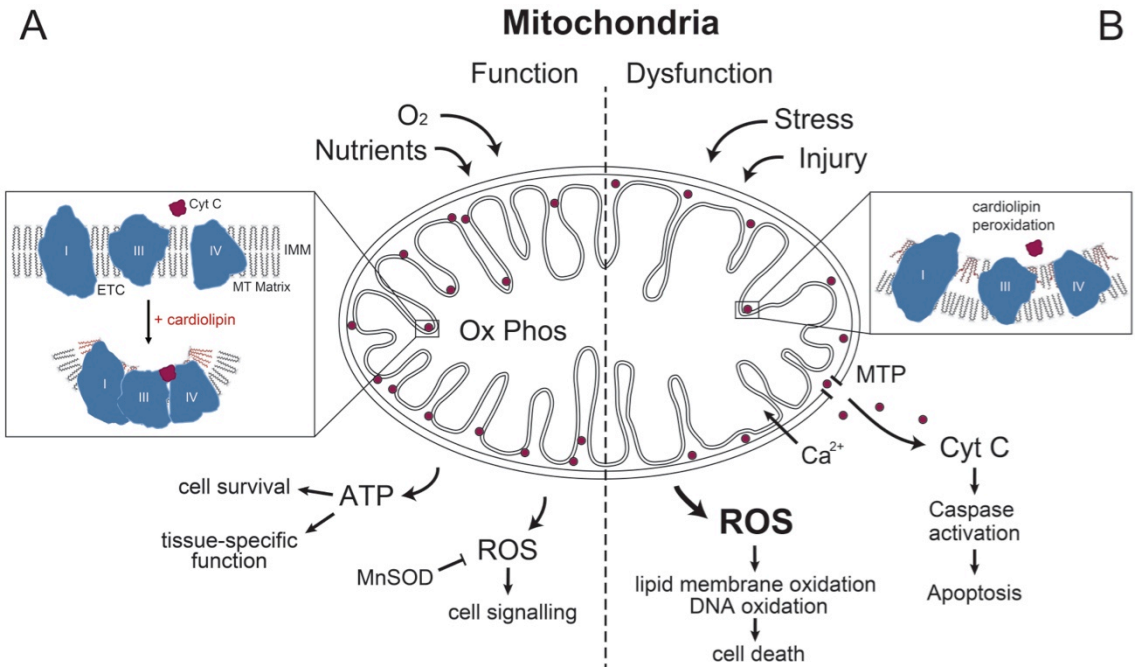

Figure 1.2. **The role of cytochrome C and cardiolipin in mitochondrial dysfunction.**
A) Cardiolipin (CL) is a cone-shaped phospholipid expressed exclusively on the inner MT membrane (IMM). Incorporation of CL into the outer leaflet of the lipid bilayer causes the IMM to bend, forming cristae structure. This organizes the electron transport chain (ETC) proteins into supercomplexes, shortening the distance between redox partners and keeps CytC closely associated to the IMM, resulting in increased efficiency of the ETC. B) During cellular stress, CL is oxidized, distorting the cristae structure, which results in decreased ATP production, increased ROS generation, and dissociation of CytC from the IMM. Damage to the outer MT membrane causes influx of Ca^{2+}, opening of the MT transition pore (MTP), and release of CytC and other MT proteins into the cytosol initiating the caspase cascade, culminating in apoptosis. (*Modified from Szeto HH, Br J Pharm, 2014 and reused with permission from John Wiley & Sons Inc.)*

Mitochondrial dysfunction in disease and aging

The term mitochondrial dysfunction is often used to describe a decline in ATP production (bioenergetic failure) but can also refer to increased ROS production/redox imbalance and the pathologic events that lead to MT-mediated cell-death (**Figure 1.2**).[28] Failure of MT energy metabolism, cumulative oxidative stress, and MT-mediated apoptosis are implicated in aging and the pathogenesis of many complex diseases including Alzheimer's, insulin resistance, cancer, and disuse muscle atrophy.[29-31] More closely related to this thesis are MT-mediated diseases initiated by mechanical injury, including intraocular pressure-induced retinopathy in glaucoma,[32] shear-induced atherosclerosis,[33,34] and neurodegeneration following traumatic brain injury.[35,36]

Evidence for mitochondrial dysfunction in osteoarthritis

MT dysfunction in established OA. Chondrocytes obtain only ~25% of cellular ATP from MT respiration (oxidative phosphorylation), which could explain why MT have received little attention in OA research. However, increasing evidence supports a role for MT dysfunction in chronic OA.[11] Many studies have identified MT dysfunction in cultured chondrocytes from end-stage OA patients.[11,12] For example, OA is associated with decreased number of chondrocyte MT and decreased ATP production.[37] Mitochondrial biogenesis is impaired in OA chondrocytes due to deficiencies in the metabolic biosensors AMPK and SIRT1, the main regulators of MT biogenesis.[38] MT dysfunction is linked to late-stage OA changes including decreased synthesis of collagen and proteoglycans, pathologic calcification of cartilage, and upregulation of matrix metalloproteinases 1, 3 and 13.[39-42] Mutations of mtDNA affecting MT function are

associated with increased incidence of knee OA.[43] These studies focused on MT in cartilage obtained from human patients with late-stage OA, whereas the goal of the current work was to investigate MT dysfunction in the acute time frame after cartilage injury.

Mitochondrial dysfunction in experimental models of PTOA in vitro. There is mounting evidence to support the concept of MT dysfunction in the initiation and early pathogenesis of PTOA. Redox imbalance and apoptosis are prominent in early PTOA, ROS are well established early mediators of the disease,[44-46] and MT-derived ROS induce chondrocyte death after cartilage injury.[29] MT may act also as intracellular mechanotransducers via strain-activated release of ROS,[16,47,48] a theory which is supported by the findings that chondrocyte compression distorts the MT network,[49] and chondrocyte cytoskeleton dissolution prevents elevated ROS and cell death in impact-injured cartilage explants.[50,51]

Mitochondrial dysfunction in experimental models of PTOA in vivo. Recently, *in vitro* models have investigated MT dysfunction in early-chronic cartilage overload models, and in chondrocytes obtained after experimental induction of OA. For example, MT superoxide:SOD_2 imbalance was found to play a role in cartilage degeneration in a mouse model of OA[52] and chondrocyte respiratory function was reduced 4 weeks after surgical destabilization of the medical meniscus in rabbits.[53] Taken together, these findings suggest MT play a central mechanobiological role in chondrocyte death after impact injury, and indicate a causal link between MT dysfunction and PTOA. However, a comprehensive study of *in situ* MT function immediately after cartilage injury has not been performed and therefore, the role of MT in the initiation of PTOA is still unclear.[12]

Failure of chondroprotective therapies

There are no effective therapies to slow the progression of PTOA.[9] Targeting downstream consequences of MT dysfunction to prevent PTOA is not a novel concept with several of the most promising drugs acting on MT-associated pathways of cell death and cartilage degradation (**Figure 1.3**). For example, antioxidants, such as N-acetyl cysteine and vitamin C, are free radical scavengers and are protective in animal models of PTOA,[52] yet fail to provide benefit in OA patients.[54-56] This is likely because they do not effectively penetrate cell membranes and thus fail to reach the MT matrix where ROS are produced.[57,58] Plasma membrane stabilizers such as the polaxamer surfactant p188 are amphipathic molecules that intercalate into phospholipid bilayers, restore membrane integrity, and prevent chondrocyte necrosis by decreasing calcium influx through damaged cell membranes.[59] P188 is superior to caspase inhibitors in prevention of chondrocyte death after injury, and it prevents radial expansion of apoptosis from the site of impact.[59-61] In a lapine model of PTOA, intra-articular administration of P188 prevented chondrocyte necrosis in the superficial layer of cartilage.[60] Plasma membrane stabilizers have not progressed to clinical trials, possibly because of their relatively non-specific mode of action. Ideally, to prevent the initiation and progression of PTOA after joint injury, drugs would act further upstream, but until recently no effective mitoprotective therapies were available.

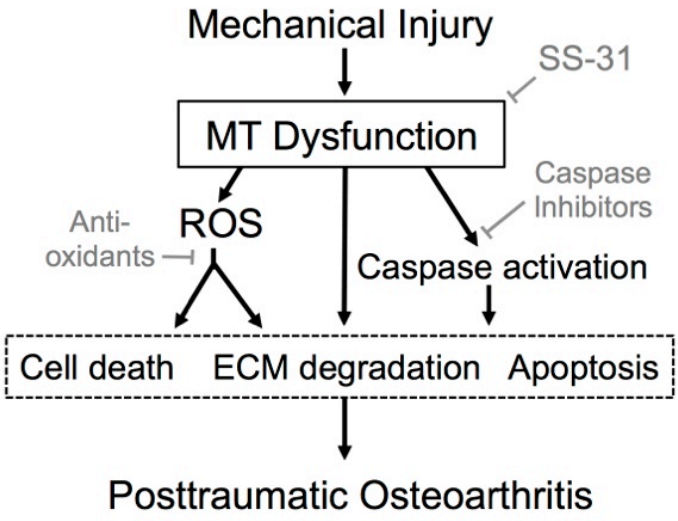

Figure 1.3. Basic mitochondria-associated pathways linking cartilage injury to posttraumatic osteoarthritis. Potential therapeutics to prevent PTOA (grey) and their likely sites of action. Note antioxidants and caspase inhibitors act downstream of mitochondrial (MT) dysfunction.

Therapeutic targeting of mitochondria

Because MT play a central role in disease and aging, they are attractive targets for drug therapy. However, many factors inhibit the development of MT-targeted drugs and currently there are no FDA-approved mitoprotective agents. Most modern drugs target single proteins in signaling pathways involved in specific disease processes. However, MT are complex, multi-compartment organelles that rely on a vast network of proteins and lipids to carry out and regulate ATP synthesis. Therefore, attempts to identify a single molecular target to improve MT function have been futile. Drug toxicity is a concern with MT targeted therapies due to the system complexity, tightly regulated processes, and vital functions. Finally, many candidate drugs are not effectively delivered to MT.

The discovery of Szeto-Schiller (SS) peptides. While attempting to synthetize μ-opioid receptor agonists capable of crossing the blood-brain barrier, pharmacologist and collaborator Dr. Hazel Szeto serendipitously discovered a novel class of highly polar, water soluble tetrapeptides. Szeto-Schiller (SS) peptides prevent MT dysfunction, stabilize the inner MT membrane, improve MT bioenergetics, reduce ROS generation, and prevent caspase-3 activation.[26] They have a unique chemical structure that confers unexpected biological properties.[26,62-64] Although these peptides have a molecular weight of ~640, and a net 3+ charge, they are highly cell permeable, and concentrate over 1000 fold on the inner MT membrane, but do not accumulate in the MT matrix. Their rapid transport across cell membranes is not energy dependent, does not rely on a transport molecule, and localization to the MT does not require the MT to be polarized. Amino acids of alternating polarity allow the two benzene rings to fold and shield the net +

charges.[65] The unique properties of this class of drugs confer their ability to provide structural protection to the cristae by specifically interacting with cardiolipin (**Figure 1.4**). By protecting cardiolipin, and modulating CytC, SS peptides optimize the efficiency of the electron transport chain by directly stabilizing the structure of the inner MT membrane, thereby preventing MT dysfunction.[26]

Clinical development of SS-31. The first SS peptide to be developed as a clinical therapeutic is SS-31 (MTP131, Bendavia™, Elamipretide™; Stealth Peptides, Newton, MA). SS-31 directly scavenges ROS and inhibits MT depolarization.[26] SS-20 is similar to SS-31, but does not scavenge ROS or inhibit MT permeability transition.[63] Nonetheless, SS-20 prevents renal ischemia-reperfusion injury in mice by improving MT bioenergetics.[66] SS-31 is in Phase 2 clinical trials for several diseases including myocardial infarction, acute renal failure, and diabetic retinopathy.[67] SS-31 is also mitoprotective after mechanical injury. It prevents mechanical ventilation-induced MT dysfunction, oxidative stress, and protease activation in the diaphragm of mice. Importantly, SS-31 treatment also prevented myofiber atrophy and contractile dysfunction.[68] SS peptides have not previously been investigated for OA.

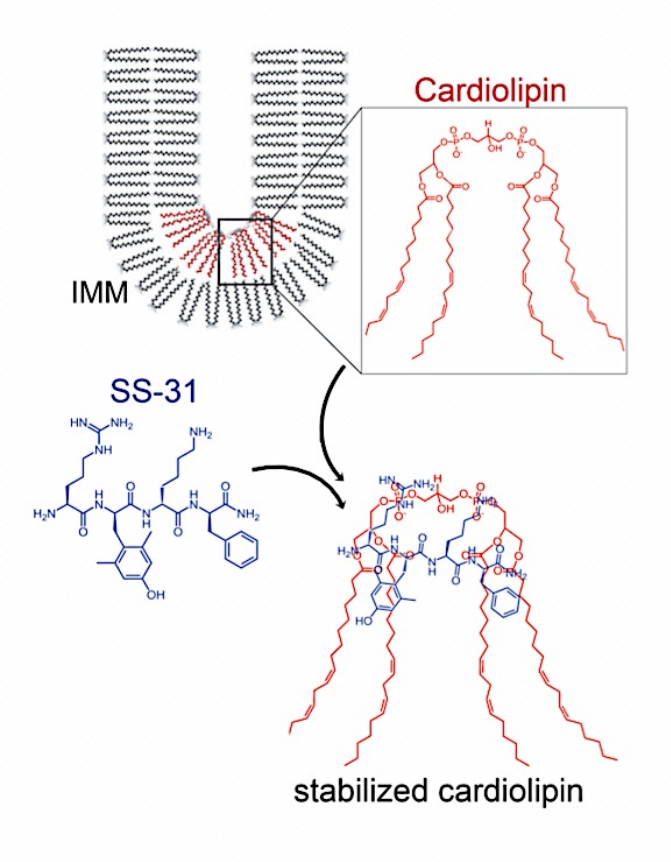

Figure 1.4. SS-31 protects mitochondrial cristae structure. SS-31 specifically binds cardiolipin, preventing oxidation of its unsaturated fatty acid tails. (*Modified from Szeto HH, Br J Pharm, 2014 and reused with permission from John Wiley & Sons Inc.)*

References

1. Ma VY, Chan L, Carruthers KJ. Incidence, Prevalence, Costs, and Impact on Disability of Common Conditions Requiring Rehabilitation in the United States: Stroke, Spinal Cord Injury, Traumatic Brain Injury, Multiple Sclerosis, Osteoarthritis, Rheumatoid Arthritis, Limb Loss, and Back Pain. *Archives of Physical Medicine and Rehabilitation*. 2014;95(5):986–995.e1. doi:10.1016/j.apmr.2013.10.032.

2. Johnson VL, Hunter DJ. The epidemiology of osteoarthritis. *Best Pract Res Clin Rheumatol*. 2014;28(1):5–15. doi:10.1016/j.berh.2014.01.004.

3. Yelin E, Murphy L, Cisternas MG, Foreman AJ, Pasta DJ, Helmick CG. Medical care expenditures and earnings losses among persons with arthritis and other rheumatic conditions in 2003, and comparisons with 1997. *Arthritis & Rheumatism*. 2007;56(5):1397–1407. doi:10.1002/art.22565.

4. Felson DT. Osteoarthritis as a disease of mechanics. *Osteoarthr Cartil*. 2013;21(1):10–15. doi:10.1016/j.joca.2012.09.012.

5. Bartell LR, Fortier LA, Bonassar LJ, Cohen I. Measuring microscale strain fields in articular cartilage during rapid impact reveals thresholds for chondrocyte death and a protective role for the superficial layer. *Journal of Biomechanics*. 2015;48(12):3440–3446. doi:10.1016/j.jbiomech.2015.05.035.

6. Anderson DD, Chubinskaya S, Guilak F, et al. Post-traumatic osteoarthritis: improved understanding and opportunities for early intervention. *J Orthop Res*. 2011;29(6):802–809. doi:10.1002/jor.21359.

7. Kramer WC, Hendricks KJ, Wang J. Pathogenetic mechanisms of posttraumatic osteoarthritis: opportunities for early intervention. *Int J Clin Exp Med*. 2011;4(4):285–298.

8. Brown TDT, Johnston RCR, Saltzman CLC, Marsh JLJ, Buckwalter JAJ. Posttraumatic osteoarthritis: a first estimate of incidence, prevalence, and burden of disease. *J Orthop Trauma*. 2006;20(10):739–744. doi:10.1097/01.bot.0000246468.80635.ef.

9. Cheng DS, Visco CJ. Pharmaceutical therapy for osteoarthritis. *PM&R*. 2012;4(5):S82–S88.

10. Lotz MK, Kraus VB. New developments in osteoarthritis. Posttraumatic osteoarthritis: pathogenesis and pharmacological treatment options. *Arthritis Research & Therapy*. 2010;12(3):211–211. doi:10.1186/ar3046.

11. Blanco FJ, Rego I, Ruiz-Romero C. The role of mitochondria in osteoarthritis. *Nat Rev Rheumatol*. 2011;7(3):161–169. doi:10.1038/nrrheum.2010.213.

12. Terkeltaub R, Johnson K, Murphy A, Ghosh S. Invited review: the mitochondrion in osteoarthritis. *Mitochondrion*. 2002;1(4):301–319. doi:10.1016/S1567-7249(01)00037-X.

13. Vafai SB, Mootha VK. Mitochondrial disorders as windows into an ancient organelle. *Nature*. 2012;491(7424):374–383. doi:10.1038/nature11707.

14. Andersson S, Zomorodipour A, Andersson JO. The genome sequence of Rickettsia prowazekii and the origin of mitochondria. *Nature*. 1998.

15. Turrens JF. Mitochondrial formation of reactive oxygen species. *The Journal of Physiology*. 2003;552(2):335–344. doi:10.1113/jphysiol.2003.049478.

16. Li D, Xie G, Wang W. Reactive oxygen species: the 2-edged sword of osteoarthritis. *Am J Med Sci*. 2012;344(6):486–490. doi:10.1097/MAJ.0b013e3182579dc6.

17. Finkel T. Signal transduction by reactive oxygen species. *The Journal of Cell Biology*. 2011;194(1):7–15. doi:10.1038/nature09663.

18. Dickinson BC, Chang CJ. Chemistry and biology of reactive oxygen species in signaling or stress responses. *Nat Chem Biol*. 2011;7(8):504–511. doi:10.1038/nchembio.607.

19. Culotta E, Koshland DE. *NO News Is Good News*. Science; 1992.

20. Contreras L, Drago I, Zampese E, Pozzan T. Biochimica et Biophysica Acta. *BBA - Bioenergetics*. 2010;1797(6-7):607–618. doi:10.1016/j.bbabio.2010.05.005.

21. Sayer RJ. Intracellular Ca2+ handling. *Adv Exp Med Biol*. 2002;513:183–196.

22. Williams GSB, Boyman L, Chikando AC, Khairallah RJ, Lederer WJ. Mitochondrial calcium uptake. *Proc Natl Acad Sci USA*. 2013;110(26):10479–10486. doi:10.1073/pnas.1300410110

23. Duchen MR. Contributions of mitochondria to animal physiology: from homeostatic sensor to calcium signalling and cell death. *The Journal of Physiology*. 1999;516 (Pt 1):1–17.

24. Green DR. Apoptotic Pathways: Ten Minutes to Dead. *Cell*. 2005;121(5):671–674. doi:10.1016/j.cell.2005.05.019.

25. Osman C, Voelker DR, Langer T. Making heads or tails of phospholipids in mitochondria. *The Journal of Cell Biology*. 2011;192(1):7–16. doi:10.1002/yea.320110602.

26. Szeto HH. BJP cardiolipin-protective compound as a therapeutic agent to restore mitochondrial bioenergetics. *Br J Pharmacol*. 2014;171(8):2029–2050.

doi:10.1111/bph.2014.171.issue-8.

27. Goldstein JC, Muñoz-Pinedo C, Ricci J-E, et al. Cytochrome c is released in a single step during apoptosis. *Cell Death Differ*. 2005;12(5):453–462. doi:10.1038/sj.cdd.4401596.

28. Brand MD, Nicholls DG. Assessing mitochondrial dysfunction in cells. *Biochem J*. 2011;435(2):297–312. doi:10.1042/BJ20110162.

29. Dai D-F, Chiao YA, Marcinek DJ, Szeto HH, Rabinovitch PS. Mitochondrial oxidative stress in aging and healthspan. *Longev Healthspan*. 2014;3:6. doi:10.1186/2046-2395-3-6.

30. Kim J-A, Wei Y, Sowers JR. Role of mitochondrial dysfunction in insulin resistance. *Circulation Research*. 2008;102(4):401–414. doi:10.1161/CIRCRESAHA.107.165472.

31. Pagano G, Talamanca AA, Castello G, et al. Oxidative stress and mitochondrial dysfunction across broad-ranging pathologies: toward mitochondria-targeted clinical strategies. *Oxid Med Cell Longev*. 2014;2014:541230. doi:10.1155/2014/541230.

32. Lee S, Van Bergen NJ, Kong GY, et al. Mitochondrial dysfunction in glaucoma and emerging bioenergetic therapies. *Exp Eye Res*. 2011;93(2):204–212. doi:10.1016/j.exer.2010.07.015.

33. Han Z, Varadharaj S, Giedt RJ, Zweier JL, Szeto HH, Alevriadou BR. Mitochondria-Derived Reactive Oxygen Species Mediate Heme Oxygenase-1 Expression in Sheared Endothelial Cells. *Journal of Pharmacology and Experimental Therapeutics*. 2009;329(1):94–101. doi:10.1124/jpet.108.145557.

34. Takabe W, Jen N, Ai L, et al. Oscillatory shear stress induces mitochondrial superoxide production: implication of NADPH oxidase and c-Jun NH2-terminal kinase signaling. *Antioxid Redox Signal*. 2011;15(5):1379–1388. doi:10.1089/ars.2010.3645.

35. Mazzeo AT, Beat A, Singh A, Bullock MR. Experimental Neurology. *Experimental Neurology*. 2009;218(2):363–370. doi:10.1016/j.expneurol.2009.05.026.

36. Sullivan PG, Thompson MB, Scheff SW. Cyclosporin A attenuates acute mitochondrial dysfunction following traumatic brain injury. *Experimental Neurology*. 1999;160(1):226–234. doi:10.1006/exnr.1999.7197.

37. Johnson K, Svensson CI, Etten DV, et al. Mediation of spontaneous knee osteoarthritis by progressive chondrocyte ATP depletion in Hartley guinea pigs. *Arthritis & Rheumatism*. 2004;50(4):1216–1225. doi:10.1002/art.20149.

38. Wang Y, Zhao X, Lotz M, Terkeltaub R, Liu-Bryan R. Mitochondrial biogenesis is impaired in osteoarthritic chondrocytes but reversible via peroxisome proliferator-activated receptor-γ coactivator 1α. *Arthritis & Rheumatology*. 2015;67(8):2141–2153. doi:10.1002/art.39182.

39. Maneiro E, Martín MA, de Andres MC, et al. Mitochondrial respiratory activity is altered in osteoarthritic human articular chondrocytes. *Arthritis & Rheumatism*. 2003;48(3):700–708. doi:10.1002/art.10837.

40. Ruiz-Romero C, Calamia V, Mateos J, et al. Mitochondrial dysregulation of osteoarthritic human articular chondrocytes analyzed by proteomics: a decrease in mitochondrial superoxide dismutase points to a redox imbalance. *Mol Cell Proteomics*. 2009;8(1):172–189. doi:10.1074/mcp.M800292-MCP200.

41. Cillero-Pastor B, Rego-Pérez I, Oreiro N, Fernandez-Lopez C, Blanco FJ. Mitochondrial respiratory chain dysfunction modulates metalloproteases -1, -3 and -13 in human normal chondrocytes in culture. *BMC Musculoskelet Disord*. 2013;14:235–235. doi:10.1186/1471-2474-14-235.

42. Johnson K, Jung A, Murphy A, Andreyev A, Dykens J, Terkeltaub R. Mitochondrial oxidative phosphorylation is a downstream regulator of nitric oxide effects on chondrocyte matrix synthesis and mineralization. *Arthritis & Rheumatism*. 2000;43(7):1560–1570. doi:10.1002/1529-0131.

43. Chang M-C, Hung S-C, Chen WY-K, et al. Accumulation of mitochondrial DNA with 4977-bp deletion in knee cartilage – an association with idiopathic osteoarthritis. *Osteoarthritis and Cartilage*. 2014;13(11):1004–1011. doi:10.1016/j.joca.2005.06.011.

44. Buckwalter JA. The role of mechanical forces in the initiation and progression of osteoarthritis. *HSS Jrnl*. 2012;8(1):37–38. doi:10.1007/s11420-011-9251-y.

45. Lotz M, Hashimoto S, Kühn K. Mechanisms of chondrocyte apoptosis. *Osteoarthr Cartil*. 1999;7(4):389–391. doi:10.1053/joca.1998.0220.

46. Del Carlo M, Loeser R. Cell death in osteoarthritis. *Curr Rheumatol Rep*. 2008;10(1):37–42. doi:10.1007/s11926-008-0007-8.

47. Szafranski JD, Grodzinsky AJ, Burger E, Gaschen V, Hung H-H, Hunziker EB. Chondrocyte mechanotransduction: effects of compression on deformation of intracellular organelles and relevance to cellular biosynthesis. *Osteoarthr Cartil*. 2004;12(12):937–946. doi:10.1016/j.joca.2004.08.004.

48. Ali MH, Pearlstein DP, Mathieu CE, Schumacker PT. Mitochondrial requirement for endothelial responses to cyclic strain: implications for mechanotransduction. *Am J Physiol Lung Cell Mol Physiol*. 2004;287(3):L486–L496. doi:10.1152/ajplung.00389.2003.

49. Patwari P, Gaschen V, James IE, et al. Ultrastructural quantification of cell death after injurious compression of bovine calf articular cartilage. *Osteoarthr Cartil*. 2004;12(3):245–252. doi:10.1016/j.joca.2003.11.004.

50. Brouillette MJ, Ramakrishnan PS, Wagner VM, et al. Strain-dependent oxidant release in articular cartilage originates from mitochondria. *Biomech Model Mechanobiol*. 2014;13(3):565–572. doi:10.1007/s10237-013-0518-8.

51. Sauter E, Buckwalter JA, McKinley TO, Martin JA. Cytoskeletal dissolution blocks oxidant release and cell death in injured cartilage. *J Orthop Res*. 2012;30(4):593–598. doi:10.1002/jor.21552.

52. Koike M, Nojiri H, Ozawa Y, et al. Mechanical overloading causesmitochondrial superoxide andSOD2 imbalance in chondrocytesresulting in cartilage degeneration. *Nature Publishing Group*. June 2015:1–16. doi:10.1038/srep11722.

53. Goetz JE, Coleman MC, Fredericks DC, et al. Time-dependent loss of mitochondrial function precedes progressive histologic cartilage degeneration in a rabbit meniscal destabilization model. *J Orthop Res*. June 2016. doi:10.1002/jor.23327.

54. Kurz B, Lemke A, Kehn M, et al. Influence of tissue maturation and antioxidants on the apoptotic response of articular cartilage after injurious compression. *Arthritis & Rheumatism*. 2004;50(1):123–130. doi:10.1002/art.11438.

55. Chubinskaya S, Wimmer MA. Key Pathways to Prevent Posttraumatic Arthritis for Future Molecule-Based Therapy. *Cartilage*. 2013;4(3 Suppl):13S–21S. doi:10.1177/1947603513487457.

56. Martin JA, McCabe D, Walter M, Buckwalter JA, McKinley TO. N-acetylcysteine inhibits post-impact chondrocyte death in osteochondral explants. *J Bone Joint Surg Am*. 2009;91(8):1890–1897. doi:10.2106/JBJS.H.00545.

57. Halliwell B. The antioxidant paradox: less paradoxical now? *Br J Clin Pharmacol*. 2013;75(3):637–644. doi:10.1111/j.1365-2125.2012.04272.x.

58. Szeto HH, Schiller PW. Novel therapies targeting inner mitochondrial membrane--from discovery to clinical development. *Pharm Res*. 2011;28(11):2669–2679. doi:10.1007/s11095-011-0476-8.

59. Phillips DM, Haut RC. The use of a non-ionic surfactant (P188) to save chondrocytes from necrosis following impact loading of chondral explants. *J Orthop Res*. 2006;22(5):1135–1142. doi:10.1016/j.orthres.2004.02.002.

60. Rundell SA, Baars DC, Phillips DM, Haut RC. The limitation of acute necrosis in retro-patellar cartilage after a severe blunt impact to the in vivo rabbit patello-femoral joint. *J Orthop Res*. 2005;23(6):1363–1369. doi:10.1016/j.orthres.2005.06.001.

61. Garrido CP, Hakimiyan AA, Rappoport L, Oegema TR, Wimmer MA, Chubinskaya S. Anti-apoptotic treatments prevent cartilage degradation after acute trauma to human ankle cartilage. *Osteoarthritis and Cartilage*. 2009;17(9):1244–1251. doi:10.1016/j.joca.2009.03.007.

62. Szeto HH. Cell-permeable, mitochondrial-targeted, peptide antioxidants. *AAPS J*. 2006;8(2):E277–E283.

63. Birk AV, Chao WM, Liu S, Soong Y, Szeto HH. Biochimica et Biophysica Acta. *BBA - Bioenergetics*. 2015;1847(10):1075–1084. doi:10.1016/j.bbabio.2015.06.006.

64. Zhao K, Zhao GM, Wu D, et al. Cell-permeable Peptide Antioxidants Targeted to Inner Mitochondrial Membrane inhibit Mitochondrial Swelling, Oxidative Cell Death, and Reperfusion Injury. *Journal of Biological Chemistry*. 2004;279(33):34682–34690. doi:10.1074/jbc.M402999200.

65. Zhao K. Transcellular Transport of a Highly Polar 3+ Net Charge Opioid Tetrapeptide. *Journal of Pharmacology and Experimental Therapeutics*. 2003;304(1):425–432. doi:10.1124/jpet.102.040147.

66. Szeto HH, Liu S, Soong Y, Birk AV. Improving mitochondrial bioenergetics under ischemic conditions increases warm ischemia tolerance in the kidney. *AJP: Renal Physiology*. 2015;308(1):F11–F21. doi:10.1152/ajprenal.00366.2014.

67. Szeto HH, Birk AV. Serendipity and the Discovery of Novel Compounds that Restore Mitochondrial Plasticity. *Clin Pharmacol Ther*. September 2014. doi:10.1038/clpt.2014.174.

68. Powers SK, Hudson MB, Nelson WB, et al. Mitochondria-targeted antioxidants protect against mechanical ventilation-induced diaphragm weakness. *Crit Care Med*. 2011;39(7):1749–1759. doi:10.1097/CCM.0b013e3182190b62.

CHAPTER 2

POST-TRAUMATIC OSTEOARTHRITIS OF THE ANKLE: A DISTINCT CLINICAL ENTITY REQUIRING NEW RESEARCH APPROACHES

Michelle L. Delco, DVM[1], John G. Kennedy, MD[2], Lawrence J. Bonassar, PhD[3], Lisa A. Fortier, DVM, PhD[1]

[1]Department of Clinical Sciences, College of Veterinary Medicine, Cornell University, Ithaca, NY

[2]Department of Foot and Ankle Surgery, Hospital for Special Surgery, New York, NY

[3]Meining School of Biomedical Engineering, Cornell University, Ithaca, NY

Manuscript accepted for publication in The Journal of Orthopedic Research special issue on Posttraumatic Osteoarthritis, August 2016.

Abstract

The diagnosis of ankle osteoarthritis (OA) is increasing as a result of advancements in non-invasive imaging modalities such as magnetic resonance imaging, improved arthroscopic surgical technology and heightened awareness among clinicians. Unlike OA of the knee, primary or age-related ankle OA is rare, with the majority of ankle OA classified as post-traumatic (PTOA). Ankle trauma, more specifically ankle sprain, is the single most common athletic injury, and no effective therapies are available to prevent or slow progression of PTOA. Despite the high incidence of ankle trauma and OA, ankle-related OA research is sparse, with the majority of clinical and basic studies pertaining to the knee joint. Fundamental differences exist between joints including their structure and molecular composition, response to trauma, susceptibility to OA, clinical manifestations of disease, and response to treatment. Considerable evidence suggests that research findings from knee should not be extrapolated to the ankle, however few ankle-specific preclinical models of PTOA are currently available. The objective of this article is to review the current state of ankle OA investigation, highlighting important differences between the ankle and knee that may limit the extent to which research findings from knee models are applicable to the ankle joint. Considerations for the development of new ankle-specific, clinically relevant animal models are discussed.

Introduction

Post-traumatic osteoarthritis (PTOA) develops secondary to joint trauma, with clinical signs of pain and dysfunction often lagging years or decades behind the initiating injury.[1,2] By conservative estimates, approximately 12% of patients with symptomatic osteoarthritis (OA) had a traumatic incident to their joint as the inciting cause. This corresponds to roughly 5.6 million Americans affected by PTOA severe enough to be evaluated by an orthopedic surgeon.[3]

Specifically in the talocrural (TC; ankle) joint, trauma is the primary cause of OA. Unlike the knee and hip joints, where only 2-10% of OA is attributed to injury, up to 90% of arthritic change in the ankle is post-traumatic in nature.[2-6] The ankle is the most commonly injured joint during sport activities, with >300,000 injuries per year reported in the US, and an estimated 52.3 ankle injuries per 1000 athletic exposures in high school-aged athletes.[7] Ankle sprains are also the most common non-combat related injury with a 15% incidence rate in over 4000 military personnel evaluated.[8] The true incidence of ankle sprains is likely much higher than reported; one prospective observational study of 10,393 basketball players found that over half of ankle injuries went unreported and were not treated by a healthcare professional.[9] Individuals with a history of ankle sprain comprise 70-85% of patients undergoing surgery for end-stage ankle PTOA.[10] The economic burden associated with ankle OA is demonstrated by the estimated 4400 total ankle replacements and 25,000 ankle fusions performed in the USA in 2010.[3,4] Additionally, patients with ankle PTOA are an average of 14 years younger at the time of diagnosis and progress more rapidly to end-stage disease compared to those with OA of other joints, resulting in increased duration of pain, loss of function, and associated economic burdens to society.[3,6,11] These data collectively indicate that the incidence, as well as the aggregate treatment costs of ankle PTOA will increase as the population ages.

Currently, no effective therapeutics are available to prevent or slow the progression of OA,[12] and increasing evidence suggests that interventions must occur early in order to modify the course of disease.[13,14] Studies of PTOA present a unique opportunity for investigating targeted therapy, because unlike other forms of OA (e.g. idiopathic), PTOA has a defined start point. Likewise, in the pursuit of effective OA therapies, modeling PTOA enables the study of very early cellular and subcellular events that initiate and perpetuate cartilage degeneration. Despite the high incidence of ankle trauma and OA, ankle-specific OA research is sparse, with the majority of clinical and basic research pertaining to the knee and hip joints. A recent meta-analysis of risk factors associated with OA of the lower limb identified only 2 of 43 studies related to the ankle.[2]

Increasingly, evidence reveals fundamental differences in cartilage structure and biology between joints, suggesting distinct mechanisms of disease.[5,14-27] For example, a recent study found significant differences in the rate of extracellular matrix turnover and collagen composition in knee versus hip OA.[28] Therefore, research findings from other joints may not be applicable to the ankle. However, few ankle-specific preclinical models of PTOA currently exist. This gap may hinder progress in the study of pathomechanisms of talocrural OA as well as the development of therapeutic interventions to prevent the initiation and progression of PTOA. Therefore, the objectives of this article are to review *ex vivo* and *in vivo* (animal model) ankle-related PTOA research, to assess the extent to which currently available models may be applicable to the ankle joint, and to discuss considerations for the development of more translational models of ankle PTOA.

Etiology of Talocrural OA - The association between cartilage injury and PTOA

Of the 70-90% of ankle OA classified as posttraumatic, the most commonly reported inciting events are severe sprain and intra-articular fracture.[1-3,6,29,30] Chronically altered joint mechanics, including malalignment, instability, and incongruity are widely accepted as contributory factors in the development of ankle PTOA.[4,6,30-34] The relative importance of these chronic abnormal loading conditions versus acute mechanical trauma to the articular surface at the time of injury remains unclear, and likely varies between ankle injury types.[33] For example, one group found that elevated joint contact stresses from residual incongruity after repair of tibial plafond fractures could predict the development of POTA in patients.[35] On the other hand, increasing evidence suggests the magnitude of injury to articular cartilage during initial trauma is the major predisposing factor in ankle PTOA development.[13,36] For example, concomitant cartilage lesions are identified arthroscopically in 63-79% of acute ankle fractures.[37,38] Although it is difficult to deconvolve chondral injury from fracture grade, long-term follow up of 109 ankle fracture patients found that initial cartilage damage is an independent predictor for the development of both clinical and radiographic PTOA.[39]

The importance of acute cartilage injury in the etiology of ankle OA is particularly evident for sprain-associated PTOA. During a typical severe ankle sprain, the medial tibial plafond is thought to impact the medial aspect of the talar dome, resulting in a talar osteochondral lesion (**Figure 2.1**). This mechanism of injury is supported by the anatomic distribution of talar osteochondral lesions (OCLs), with the medial talus affected nearly twice as frequently as the lateral talus, and the mid-one third of the talar dome affected 4 times more commonly than the anterior and posterior thirds combined.[40] Evidence suggest that the majority (as high as 95%) of severe ankle sprains result in OCLs and over half of patients with OCLs

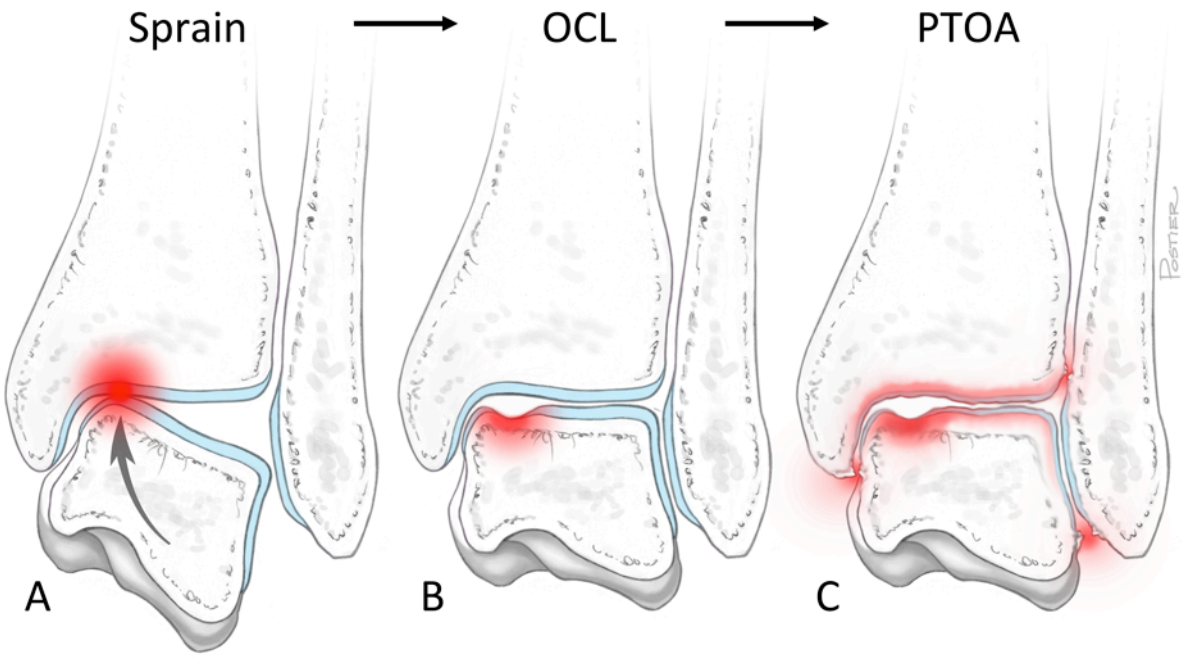

Figure 2.1. The proposed mechanism of posttraumatic osteoarthritis after a severe ankle sprain. A) During a typical lateral ankle sprain (inversion) the medial aspect of the talus likely impacts the tibial plafond which may result in B) a talar osteochondral lesion (OCL). Direct trauma to the articular surface can initiate progressive, irreversible joint destruction culminating in C) late-stage posttraumatic osteoarthritis (PTOA) years to decades after the original injury.

develop OA.[41,42] Ligament injury resulting in chronic ankle instability is a common sequelae to severe sprain, and approximately 15% of ankle sprains are recurrences.[43] However, instability alone cannot account for the incidence of resulting PTOA.[10] In a population of patients presenting to orthopedic surgeons with severe ankle OA, approximately equal numbers of patients reported a single ankle sprain as those reporting recurrent sprains (i.e. chronic instability).[3] Notably, one study reported that the mean latency time between injury and end-stage OA was 12 years shorter for patients who suffered a single ankle sprains than those who experienced chronic recurrent sprains. The authors speculate that the more rapid progression of PTOA in patients without chronic joint instability could be explained by the degree of cartilage damage sustained at the time of injury.[11] Finally, no clinical study to date has demonstrated that any conservative or surgical therapies to stabilize the ankle joint after injury decrease the incidence of PTOA, further suggesting that the magnitude of the initial cartilage/subchondral bone injury is the primary inciting cause of ankle PTOA.[10,44-47]

In patients presenting for ankle pain, MRI is the imaging modality of choice because of its ability to identify ligamentous injury, subchondral bone edema, and cartilage pathology.[48-50] However, diagnosing subtle talar cartilage lesions and the early phases of PTOA remains challenging.[45] In one study, 107 ankles in 101 patients (mean age 28.7 years) with chronic lateral ligament instability secondary to ankle sprain were examined arthroscopically to assess the articular cartilage prior to ligament reconstruction. In 99 ankles without abnormalities diagnosed on radiographs or MRI, 77% had chondral lesions identified during arthroscopy.[51] In a recent study, 3T MRI of the ankle joint had a reported 71% sensitivity and 74% specificity for detecting talar dome articular cartilage defects (Outerbridge grades 3 and 4) that were confirmed on arthroscopy.[49] A similar study reported a sensitivity of only 46% for the diagnosis of talar OCLs

on 1.5T MRI.[50] In one cohort of young, active individuals who had experienced an ankle sprain within 5 years of evaluation, T2 relaxation times were increased in injured ankles with and without instability relative to uninjured controls, indicating early subclinical cartilage degeneration.[48] These findings suggest that while diagnostic imaging modalities continue to improve, the incidence of chondral lesions and early PTOA may be higher than previously recognized.

Differences between the ankle and knee joint

Differences between the ankle and knee, summarized in **Table 2.1,** are important considerations when extrapolating clinical or basic OA research knowledge of the knee to the ankle. Overall, the knee has an approximately ninefold higher incidence of clinical OA than the ankle, however the proportion of PTOA is at least sevenfold higher in the ankle.[3] Improved understanding of the biological and mechanical factors underlying this disparity may contribute to the development of joint-specific therapies.

Differences between ankle and knee joint anatomy and biomechanics

The articular surfaces of the talocrural joint are highly congruent resulting in intrinsic stability of the ankle based on bony anatomy alone[52] (**Figure 2.2**). Furthermore, during weight-bearing, redistribution of contact stresses over the tibiotalar articular surfaces increase ankle joint stability.[52] Only at the extremes of the normal range of motion is stability of the ankle joint maintained by soft tissue structures including the anterior and posterior tibiofibular ligaments and the calcaneofibular ligament.[53] In contrast, the rounded femoral condyles are

Table 2.1. Summary of important differences between the knee and ankle joints. The ankle has a low prevalence of primary OA, but a high proportion of PTOA. The ankle joint is more congruent and has higher intrinsic stability than the knee. The extracellular matrix (ECM) properties of ankle cartilage may protect against primary OA and ankle chondrocytes may also have improved homeostatic mechanisms compared to that of knee chondrocytes. OA = osteoarthritis, sGAG = sulfated glycosaminoglycans, PG = proteoglycan, CII =type II collagen, IL-1 = interleukin-1, Fn-F = fibronectin fragments.

	Ankle	Knee
Prevalence of primary OA	Low	Higher (ninefold)
Proportion of OA secondary to trauma	High (80%)	Low (10%)
Anatomy and Mechanics		
Joint congruity	High	Low
Articular contact area	Low	High
Cartilage thickness	Thin (0.7-1.62mm)	Thick (1.5 -2.6mm)
Cartilage stiffness (Compressive modulus)	High	Lower
ECM properties		
sGAG content	Higher (twofold)	Lower
Water content	Lower	Higher
Collagen content	No difference	Similar
Metabolism		
Basal PG synthesis and turnover	High	Low
Response to mechanical loading		
Upregulation of collagen synthesis marker (CII)	Yes	No
Upregulation of aggrecan mRNA	Yes	No
Response to catabolic signals		
Net response	Anabolic	Catabolic
IL-1 inhibition of PG synthesis	Low	Higher (eightfold)
IL-1 induced PG degradation	No	Yes
Fn-f induced PG loss	Low	High (30-50% loss)

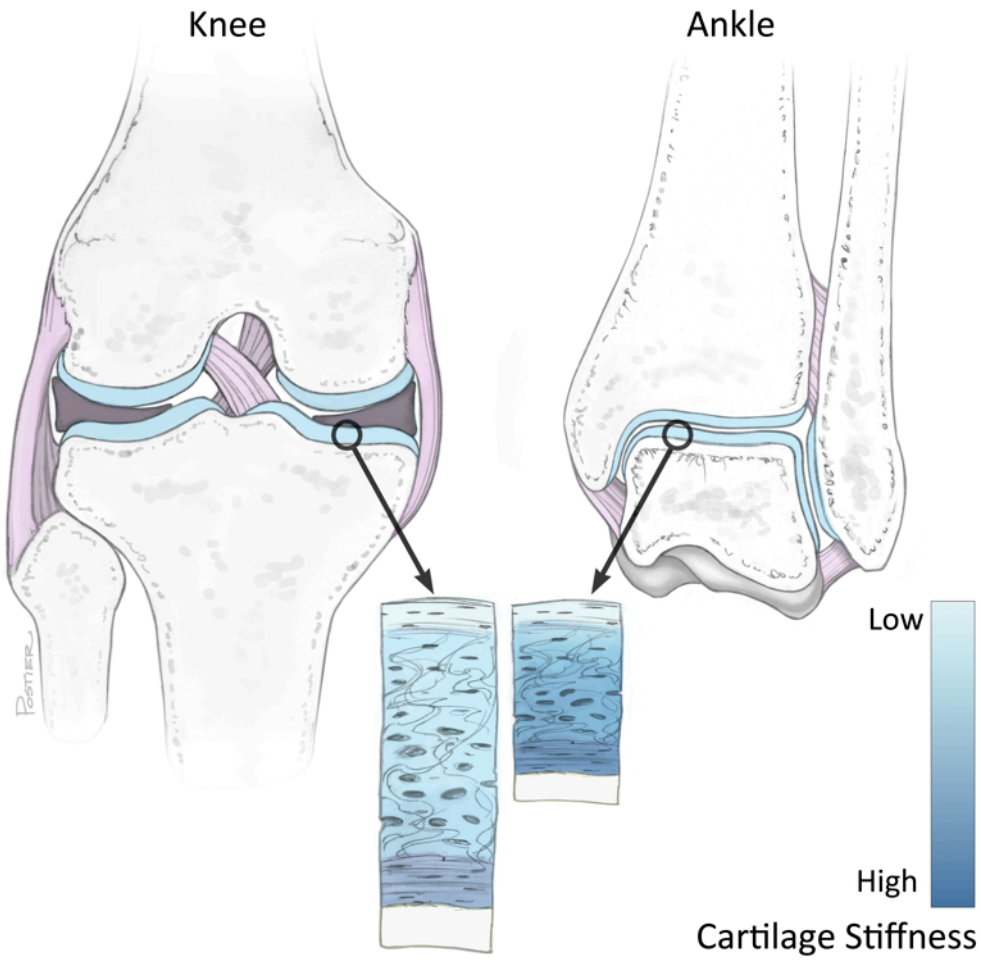

Figure 2.2. A comparison between the knee and ankle joints. The contact surface area of knee joint is approximately three times larger than the ankle. The ankle has more bony congruity than the knee, and is therefore less reliant on supporting soft tissues (pink-purple) to maintain stability. Ankle cartilage (blue) is approximately half the thickness of knee cartilage, although the superficial zone thickness is similar between joints. The extracellular matrix of ankle cartilage is more dense than that of the knee and has a higher dynamic stiffness and compressive modulus.

incongruent with the flat surface of the tibial plateau, making the knee joint highly reliant on soft tissues such as menisci, collateral ligaments, and cruciate ligaments, to maintain stability during loading.[54] The motion of the ankle joint is "rolling" with the center of rotation changing throughout a range of motion of 50 degrees plantar flexion to 20 degrees of dorsiflexion. The point of articulation is slightly oblique to the long axis of the tibia resulting in a slight (~3 degree) valgus conformation and an outward deviation of the foot with dorsiflexion and inward deviation with plantar flexion.[55,56] In contrast, the normal motion of the knee joint is a combination of sliding, rolling, and rotation.[54]

The articular cartilage in the ankle is approximately half the thickness of knee cartilage (**Figure 2.2**), with a mean thickness of 0.7 - 1.62mm in the ankle versus 1.5 - 2.6mm in the knee.[57,58] The relatively smaller size of the ankle joint results in a contact surface area approximately one-third that of the knee, which translates to higher force per area (stress) during loading.[59] In plantar flexion, the contact area of the ankle joint decreases by greater than 40% with corresponding increases in peak stresses.[60] This may partially explain the high incidence of ankle OA in retired ballet dancers[61] and early subclinical disease in a cohort of active professional dancers.[62] During eversion and inversion, contact area also decreases, and peak stresses increase.[60] One study estimated that with 1 mm of lateral talar displacement, as might occur during a typical ankle sprain, contact area of the ankle joint is decreased by 42%.[63] A computer simulation modeling study found that plantar flexion and inversion during forefoot loading increases the likelihood of ankle sprain,[64] which is consistent with the high prevalence of sprains during jump landing in the sport of basketball.[65] Accidental sprains incurred by subjects during controlled laboratory testing consistently accompanied internal rotation and rapid inversion, with or without plantar flexion.[10]

Differences between ankle and knee cartilage extracellular matrix properties and chondrocyte distribution

The extracellular matrix (ECM) of articular cartilage, comprised mainly of proteoglycans and type 2 collagen, functions in load bearing and supports near-frictionless joint movement. In the ankle, the ECM is more dense than that of the knee, with lower water and higher glycosaminoglycan (GAG) concentrations.[16] In compression, ankle cartilage has a higher dynamic stiffness and compressive modulus than knee cartilage[16] (**Figure 2.2**). These physical properties of ankle cartilage translate to an increased resistance to compressive loads, but do not necessarily explain why the ankle might be more resistant to mechanical damage than the knee. Recently, increased attention has been directed toward resolving depth-dependent mechanical properties of articular cartilage, revealing that the superficial layer is more compliant (lower compressive stiffness) and dissipates more shear energy than the deeper tissue.[66-68] For example, the superficial 500um of the articular surface has a shear modulus 2 orders of magnitude lower than that of the deep zone, and acts to dissipate nearly 90% of shear energy.[69] Although ankle cartilage is roughly half as thick as knee cartilage, the superficial zone thickness is similar between joints, therefore the superficial zone comprises a relatively higher proportion of cartilage in the ankle than the knee (**Figure 2.2**). This relative difference has been suggested to play an important protective role during physiologic loading in the ankle,[16] and could have important implications in the development of ankle-specific therapies.

Chondrocytes are the sole cell type within articular cartilage and are responsible for maintaining the surrounding ECM.[70] Cell density in full thickness ankle cartilage ($41 \pm 34 \times 10^3$ cells/mg) has been reported to be 48% higher than knee cartilage ($28 \pm 26 \times 10^3$ cells/mg).[19] Interestingly, the spatial organization of superficial zone chondrocytes differ between the ankle

and knee joints, and the understanding of these differences have evolved with improved imaging techniques.[71,72] In the human ankle joint, superficial zone chondrocytes are predominantly arranged in pairs, but in the in the femoral condyles of the knee, they are arranged in horizontally oriented strings. These distinct patterns are likely related to predominant collagen fiber orientation within the superficial zone, but it remains unclear if they are causally linked to local biomechanical forces or have implications in chondrocyte function or mechanotransduction. These predictable patterns of organization in the superficial zone chondrocytes change in early OA, both within areas of focal OA and in intact cartilage remote to focal lesions, indicating a coordinated response of chondrocytes to injury, and may serve as sensitive indicators of early preclinical OA and/or focal cartilage lesions elsewhere in the joint.[72,73]

Differences between ankle and knee cartilage matrix homeostasis and response of chondrocytes to biochemical and mechanical stimulation

In matched pairs of ankle and knee cartilage from healthy cadaver joints, ankle chondrocytes had increased proteoglycan (PG) and collagen synthetic rates compared to knee chondrocytes, and these differences persisted throughout life.[18,19] In diseased cartilage with surface fibrillations and fissuring consistent with early OA, markers of collagen synthesis (CPII) and aggrecan turnover (epitope 846) are increased in the ankle, but down-regulated in the knee. Markers consistent with collagen degradation (Col2-3/4C short) are higher in the knee than the ankle.[25] These findings may explain the observation that age-related degeneration of the ECM does not occur in the ankle, or it happens at a much slower rate than in the knee.[17]

Ankle and knee cartilage also differ in their response to catabolic signals. Knee chondrocytes are approximately eight times more sensitive to inhibition of PG synthesis by the

catabolic cytokine interleukin-1 (IL-1).[18] The ankle is also less susceptible to fibronectin fragment (Fn-f)-mediated degradation.[21,74] PG content was decreased by 30-50% in knee cartilage exposed to Fn-f for two weeks, whereas it was essentially unaffected in ankle cartilage after FN-f exposure for a month.[74]

More specifically with respect to PTOA, differences between ankle and knee cartilage are evident in their disparate response to injurious compression. In adult knee cartilage, injurious compression (65% fixed strain, 2 mm/s fixed velocity, strain rate approximately 400%/s) resulted in matrix damage in 46% of samples and a net loss of about 1.2% of total GAG in knee explants. Ankle cartilage subjected to the same magnitude of injury sustained little damage and no GAG loss, suggesting that ankle cartilage is more resistant to mechanical injury.[22] An approximately 2-fold increase in aggrecan mRNA expression was observed in knee versus ankle chondrocytes in response to mechanical stimulation. Ankle chondrocytes express higher levels of integrin-associated proteins CD98, CD147 and galectin 3 than knee chondrocytes, suggesting differences in integrin-associated mechanotransduction and matrix remodeling.[75] Collectively, these data suggest that ankle chondrocytes have superior homeostatic mechanisms compared to knee chondrocytes.

Despite this convincing body of literature indicating ankle chondrocytes are inherently more anabolic and less catabolic than knee chondrocytes, there is also interesting evidence to suggest otherwise. No differences in the synthetic capabilities or response to catabolic stimuli were detected in pellet cultures of chondrocytes from the ankle and knee of the same individual.[76] In this study, chondrocytes from both joints were similar in expression of type 1 and type 2 collagen mRNA. Pellet ECM contained equivalent concentrations of GAG and type II collagen and the synthetic rates of GAG and collagen were similarly decreased in response to IL-

1 treatment.[76] These findings suggest that characteristic differences between ankle and knee chondrocytes are lost once the cells are isolated from their native ECM and expanded ex vivo, implying that the native tissue environment may be more important in dictating the characteristic properties of ankle and knee chondrocytes than intrinsic differences between cell types.

Taken together, these findings suggest that major differences exist between joints, which are likely to influence disease pathomechanisms and affect clinical response to OA therapies. Therefore, ankle-specific and injury-specific modeling of PTOA may accelerate progress in basic and clinical research.

Ex vivo ankle cartilage injury models

In addition to the cartilage injury models mentioned above, several groups have used explanted ankle cartilage to investigate early disease mechanisms and response to therapeutic interventions. For example in one model, fresh cadaveric human tali were subjected to a single pressure-controlled impact injury (1Ns; up to 600N within 2ms).[77] Explants were removed from the bone and cultured for up to 2 weeks. Chondrocyte viability was assessed using live-dead cell staining and apoptosis was assessed using a Tunnel assay. Histopathology was performed and a Modified Mankin score was used to assess cartilage injury. Explants were treated 1 hour prior to injury or 48 hours after injury with one of 3 cytoprotective drugs. The polaxamer surfactant P188, a plasma membrane stabilizer, was found to be superior to caspase-3 and caspase-9 inhibitors in preventing impact-induced chondrocyte death and the radial expansion of apoptosis from the site of impact.

A major strength of these types of *ex vivo* models is that they allow injury-induced cellular responses to be studied *in situ* (i.e. in chondrocytes within their native extracellular

matrix) immediately after cartilage injury, and over time.[78] Additionally, *ex vivo* models allow preliminary testing of putative early interventional therapies.[79] A drawback of *ex vivo* models is that they fail to capture important aspects of disease pathogenesis including the inflammatory response, joint loading conditions, etc. Therefore, *in vivo* analogs of these injury- and joint-specific *ex vivo* models are important for preclinical testing of therapeutics.

Non-traumatic animal models of ankle osteoarthritis

Several non-traumatic rodent models of ankle OA have been published. These models utilize the ankle joint to investigate cartilage degeneration secondary to acute joint inflammation, joint immobilization or spontaneous/age-associated OA. Despite limitations in the translatability of these models to clinical ankle PTOA, they may serve as useful tools to explore specific aspects of ankle OA pathophysiology. Furthermore, several of these studies have directly compared the ankle and knee joints within the same individual, and will therefore be reviewed.

Intraarticular IL-1β model of acute ankle inflammation in rats. Scott, et al. described injection of IL-1β into the ankle of rats as an acute model of joint inflammation.[80] Biochemical changes in joint lavage fluid, gene expression changes in whole joint tissues, and histopathology were assessed up to 24 hours after injection. They found that 100ng of IL-1β caused joint swelling and hyperalgesia, as well as gene expression of pro-inflammatory and catabolic mediators, including IL-6, PTGS2, NOS2, TNFα, NFκB, ADAMTS5 and IL-1β. Biochemical analysis of joint lavage fluid revealed accumulation of GAG, IL-6 protein and NO. Histopathology at 24 hours showed evidence of synovitis. Although there was no histological evidence of cartilage destruction in this short time frame, the release of GAG into joint lavage fluids likely indicates early ECM degradation. Strengths of this model include the induction of

reproducible joint inflammation and GAG release within 4 hours. This model is potentially useful for the initial evaluation of antagonists of the IL-1 pathway. The utility of this model is limited by the short study duration and non-physiologic method of disease initiation.

Short-term ankle immobilization model of cartilage atrophy in rats. Renner, et al. evaluated the effect of a passive muscle stretching protocol on the articular cartilage of normal and previously immobilized rat ankles.[81] One ankle in each mouse was immobilized non-invasively for four weeks and histology was performed at 7 weeks. Unilateral ankle immobilization caused increased cellularity and chondrocyte cloning in both the immobilized and non-immobilized limb over control animals. Similarly, proteoglycan depletion was present in both limbs of unilaterally immobilized mice, worse in the immobilized than the contralateral limb. No differences in cartilage thickness were observed.

When passive muscle stretching was instituted for 3 weeks following remobilization, higher cellularity was observed in treated ankles of the stretched group and chondrocyte cloning was observed in the contralateral limb. Notably, immobilized/stretched ankles had the highest PG loss of all the groups calling into question the utility of this modality or the methodology by which it was employed in this model. This model may be useful to investigate therapies to prevent cartilage atrophy following ankle immobilization, and in combination with an ankle destabilization model, could possibly provide insight into the relative importance of joint immobilization in the degenerative and healing processes after destabilizing ankle injuries.

Spontaneous ankle OA model in guinea pigs. Han, et al. were the first to report OA-like lesions occurring spontaneously in the guinea pig ankle.[82] They performed histologic examination and assessed collagen fiber orientation in knee and ankle pairs from male Dunkin-

Hartley guinea pigs at 3 and 6 months of age. Changes in the ankles were evenly distributed between the tibial and talar joint surfaces. At 3 months of age, synovitis was present in all ankle joints and mild focal degenerative cartilage changes were present in some ankles, but histologic scores were not different than controls. At 6 months, moderate focal cartilage lesions, chondrocyte loss and loss of PG staining were present in all ankles. While ankle joint scores were only elevated at 6 months, knee joint scores were significantly elevated at 3 and 6 months. In areas of intact cartilage, changes in collagen fiber orientation were identified and correlated to PG loss indicating that remodeling of the ECM plays a role in early disease and may precede histologic changes this model of spontaneous OA.

STR/ORT mouse model of spontaneous ankle OA. The STR/ORT mouse is a well-established model of spontaneous knee OA, and its utility has been reviewed.[83] Males are preferentially affected, and early calcification of periarticular soft tissue structures is a prominent feature of this model. Evans, et al. described the radiographic changes and Collins, et al. described the histopathological changes in the knees and ankles of STR/ORT mice from 3-10 months of age.[84,85] The radiographic progression of OA in knee and ankle joints was different; in male mice, knee OA worsened directly with age, whereas ankle OA scores increased markedly at 5-6 months, then plateaued. Histology revealed extensive new bone formation in the entheses around the ankle and mineralization of the talar interosseous ligaments starting around 3 months of age. The development of knee and ankle OA was found to be independent within a single mouse.

The etiology of OA in STR/ORT mice is not entirely clear but recently, meta-analysis of transcription profiles revealed increased expression of genes related to endochondral ossification, increased MMP-13 and type X collagen expression as well as differential expression of

regulators of tissue mineralization, suggesting an inherent chondrocyte defect related to endochondral growth.[86] The excessive soft tissue calcification, which precedes cartilage degeneration in this model suggests that the pathophysiology is unlikely to be reflective of human ankle OA.[83,87]

BCBC/Y mouse model of anklylosing ankle OA. Yamamoto, et al. described a mutant B6C3F$_1$ mouse with a light coat color displaying progressive ankle swelling starting at around 9 months.[88] By 10-20 months, these mice display an abnormal stance and gait, with progressive ankylosis of the tarsus on radiographs. On histologic examination, early cartilage lesions included chondrocyte necrosis, cartilage fibrillation and thinning. Later changes included full-thickness erosions in conjunction with a hyperplastic cartilage response.[89] Severe osteophyte formation progressed to bridging ankylosis and finally complete joint fusion of the tarsal joints. Despite these dramatic changes, no synovial inflammation was identified. There is a strong sex predilection, with 87% of males affected and 21% of females. The disease mechanisms and underlying genetic basis of this atypical arthropathy, with a strong predilection for the ankle joints has not been identified.

Aging model of ankle OA in rats. Although spontaneous knee OA is rarely reported in rats,[90,91] Mohr and Lehman describe spontaneous ankle OA in 26 month old CD/BR Sprague Dawley rats.[92] Histology was performed on the talocrural and subtalar joints and morphologic changes were scored semi-quantitatively on a 40-point scale. Lesions ranged from focal chondrocyte necrosis, to loss of proteoglycan staining to fibrillation to partial and total loss of hyaline cartilage to full thickness lesions involving the calcified cartilage layer. Synovitis was rarely present. Although disease mechanisms were not investigated, changes were commonly

present on opposing articular surfaces, suggesting localized increased contact pressures may play a role. Males had more severe lesions compared to females, which could be related to mechanical factors due to the higher body weight of males and/or endocrine factors.

This model was subsequently used to study the effect of meloxicam, a non-steroidal anti-inflammatory drug, on ankle OA.[93] While no drug effect was found, this study demonstrated that the incidence and severity of OA changes are highest in the ankle compared to the hip and knee joints in this model. A consideration in the application of this model is that in humans, age-associated cartilage degeneration in the knee is consistently more severe than in the ankle of the same individual.[26,94] A limitation of any of these spontaneous models of ankle OA is that in humans, primary ankle OA is uncommon.

Modeling ankle posttraumatic osteoarthritis in vivo

Many preclinical PTOA models are available and have been well reviewed.[95-102] Appropriate use of existing models and the development of preclinical models with improved translatability is an ongoing topic of discussion within and beyond the field of OA research.[103-105] The majority of in vivo PTOA models utilize the knee joint, but the numerous anatomical, biomechanical, and biochemical differences between the ankle and the knee suggest that an ankle-specific model is appropriate when targeting therapy for ankle OA. Recently, two surgically induced models of ankle OA have been described.

Destabilization models of ankle OA in the mouse. Recently, Change et al. described an aging model, as well as three destabilization models of mouse ankle OA.[106] First, ankle and knee cartilage from 25 month-old mice were compared to cartilage obtained from humans undergoing joint replacement surgery. OARSI scores for tibiotalar cartilage were lower than for the medial

compartment of the knee, indicating the mouse ankle is more resistant to age-associated cartilage degeneration than the knee, similar to humans. They also found that like humans, mouse talar cartilage is approximately half as thick, and talar subchondral bone was denser compared to the medial tibial plateau. This serves as an important baseline reference, and indicates that this model may have better translatability for the study of age-related ankle OA than those previously mentioned. One caveat to the interpretation of these findings is that normal, aged mouse tissues were compared to cartilage from end-stage OA joints in humans.

The authors go on to describe three methods of ankle joint destabilization in young mice. The medial model involved transection of the tibialis posterior tendon and deltoid ligament and incision of the medial joint capsule. This technique resulted in progressive cartilage degeneration in the talocrural joint over the 8 weeks following surgery. Increased MMP-13 and ADAMTS5 were detected on immunohistochemistry and chondrocyte apoptosis was identified on TUNEL staining. A lateral destabilization model resulted in subtalar OA changes, while a bilateral model resulted in both talocrural and subtalar OA.

The major strengths of the medial destabilization model is that it captures many important features of human disease, including progression of tibiotalar cartilage lesions, chondrocyte apoptosis and inflammatory cytokines, and also lacks the excessive osteophyte formation present in other mouse models. The differences in disease phenotype induced by the three surgical techniques highlights the importance of increased specificity in the type of injury used to study PTOA subtypes. In humans, injury to the lateral soft tissues are more commonly associated with ankle sprain and OA.[107,108] In the mouse, complete transection of the major lateral stabilizing soft tissues and invasion of the joint capsule did not result in significant talocrural joint OA.

Intraarticular fracture model of ankle OA in the Yucatan miniature pig. Goetz, et al. recently developed a porcine distal tibia intraarticular fracture/stabilization model to assess the effects of poor anatomic reconstruction on the development of ankle PTOA.[109] Fractures of the distal tibia were created using an open joint approach and repaired using internal fixation with a bone plate. Synovial fluid analysis, radiographic monitoring and force plate analysis were performed after surgery and animals were sacrificed at 12 weeks. Osteochondral histology was performed and scored using automated Mankin scoring. By 12 weeks post-operatively, all fractures were healed and limb loading had returned to normal. Inflammatory cytokine concentrations in synovial fluid, including TNFα, IL1β, IL6, and IL8 were elevated transiently during the 2 weeks after fracture. Histology scores were worse in joints with articular incongruity compared to those that were anatomically reconstructed.

This is a well-validated model to investigate intraarticular fracture-induced PTOA and the effects of chronically altered ankle joint mechanics due to articular surface incongruity. Strengths of this model include a consistent fracture geometry, with reporting of the energy absorbed during fracture, and clinically relevant outcome measures including intra- and post-operative imaging and analysis, gait analysis to quantify pain/joint dysfunction, synovial fluid biomarkers and osteochondral histology, although synovial membrane was not assessed. Internal fixation techniques are similar to those used in human clinical patients. In this report, 27% (6/22) of the animals were lost post-operatively due to orthopedic complications. Longer-term follow up will be required if this model is to be used to test biological treatments to reduce the incidence of fracture-associated ankle PTOA.

Considerations for development of new preclinical models of ankle PTOA

Method of OA induction

When modeling PTOA, the induction method would ideally mimic that of naturally occurring disease. The majority of PTOA models utilize the knee (stifle) joint and rely on surgical destabilization of supporting soft tissue such as the meniscus or anterior cruciate ligament.[95-100] PTOA models involving joint instability or the generation of an osteochondral fragment are valuable tools, however these models do not reflect the contributions of acute trauma to the articular cartilage at the time of injury. Although the specific injury parameters required to initiate clinical PTOA remain unclear, these mechanical thresholds have been studied in many model systems, and experimental evidence supports the importance of loading magnitude and rate as predictors of cartilage degeneration.[13,22,31,110-113]

To more specifically investigate mechanical overloading of the articular surface, single-impact load models are becoming more prevalent in PTOA research, and have been validated to initiate early OA-like lesions in the knee, but have not been applied to the ankle.[114-116] This reductionist approach allows investigators to gain new insight into the cartilage-specific contributions to PTOA *ex vivo*, investigate mechanical thresholds for peracute cellular and subcellular responses to cartilage injury, and test targeted drugs to prevent PTOA in animal models. For example, a recent study examined microscale mechanics and corresponding chondrocyte death in articular cartilage following rapid impact injury.[117] This new technique revealed that chondrocyte death is highly correlated with a threshold of 8% microscale strain. When the superficial layer of the cartilage was removed, cell death penetrated deeper into the cartilage, indicating a protective role for the superficial layer. Additionally, chondrocyte death developed within 2 hours of impact, suggesting a narrow window for early therapeutic

intervention after injury.[117] In summary, an overly aggressive model with rapid progression to end-stage OA may not provide a sufficiently dynamic range of disease to evaluate therapeutic effects in a preclinical ankle model and a single, rapid impact model is most consistent with the likely etiopathogenesis of ankle PTOA.

Species Choice

Rodent models have the advantages of being low cost, genetically similar within a specific breed strain, and amenable to genetic manipulation. Rodent models have therefore been used extensively as screening tools for drug development and to investigate specific molecular pathways involved in OA pathogenesis.[95,96,99,102,118,119] The most significant shortcomings of small animal models are the dissimilarities in cartilage structure and disparate loading compared to a human joint. An optimal preclinical model would be scaled appropriately to mimic joint size (**Figure 2.3**), load, age and skeletal maturity of human clinical patients. The cartilage lesion should be located in an analogous location in ankle, and be of similar size, type and depth as clinically observed lesions, which is difficult or impossible to control in rodents. Recently, a mouse model of ankle OA was described based on surgical destabilization.[106] Rabbit models are slightly larger and have been used in single impact studies of knee PTOA without the confounding variables of instability.[114,120]

Common large animal species used in OA research include the dog, sheep, goat, pig and horse.[95,99-101,104,116,121-124] A benefit common to these larger species is increased joint size, allowing OA outcome measures such as synovial fluid collection, clinical cartilage imaging modalities including MRI, quantitative gait analysis, arthroscopic joint examination, topographical evaluation within a single joint and ample tissue for histological, biochemical,

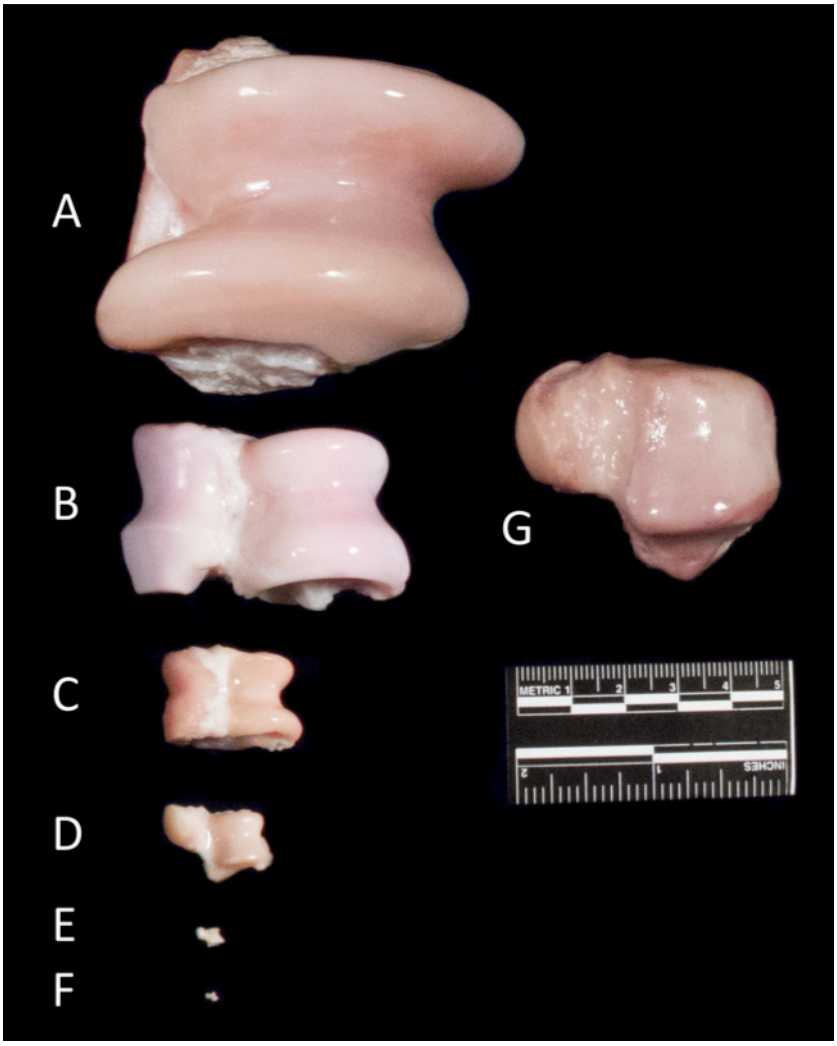

Figure 2.3. Comparative talus anatomy. Size comparison of left tali from species commonly used as animal models in osteoarthritis research; A) horse, B) pig, C) sheep, D) dog, E) rat, F) mouse, compared to the G) human.

biomechanical, and molecular analyses. Large joint size is a particularly important feature if precise anatomical placement of articular surface trauma is to be employed.

The dog knee has been widely used in preclinical models of knee OA, therefore validated outcome measures have been established in that joint.[99,123] Most commonly, OA is induced by surgical destabilization, however single impact models have recently been described.[116] Dogs are an athletic species and are prone to naturally occurring OA, however as a popular companion animal species, their use in biomedical research draws heightened scrutiny by the public. Sheep and goats have been used in several destabilization models of knee OA as well as a femoral condyle impact model.[125] Sheep and goats have joints that are closer in size to the human ankle than dogs (**Figure 2.3**), however naturally occurring OA is rare to non-existent, and these species may be less susceptible to OA after surgical induction, as ACL transection leads to joint instability but not significant OA in the goat knee.[122,126] When considering the development of preclinical models, small ruminants (sheep and goats) have the particular disadvantage of being foregut fermenters, and therefore bioavailability of orally administered therapeutics differ significantly from monogastric species (i.e. humans, horses, dogs, pigs).

The horse is an established model organism for PTOA research and offers several advantages over other species. The horse is the largest model available and equine cartilage most closely approximates human cartilage thickness and biomechanical loading.[127,128] Similar to humans, the cartilage of the equine talocrural joint has a higher GAG content, and is stiffer than that of the knee.[129] The equine species is naturally prone to OA.[130] Similar to the human ankle, the equine TC joint has a high degree of intrinsic bony stability and rarely suffers OA in the absence of injury.[131,132] As in humans, equine TC PTOA does occur secondary to ligamentous injury, blunt trauma, OCLs and intraarticular fractures.[131-133] The dimensions of the equine

talocrural joint are well suited to arthroscopic examination and manipulation and it is among the most common arthroscopically approached joints in equine surgical practice. In addition to the potential to perform serial arthroscopic examinations, MRI is a well validated diagnostic modality to assess the equine TC joint, therefore the horse may be considered for studies where longitudinal evaluations of cartilage are needed.[134-136]

Outcome measures

Histopathology remains the gold standard for assessing OA progression. Many systems have been used to evaluate OA changes, and these have been extensively reviewed.[137] Commonly used scoring systems in animal research models are the Mankin Score,[138] the OARSI scoring system [139]and the ICRS score for cartilage repair.[140] Recently, species-specific consensus scoring systems have been developed for the most important species used in OA research including dog, guinea pig, horse, mouse, rabbit, rat, and sheep/goat.[101] To reduce the number of animal sacrifices at each time point, longitudinal outcome assessments are preferred, including imaging, biochemical and genetic biomarkers, as well as assessments of pain, joint function and gait. Appropriate ankle-specific biomarkers will need to be identified and validated in order to develop translational PTOA models that more closely represent clinical subgroups of disease.[141]

MRI allows objective measures of soft tissue injuries and cartilage health in human and large animal veterinary patients, and its use and utility in preclinical animal models will continue to increase. Bone bruising is identified on MRI in 16-40% of patients after ankle sprain, and in up to 50% of patients with ligament injuries.[142,143] Therefore, the assessment of subchondral bone should be included in the characterization of ankle injury models. Highly congruent joints with relatively thin articular cartilage are more challenging to assess using MRI, however steady

advancements in imaging technology have allowed evaluation of subtle cartilage lesions in the ankle.[144,145] Contemporary compositional MRI techniques including dGEMRIC and T1-rho, and T2 mapping have become increasingly useful for assessing cartilage degeneration and allow examination of biochemical or ultrastructural composition of articular cartilage relevant to OA research.[145,146] Combining clinical and research data pertaining to the ankle may allow identification of preclinical disease. As discussed, evidence in patients with ankle injuries suggests that, in addition to advanced imaging, arthroscopic examination is particularly important in identifying early ankle PTOA. Therefore, the ideal model would allow serial arthroscopic examination of the talocrural joint.

A major challenge in developing appropriate preclinical animal models of OA is the ability to quantify pain as a clinical endpoint. Chronic pain is a hallmark of OA, and the ability to evaluate pain and joint dysfunction is integral to the relevance and utility of models in translational research. This is especially relevant for less severe models of OA, when the goal is to study and develop therapies targeted at early OA in humans.[104] Numerous measures of pain and joint dysfunction that have been developed in multiple species, and it is not clear which of these will prove the most useful in ankle PTOA models. As an example, gait abnormalities are well-established indicators for pain. In horses and dogs, quantitative gait analysis has been used for over two decades to evaluate naturally occurring and experimental lameness. Studies have employed force plate, pressure plate, accelerometers and kinematic image analysis, and these outcome measures are well validated.[147-154] In small animal models, pain and joint dysfunction have been less commonly reported outcome measures, although more recently these systems have been developed and validated for rodents.[151,155,156] Quantitative gait analysis is possible in pigs, sheep, and goats, however their temperament is less amenable to pain assessment using

standard techniques such as force plate analysis. New mechanisms of pain are being identified in OA patients, and appropriate outcome measures will need to be identified as new joint-specific and injury-specific PTOA models are developed.[104,155,157,158]

Conclusion

OA is the most common cause of chronic disability in the United States, and as the population ages, it will become increasingly burdensome to society. The ankle is the most commonly injured joint, and ankle PTOA disproportionately affects populations of young adults, athletes and military personnel. Laboratory and animals model studies will continue to reveal pathomechansisms of ankle PTOA. Remaining unmet needs related ankle OA include early interventional therapies (so called "point of injury care") to prevent progression of early PTOA, as well as methods to treat established/late-stage OA. To address these knowledge gaps, an appropriate ankle-specific preclinical PTOA model would allow investigation of the early initiating events following talocrural cartilage injury, as well as longitudinal testing of targeted therapies in a clinically relevant species.

Acknowledgements

The authors acknowledge Jim Postier for technical drawing. We thank David C. Jones for photography, Youichi Yasui for logistical support and Margaret Goodale for technical support. MD was supported by NIH 5T32OD011000-20 and NIH 1K08AR068470.

References

1. Kramer WC, Hendricks KJ, Wang J. Pathogenetic mechanisms of posttraumatic osteoarthritis: opportunities for early intervention. *Int J Clin Exp Med*. 2011;4(4):285–298.

2. Richmond SA, Fukuchi RK, Ezzat A, Schneider K, Schneider G, Emery CA. Are Joint Injury, Sport Activity, Physical Activity, Obesity, or Occupational Activities Predictors for Osteoarthritis? A Systematic Review. *J Orthop Sports Phys Ther*. 2013;43(8):515–B519. doi:10.2519/jospt.2013.4796.

3. Brown TDT, Johnston RCR, Saltzman CLC, Marsh JLJ, Buckwalter JAJ. Posttraumatic osteoarthritis: a first estimate of incidence, prevalence, and burden of disease. *J Orthop Trauma*. 2006;20(10):739–744. doi:10.1097/01.bot.0000246468.80635.ef.

4. Weatherall JM, Mroczek K, McLaurin T, Ding B, Tejwani N. Post-traumatic ankle arthritis. *Bull Hosp Jt Dis (2013)*. 2013;71(1):104–112.

5. Wilson MG, Michet CJJ, Ilstrup DM, Melton LJ3. Idiopathic symptomatic osteoarthritis of the hip and knee: a population-based incidence study. *Mayo Clin Proc*. 1990;65(9):1214–1221.

6. Valderrabano V, Horisberger M, Russell I, Dougall H, Hintermann B. Etiology of Ankle Osteoarthritis. *Clin Orthop Relat Res*. 2008;467(7):1800–1806. doi:10.1007/s11999-008-0543-6.

7. Nelson AJ, Collins CL, Yard EE, Fields SK, Comstock RD. Ankle injuries among United States high school sports athletes, 2005-2006. *J Athl Train*. 2007;42(3):381–387.

8. Belmont PJJ, Goodman GP, Waterman B, DeZee K, Burks R, Owens BD. Disease and nonbattle injuries sustained by a U.S. Army Brigade Combat Team during Operation Iraqi Freedom. *Mil Med*. 2010;175(7):469–476.

9. McKay G, Goldie P, Payne WR, Oakes BW, Watson LF. A prospective study of injuries in basketball: A total profile and comparison by gender and standard of competition. *J Sci Med Sport*. 2001;4(2):196–211.

10. Gribble PA, Bleakley CM, Caulfield BM, et al. Evidence review for the 2016 International Ankle Consortium consensus statement on the prevalence, impact and long-term consequences of lateral ankle sprains. *Br J Sports Med*. June 2016. doi:10.1136/bjsports-2016-096189.

11. Valderrabano V, Hintermann B, Horisberger M, Fung TS. Ligamentous posttraumatic ankle osteoarthritis. *The American Journal of Sports Medicine*. 2006;34(4):612–620. doi:10.1177/0363546505281813.

12. Cheng DS, Visco CJ. Pharmaceutical therapy for osteoarthritis. *PM&R*. 2012;4(5):S82–S88.

13. Anderson DD, Chubinskaya S, Guilak F, et al. Post-traumatic osteoarthritis: improved understanding and opportunities for early intervention. *J Orthop Res*. 2011;29(6):802–809. doi:10.1002/jor.21359.

14. Lotz MK, Kraus VB. New developments in osteoarthritis. Posttraumatic osteoarthritis: pathogenesis and pharmacological treatment options. *Arthritis Research & Therapy*. 2010;12(3):211–211. doi:10.1186/ar3046.

15. Quinn TM, Häuselmann H-J, Shintani N, Hunziker EB. Cell and matrix morphology in articular cartilage from adult human knee and ankle joints suggests depth-associated adaptations to biomechanical and anatomical roles. *Osteoarthritis and Cartilage*. October, 2013; 21(12):1904-12. doi:10.1016/j.joca.2013.09.011.

16. Treppo S, Koepp H, Quan EC, Cole AA, Kuettner KE, Grodzinsky AJ. Comparison of biomechanical and biochemical properties of cartilage from human knee and ankle pairs. *J Orthop Res*. 2000;18(5):739–748. doi:10.1002/jor.1100180510.

17. Aurich M, Poole AR, Reiner A, et al. Matrix homeostasis in aging normal human ankle cartilage. *Arthritis & Rheumatism*. 2002;46(11):2903–2910. doi:10.1002/art.10611.

18. Eger W, Schumacher BL, Mollenhauer J, Kuettner KE, Cole AA. Human knee and ankle cartilage explants: catabolic differences. *J Orthop Res*. 2002;20(3):526–534. doi:10.1016/S0736-0266(01)00125-5.

19. Huch K. Knee and ankle: human joints with different susceptibility to osteoarthritis reveal different cartilage cellularity and matrix synthesis in vitro. *Arch Orthop Trauma Surg*. 2001;121(6):301–306.

20. Huch K, Kuettner KE, Dieppe P. Osteoarthritis in ankle and knee joints. *Semin Arthritis Rheum*. 1997;26(4):667–674.

21. Dang Y, Cole AA, Homandberg GA. Comparison of the catabolic effects of fibronectin fragments in human knee and ankle cartilages. *Osteoarthr Cartil*. 2003;11(7):538–547.

22. Patwari P, Cheng DM, Cole AA, Kuettner KE, Grodzinsky AJ. Analysis of the Relationship between Peak Stress and Proteoglycan Loss following Injurious Compression of Human Post-mortem Knee and Ankle Cartilage. *Biomech Model Mechanobiol*. 2006;6(1-2):83–89. doi:10.1007/s10237-006-0037-y.

23. Hendren L, Beeson P. A review of the differences between normal and osteoarthritis articular cartilage in human knee and ankle joints. *Foot (Edinb)*. 2009;19(3):171–176. doi:10.1016/j.foot.2009.03.003.

24. Aurich, M., Hofmann, G. O., Rolauffs, B., & Gras, F. (2014). Differences in injury pattern and prevalence of cartilage lesions in knee and ankle joints: a retrospective cohort study. Orthopedic Reviews, 6(4), 5611. http://doi.org/10.4081/or.2014.5611

25. Aurich M, Hofmann GO, Rolauffs B, Gras F. Differences in injury pattern and

prevalence of cartilage lesions in knee and ankle joints: a retrospective cohort study. *Orthop Rev (Pavia)*. 2014;6(4):5611. doi:10.4081/or.2014.5611.

26. Koepp H, Eger W, Muehleman C, et al. Prevalence of articular cartilage degeneration in the ankle and knee joints of human organ donors. *J Orthop Sci*. 1999;4(6):407–412.

27. Novakofski KD, Berg LC, Bronzini I, et al. Joint-dependent response to impact and implications for post-traumatic osteoarthritis. *Osteoarthritis and Cartilage*. 2015;23(7):1130–1137. doi:10.1016/j.joca.2015.02.023.

28. Catterall JB, Zura RD, Bolognesi MP, Kraus VB. Aspartic acid racemization reveals a high turnover state in knee compared with hip osteoarthritic cartilage. *Osteoarthritis and Cartilage*. 2016;24(2):374–381. doi:10.1016/j.joca.2015.09.003.

29. Barg A, Pagenstert GI, Hügle T, et al. Ankle osteoarthritis: etiology, diagnostics, and classification. *Foot Ankle Clin*. 2013;18(3):411–426. doi:10.1016/j.fcl.2013.06.001.

30. Saltzman CL, Salamon ML, Blanchard GM, et al. Epidemiology of ankle arthritis: report of a consecutive series of 639 patients from a tertiary orthopaedic center. *Iowa Orthop J*. 2005;25:44–46.

31. Buckwalter JA. The role of mechanical forces in the initiation and progression of osteoarthritis. *HSS Jrnl*. 2012;8(1):37–38. doi:10.1007/s11420-011-9251-y.

32. Blalock D, Miller A, Tilley M, Wang J. Joint instability and osteoarthritis. *Clin Med Insights Arthritis Musculoskelet Disord*. 2015;8:15–23. doi:10.4137/CMAMD.S22147.

33. McKinley TO, Rudert MJ, Koos DC, Brown TD. Incongruity versus Instability in the Etiology of Posttraumatic Arthritis. *Clin Orthop Relat Res*. 2004;423:44–51. doi:10.1097/01.blo.0000131639.89143.26.

34. Bischof JE, Spritzer CE, Caputo AM, et al. Journal of Biomechanics. *Journal of Biomechanics*. 2010;43(13):2561–2566. doi:10.1016/j.jbiomech.2010.05.013.

35. Anderson DD, Van Hofwegen C, Marsh JL, Brown TD. Is elevated contact stress predictive of post-traumatic osteoarthritis for imprecisely reduced tibial plafond fractures? *J Orthop Res*. 2010;29(1):33–39. doi:10.1002/jor.21202.

36. McKinley TO, Borrelli J, D'Lima DD, Furman BD, Giannoudis PV. Basic science of intra-articular fractures and posttraumatic osteoarthritis. *J Orthop Trauma*. 2010;24(9):567–570. doi:10.1097/BOT.0b013e3181ed298d.

37. Hintermann B, Regazzoni P, Lampert C, Stutz G, Gächter A. Arthroscopic findings in acute fractures of the ankle. *J Bone Joint Surg Br*. 2000;82(3):345–351.

38. Loren GJ, Ferkel RD. Arthroscopic assessment of occult intra-articular injury in acute ankle fractures. *Arthroscopy*. 2002;18(4):412–421. doi:10.1053/jars.2002.32317.

39. Stufkens SA, Knupp M, Horisberger M, Lampert C, Hintermann B. Cartilage lesions and the development of osteoarthritis after internal fixation of ankle fractures: a prospective study. *J Bone Joint Surg Am*. 2010;92(2):279–286. doi:10.2106/JBJS.H.01635.

40. Raikin SM, Elias I, Zoga AC, Morrison WB, Besser MP, Schweitzer ME. Osteochondral Lesions of the Talus: Localization and Morphologic Data from 424 Patients Using a Novel Anatomical Grid Scheme. *Foot Ankle Int*. 2007;28(2):154–161. doi:10.3113/FAI.2007.0154.

41. Taga I, Shino K, Inoue M, Nakata K, Maeda A. Articular cartilage lesions in ankles with lateral ligament injury. An arthroscopic study. *The American Journal of Sports Medicine*. 1993;21(1):120–6–discussion126–7.

42. Klammer G, Maquieira GJ, Spahn S, Vigfusson V, Zanetti M, Espinosa N. Natural history of nonoperatively treated osteochondral lesions of the talus. *Foot & ankle international / American Orthopaedic Foot and Ankle Society [and] Swiss Foot and Ankle Society*. 2015;36(1):24–31. doi:10.1177/1071100714552480.

43. Swenson DM, Collins CL, Fields SK, Comstock RD. Epidemiology of U.S. high school sports-related ligamentous ankle injuries, 2005/06-2010/11. *Clin J Sport Med*. 2013;23(3):190–196. doi:10.1097/JSM.0b013e31827d21fe.

44. Marsh JL, Buckwalter J, Gelberman R, et al. Articular fractures: Does an anatomic reduction really change the result? *J Bone Joint Surg Am*. 2002;84A(7):1259–1271.

45. O'Loughlin PF, Heyworth BE, Kennedy JG. Current Concepts in the Diagnosis and Treatment of Osteochondral Lesions of the Ankle. *The American Journal of Sports Medicine*. 2010;38(2):392–404. doi:10.1177/0363546509336336.

46. Lynch SA, Renström PA. Treatment of acute lateral ankle ligament rupture in the athlete. Conservative versus surgical treatment. *Sports Med*. 1999;27(1):61–71.

47. Petersen W, Rembitzki IV, Koppenburg AG, et al. Treatment of acute ankle ligament injuries: a systematic review. *Arch Orthop Trauma Surg*. 2013;133(8):1129–1141. doi:10.1007/s00402-013-1742-5.

48. Golditz T, Steib S, Pfeifer K, et al. Functional ankle instability as a risk factor for osteoarthritis: using T2-mapping to analyze early cartilage degeneration in the ankle joint of young athletes. *Osteoarthr Cartil*. 2014;22(10):1377–1385. doi:10.1016/j.joca.2014.04.029.

49. Gatlin CC, Matheny LM, HO CP, Johnson NS, Clanton TO. Diagnostic accuracy of 3.0 Tesla magnetic resonance imaging for the detection of articular cartilage lesions of the talus. *Foot & ankle international / American Orthopaedic Foot and Ankle Society [and] Swiss Foot and Ankle Society*. 2015;36(3):288–292. doi:10.1177/1071100714553469.

50. Roemer FW, Jomaah N, Niu J, et al. Ligamentous Injuries and the Risk of Associated

Tissue Damage in Acute Ankle Sprains in Athletes: A Cross-sectional MRI Study. *The American Journal of Sports Medicine*. 2014;42(7):1549–1557. doi:10.1177/0363546514529643.

51. Sugimoto K, Takakura Y, Okahashi K, Samoto N, Kawate K, Iwai M. Chondral injuries of the ankle with recurrent lateral instability: an arthroscopic study. *J Bone Joint Surg Am*. 2009;91(1):99–106. doi:10.2106/JBJS.G.00087.

52. Tochigi Y, Rudert MJ, Saltzman CL, Amendola A, Brown TD. Contribution of articular surface geometry to ankle stabilization. *J Bone Joint Surg Am*. 2006;88(12):2704–2713. doi:10.2106/JBJS.E.00758.

53. Fong DT, Chan Y-Y, Mok K-M, Yung PS, Chan K-M. Understanding acute ankle ligamentous sprain injury in sports. *Sports Med Arthrosc Rehabil Ther Technol*. 2009;1(1):14. doi:10.1186/1758-2555-1-14.

54. Madeti BK, Chalamalasetti SR, Bolla Pragada SKSSR. Biomechanics of knee joint — A review. *Front Mech Eng*. 2015;10(2):176–186. doi:10.1007/s11465-014-0306-x.

55. Deland JT, Morris GD, Sung IH. Biomechanics of the ankle joint. A perspective on total ankle replacement. *Foot Ankle Clin*. 2000;5(4):747–759.

56. Stauffer RN, Chao EY, Brewster RC. Force and motion analysis of the normal, diseased, and prosthetic ankle joint. *Clin Orthop Relat Res*. 1977;(127):189–196.

57. D Shepherd BS. Thickness of human articular cartilage in joints of the lower limb. *Annals of the Rheumatic Diseases*. 1999;58(1):27.

58. Adam C, Eckstein F, Milz S, Putz R. The distribution of cartilage thickness within the joints of the lower limb of elderly individuals. *J Anat*. 1998;193 (Pt 2):203–214.

59. DeSmet AA, Dalinka MK, Alazraki N, et al. Chronic ankle pain. American College of Radiology. ACR Appropriateness Criteria. *Radiology*. 2000;215 Suppl:321–332.

60. Calhoun JH, Li F, Ledbetter BR, Viegas SF. A comprehensive study of pressure distribution in the ankle joint with inversion and eversion. *Foot Ankle Int*. 1994;15(3):125–133.

61. van Dijk CN, Lim LS, Poortman A, Strubbe EH, Marti RK. Degenerative joint disease in female ballet dancers. *The American Journal of Sports Medicine*. 1995;23(3):295–300.

62. Angioi M, Maffulli GD, McCormack M, Morrissey D, Chan O, Maffulli N. Early signs of osteoarthritis in professional ballet dancers: a preliminary study. *Clin J Sport Med*. 2014;24(5):435–437. doi:10.1097/JSM.0000000000000035.

63. Ramsey PL, Hamilton W. Changes in tibiotalar area of contact caused by lateral talar shift. *J Bone Joint Surg Am*. 1976;58(3):356–357.

64. Wright IC, Neptune RR, van den Bogert AJ, Nigg BM. The influence of foot positioning on ankle sprains. *Journal of Biomechanics*. 2000;33(5):513–519. doi:10.1016/S0021-9290(99)00218-3.

65. McKay GD, Goldie PA, Payne WR, Oakes BW. Ankle injuries in basketball: injury rate and risk factors. *Br J Sports Med*. 2001;35(2):103–108.

66. Buckley MR, Bonassar LJ, Cohen I. Localization of Viscous Behavior and Shear Energy Dissipation in Articular Cartilage Under Dynamic Shear Loading. *J Biomech Eng*. 2013;135(3):031002. doi:10.1115/1.4007454.

67. Silverberg JL, Barrett AR, Das M, Petersen PB, Bonassar LJ, Cohen I. Structure-Function Relations and Rigidity Percolation in the Shear Properties of Articular Cartilage. *Biophysj*. 2014;107(7):1721–1730. doi:10.1016/j.bpj.2014.08.011.

68. Korhonen RK, Wong M, Arokoski J, et al. Importance of the superficial tissue layer for the indentation stiffness of articular cartilage. *Med Eng Phys*. 2002;24(2):99–108.

69. Silverberg JL, Dillavou S, Bonassar L, Cohen I. Anatomic variation of depth-dependent mechanical properties in neonatal bovine articular cartilage. *J Orthop Res*. 2012;31(5):686–691. doi:10.1002/jor.22303.

70. Poole AR, Kojima T, Yasuda T, Mwale F, Kobayashi M, Laverty S. Composition and structure of articular cartilage: a template for tissue repair. *Clin Orthop Relat Res*. 2001;(391 Suppl):S26–S33.

71. Schumacher BL, Su J-L, Lindley KM, Kuettner KE, Cole AA. Horizontally oriented clusters of multiple chondrons in the superficial zone of ankle, but not knee articular cartilage. *Anat Rec*. 2002;266(4):241–248. doi:10.1002/ar.10063.

72. Aicher WK, Rolauffs B. The spatial organisation of joint surface chondrocytes: review of its potential roles in tissue functioning, disease and early, preclinical diagnosis of osteoarthritis. *Annals of the Rheumatic Diseases*. 2014;73(4):645–653. doi:10.1136/annrheumdis-2013-204308.

73. Rolauffs B, Rothdiener M, Bahrs C, et al. Onset of preclinical osteoarthritis: The angular spatial organization permits early diagnosis. *Arthritis & Rheumatism*. 2011;63(6):1637–1647. doi:10.1002/art.30217.

74. Kang Y, Koepp H, Cole AA, Kuettner KE, Homandberg GA. Cultured human ankle and knee cartilage differ in susceptibility to damage mediated by fibronectin fragments. *J Orthop Res*. 1998;16(5):551–556. doi:10.1002/jor.1100160505.

75. Orazizadeh M, Cartlidge C, Wright MO, et al. Mechanical responses and integrin associated protein expression by human ankle chondrocytes. *Biorheology*. 2006;43(3-4):249–258.

76. Candrian C, Bonacina E, Frueh JA, et al. Intra-individual comparison of human ankle

and knee chondrocytes in vitro: relevance for talar cartilage repair. *Osteoarthritis and Cartilage*. 2009;17(4):489–496. doi:10.1016/j.joca.2008.05.023.

77. Garrido CP, Hakimiyan AA, Rappoport L, Oegema TR, Wimmer MA, Chubinskaya S. Anti-apoptotic treatments prevent cartilage degradation after acute trauma to human ankle cartilage. *Osteoarthritis and Cartilage*. 2009;17(9):1244–1251. doi:10.1016/j.joca.2009.03.007.

78. Kurz B, Lemke AK, Fay J, Pufe T, Grodzinsky AJ, Schünke M. Pathomechanisms of cartilage destruction by mechanical injury. *Annals of Anatomy - Anatomischer Anzeiger*. 2005;187(5-6):473–485. doi:10.1016/j.aanat.2005.07.003.

79. Chubinskaya S, Wimmer MA. Key Pathways to Prevent Posttraumatic Arthritis for Future Molecule-Based Therapy. *Cartilage*. 2013;4(3 Suppl):13S–21S. doi:10.1177/1947603513487457.

80. Scott I, Midha A, Rashid U, et al. Correlation of gene and mediator expression with clinical endpoints in an acute interleukin-1b-driven model of joint pathology. *Osteoarthritis and Cartilage*. 2009;17(6):790–797. doi:10.1016/j.joca.2008.09.016.

81. Renner AF, Carvalho E, Soares E, Mattiello-Rosa S. The effect of a passive muscle stretching protocol on the articular cartilage. *Osteoarthritis and Cartilage*. 2006;14(2):196–202. doi:10.1016/j.joca.2005.08.011.

82. Han B, Cole AA, Shen Y, Brodie T, Williams JM. Early alterations in the collagen meshwork and lesions in the ankles are associated with spontaneous osteoarthritis in guinea-pigs. *Osteoarthritis and Cartilage*. 2002;10(10):778–784. doi:10.1053/joca.2002.0822.

83. Mason RM, Chambers MG, Flannelly J, Gaffen JD, Dudhia J, Bayliss MT. The STR/ort mouse and its use as a model of osteoarthritis. *Osteoarthritis and Cartilage*. 2001;9(2):85–91. doi:10.1053/joca.2000.0363.

84. Collins C, Evans RG, Ponsford F, Miller P, Elson CJ. Chondro-osseous metaplasia, bone density and patellar cartilage proteoglycan content in the osteoarthritis of STR/ORT mice. *Osteoarthr Cartil*. 1994;2(2):111–118.

85. Evans RG, Collins C, Miller P, Ponsford FM, Elson CJ. Radiological scoring of osteoarthritis progression in STR/ORT mice. *Osteoarthr Cartil*. 1994;2(2):103–109.

86. Staines KA, Madi K, Mirczuk SM, et al. Endochondral Growth Defect and Deployment of Transient Chondrocyte Behaviors Underlie Osteoarthritis Onset in a Natural Murine Model. *Arthritis & Rheumatology*. 2016;68(4):880–891. doi:10.1002/art.39508.

87. Das-Gupta EP, Lyons TJ, Hoyland JA, Lawton DM, Freemont AJ. New histological observations in spontaneously developing osteoarthritis in the STR/ORT mouse questioning its acceptability as a model of human osteoarthritis. *International Journal of Experimental Pathology*. 1993;74(6):627–634.

88. Yamamoto H, Iwase N. Spontaneous osteoarthritic lesions in a new mutant strain of the mouse. *Exp Anim*. 1998;47(2):131–135.

89. Yamamoto H, Iwase N, Kohno M. Histopathological characterization. *Experimental and toxicologic pathology*. 1999;51(1):15–20. doi:10.1016/S0940-2993(99)80051-7.

90. Gerwin N, Bendele AM, Glasson S, Carlson CS. The OARSI histopathology initiative. *Osteoarthr Cartil*. 2010;18(S3):S24–S34. doi:10.1016/j.joca.2010.05.030.

91. Moriyama H, Kanemura N, Brouns I, et al. Effects of aging and exercise training on the histological and mechanical properties of articular structures in knee joints of male rat. *Biogerontology*. 2012;13(4):369–381. doi:10.1007/s10522-012-9381-8.

92. Mohr W, Lehmann H. Osteoarthrosis of the ankle joints in old rats. *Z Rheumatol*. 1992;51(1):35–40.

93. Mohr W, Lehmann H, Engelhardt G. Chondroneutrality of meloxicam in rats with spontaneous osteoarthrosis of the ankle joint. *Z Rheumatol*. 1997;56(1):21–30. doi:10.1007/s003930050017.

94. Kuettner KE, Cole AA. Cartilage degeneration in different human joints. *Osteoarthritis and Cartilage*. 2005;13(2):93–103. doi:10.1016/j.joca.2004.11.006.

95. Little CB, Hunter DJ. Post-traumatic osteoarthritis: from mouse models to clinical trials. *Nat Rev Rheumatol*. 2013;9(8):485–497. doi:10.1038/nrrheum.2013.72.

96. Little CB, Smith MM. Animal Models of Osteoarthritis. *Curr Rheumatol Rev*. 2008;4(3):175–182. doi:10.2174/157339708785133523.

97. Bendele AM. Animal models of osteoarthritis. *J Musculoskelet Neuronal Interact*. 2001;1(4):363–376.

98. Mastbergen SC, Lafeber FP. Animal models of osteoarthritis—why choose a larger model. *US Musculoskeletal Review*. 2009; 11-17.

99. Gregory MH, Capito N, Kuroki K, Stoker AM, Cook JL, Sherman SL. A Review of Translational Animal Models for Knee Osteoarthritis. *Arthritis*. 2012;2012(7):1–14. doi:10.1002/jor.20135.

100. Lampropoulou-Adamidou K, Lelovas P, Karadimas EV, et al. Useful animal models for the research of osteoarthritis. *Eur J Orthop Surg Traumatol*. 2013;24(3):263–271. doi:10.1007/s00590-013-1205-2.

101. Aigner T, Cook JL, Gerwin N, et al. Histopathology atlas of animal model systems. *Osteoarthritis and Cartilage*. 2010;18(S3):S2–S6. doi:10.1016/j.joca.2010.07.013.

102. McCoy AM. Animal Models of Osteoarthritis: Comparisons and Key Considerations. *Vet Pathol*. 2015;52(5):803–818. doi:10.1177/0300985815588611.

103. Malfait A-M, Little CB. On the predictive utility of animal models of osteoarthritis. *Arthritis Research & Therapy*. 2015;17:225. doi:10.1186/s13075-015-0747-6.

104. Poole R, Blake S, Buschmann M, et al. Recommendations for the use of preclinical models in the study and treatment of osteoarthritis. *Osteoarthritis and Cartilage*. 2020;18(S3):S10–S16. doi:10.1016/j.joca.2010.05.027.

105. Wendler A, Wehling M. The translatability of animal models for clinical development: biomarkers and disease models. *Current Opinion in Pharmacology*. 2010;10(5):601–606. doi:10.1016/j.coph.2010.05.009.

106. Chang SH, Yasui T, Taketomi S, et al. Comparison of mouse and human ankles and establishment of mouse ankle osteoarthritis models by surgically-induced instability. *Osteoarthritis and Cartilage*. 2016;24(4):688–697. doi:10.1016/j.joca.2015.11.008.

107. Czajka CM, Tran E, Cai AN, DiPreta JA. Ankle sprains and instability. *Med Clin North Am*. 2014;98(2):313–329. doi:10.1016/j.mcna.2013.11.003.

108. Kerkhoffs GM, Blankevoort L, van Poll D, Marti RK, van Dijk CN. Anterior lateral ankle ligament damage and anterior talocrural-joint laxity: an overview of the in vitro reports in literature. *Clin Biomech (Bristol, Avon)*. 2001;16(8):635–643. doi:10.1016/S0268-0033(01)00054-7.

109. Goetz JE, Fredericks D, Petersen E, et al. A clinically realistic large animal model of intra-articular fracture that progresses to post-traumatic osteoarthritis. *Osteoarthritis and Cartilage*. 2015;23(10):1797–1805. doi:10.1016/j.joca.2015.05.022.

110. Buckwalter JA, Brown TD. Joint Injury, Repair, and Remodeling. *Clin Orthop Relat Res*. 2004;423:7–16. doi:10.1097/01.blo.0000131638.81519.de.

111. Ewers BJ, Dvoracek-Driksna D, Orth MW, Haut RC. The extent of matrix damage and chondrocyte death in mechanically traumatized articular cartilage explants depends on rate of loading. *J Orthop Res*. 2001;19(5):779–784. doi:10.1016/S0736-0266(01)00006-7.

112. Diestelmeier BW, Rudert MJ, Tochigi Y, Baer TE, Fredericks DC, Brown TD. An Instrumented Pendulum System for Measuring Energy Absorption During Fracture Insult to Large Animal Joints in Vivo. *J Biomech Eng*. 2014;136(6):064502. doi:10.1115/1.4025113.

113. Bonnevie ED, Delco ML, Fortier LA, Alexander PG, Tuan RS, Bonassar LJ. Characterization of Tissue Response to Impact Loads Delivered Using a Hand-Held Instrument for Studying Articular Cartilage Injury. *Cartilage*. 2015;6(4):226–232. doi:10.1177/1947603515595071.

114. Alexander PG, McCarron JA, Levine MJ, et al. An In Vivo Lapine Model for Impact-Induced Injury and Osteoarthritic Degeneration of Articular Cartilage. *Cartilage*. 2012;3(4):323–333. doi:10.1177/1947603512447301.

115. Rickey EJ, Cruz AM, Trout DR, McEwen BJ, Hurtig MB. Evaluation of experimental impact injury for inducing post-traumatic osteoarthritis in the metacarpophalangeal joints of horses. *American Journal of Veterinary Research*. 2012;73(10):1540–1552. doi:10.2460/ajvr.73.10.1540.

116. Brimmo OA, Pfeiffer F, Bozynski CC, et al. Development of a Novel Canine Model for Posttraumatic Osteoarthritis of the Knee. *J Knee Surg*. 2016;29(3):235–241. doi:10.1055/s-0035-1549026.

117. Bartell LR, Fortier LA, Bonassar LJ, Cohen I. Measuring microscale strain fields in articular cartilage during rapid impact reveals thresholds for chondrocyte death and a protective role for the superficial layer. *Journal of Biomechanics*. 2015;48(12):3440–3446. doi:10.1016/j.jbiomech.2015.05.035.

118. Christiansen BA, Guilak F, Lockwood KA, et al. Non-invasive mouse models of post-traumatic osteoarthritis. *Osteoarthritis and Cartilage*. 2015;23(10):1627–1638. doi:10.1016/j.joca.2015.05.009.

119. Chang S, Yasui T, Tanaka S, Saito T. Establishment of surgical destabilization model of mouse ankle osteoarthritis. *Osteoarthritis and Cartilage*. 2015;23, Supplement 2 IS - (S2):A291–A292. doi:10.1016/j.joca.2015.02.529.

120. Alexander PG, Song Y, Taboas JM, et al. Development of a Spring-Loaded Impact Device to Deliver Injurious Mechanical Impacts to the Articular Cartilage Surface. *Cartilage*. 2012;4(1):52–62. doi:10.1177/1947603512455195.

121. McIlwraith CW, Frisbie DD, Kawcak CE, Fuller CJ, Hurtig M, Cruz A. The OARSI histopathology initiative. *Osteoarthritis and Cartilage*. 2020;18(S3):S93–S105. doi:10.1016/j.joca.2010.05.031.

122. Little CB, Smith MM, Cake MA, Read RA, Murphy MJ, Barry FP. The OARSI histopathology initiative. *Osteoarthritis and Cartilage*. 2010;18(S3):S80–S92. doi:10.1016/j.joca.2010.04.016.

123. Cook JL, Kuroki K, Visco D, Pelletier JP, Schulz L, Lafeber FPJG. The OARSI histopathology initiative. *Osteoarthritis and Cartilage*. 2010;18(S3):S66–S79. doi:10.1016/j.joca.2010.04.017.

124. Boyce MK, Trumble TN, Carlson CS, Groschen DM, Merritt KA, Brown MP. Non-terminal animal model of post-traumatic osteoarthritis induced by acute joint injury. *Osteoarthritis and Cartilage*. 2013;21(5):746–755. doi:10.1016/j.joca.2013.02.653.

125. Hurtig M, Chubinskaya S, Dickey J, Rueger D. BMP-7 protects against progression of cartilage degeneration after impact injury. *J Orthop Res*. 2009;27(5):602–611. doi:10.1002/jor.20787.

126. Rorvik AM, Teige J. Unstable stifles without clinical or radiographic osteoarthritis in young goats: an experimental study. *Acta Vet Scand*. 1996;37(3):265–272.

127. Malda J, de Grauw JC, Benders KEM, et al. Of Mice, Men and Elephants: The Relation between Articular Cartilage Thickness and Body Mass. Orgel JPRO, ed. *PLoS ONE*. 2013;8(2):e57683. doi:10.1371/journal.pone.0057683.t002.

128. Frisbie DD, Cross MW, McIlwraith CW. A comparative study of articular cartilage thickness in the stifle of animal species used in human pre-clinical studies compared to articular cartilage thickness in the human knee. *Veterinary and Comparative Orthopaedics and Traumatology*. 2006;19(3):142–146.

129. Garcia-Seco E, Wilson DA, Cook JL, Kuroki K, Kreeger JM, Keegan KG. Measurement of Articular Cartilage Stiffness of the Femoropatellar, Tarsocrural, and Metatarsophalangeal Joints in Horses and Comparison with Biochemical Data. *Veterinary Surgery*. 2005;34(6):571–578. doi:10.1111/j.1532-950X.2005.00090.x.

130. McIlwraith CW, Frisbie DD, Kawcak CE. The horse as a model of naturally occurring osteoarthritis. *Bone and Joint Research*. 2012;1(11):297–309. doi:10.1302/2046-3758.111.

131. Fleck SKV, Dyson SJ. Lameness associated with tarsocrural joint pathology in 17 mature horses (1997-2010). *Equine Veterinary Education*. 2012;24(12):628–638. doi:10.1111/j.2042-3292.2012.00415.x.

132. Barker WHJ, SMITH MRW, Minshall GJ, Wright IM. Soft tissue injuries of the tarsocrural joint: A retrospective analysis of 30 cases evaluated arthroscopically. *Equine Veterinary Journal*. 2012;45(4):435–441. doi:10.1111/j.2042-3306.2012.00685.x.

133. Lamb L, Zubrod C, Hague B, Brakenhoff J, Major M. Clinical outcome of collateral ligament injuries of the tarsus. *Can Vet J*. 2012;53(5):518–524.

134. Latorre R, Arencibia A, Gil F, et al. Correlation of magnetic resonance images with anatomic features of the equine tarsus. *American Journal of Veterinary Research*. 2006;67(5):756–761. doi:10.2460/ajvr.67.5.756.

135. Raes EV, Bergman EHJ, van der Veen H, Vanderperren K, Van der Vekens E, Saunders JH. Comparison of cross-sectional anatomy and computed tomography of the tarsus in horses. *American Journal of Veterinary Research*. 2011;72(9):1209–1221. doi:10.2460/ajvr.72.9.1209.

136. Chu CR, Szczodry M, Bruno S. Animal models for cartilage regeneration and repair. *Tissue Eng Part B Rev*. 2010;16(1):105–115. doi:10.1089/ten.TEB.2009.0452.

137. Rutgers M, van Pelt MJP, Dhert WJA, Creemers LB, Saris DBF. ReviewEvaluation of histological scoring systems for tissue-engineered, repaired and osteoarthritic cartilage. *Osteoarthritis and Cartilage*. 2010;18(1):12–23. doi:10.1016/j.joca.2009.08.009.

138. Mankin HJ, Dorfman H, Lippiello L, Zarins A. Biochemical and metabolic abnormalities in articular cartilage from osteo-arthritic human hips. II. Correlation of morphology with biochemical and metabolic data. *J Bone Joint Surg Am*.

1971;53(3):523–537.

139. Pritzker K, Gy S, Jiminez S, et al. Osteoarthritis cartilage histopathology: grading and staging1, 2. *Osteoarthritis and Cartilage*. 2006;14(1):13–29. doi:10.1016/j.joca.2005.07.014.

140. Mainil-Varlet P, Aigner T, Brittberg M, et al. Histological assessment of cartilage repair: a report by the Histology Endpoint Committee of the International Cartilage Repair Society (ICRS). *J Bone Joint Surg Am*. 2003;85-A Suppl 2:45–57.

141. Dell'Isola A, Allan R, Smith SL, Marreiros SSP, Steultjens M. Identification of clinical phenotypes in knee osteoarthritis: a systematic review of the literature. *BMC Musculoskelet Disord*. 2016;17(1):425. doi:10.1186/s12891-016-1286-2.

142. Pinar H, Akseki D, Kovanlikaya I, Araç S, Bozkurt M. Bone bruises detected by magnetic resonance imaging following lateral ankle sprains. *Knee Surg Sports Traumatol Arthrosc*. 1997;5(2):113–117. doi:10.1007/s001670050036.

143. Labovitz JM, Schweitzer ME. Occult osseous injuries after ankle sprains: incidence, location, pattern, and age. *Foot Ankle Int*. 1998;19(10):661–667.

144. Welsch GH, Mamisch TC, Weber M, Horger W, Bohndorf K, Trattnig S. High-resolution morphological and biochemical imaging of articular cartilage of the ankle joint at 3.0 T using a new dedicated phased array coil: in vivo reproducibility study. *Skeletal Radiol*. 2008;37(6):519–526. doi:10.1007/s00256-008-0474-z.

145. Lee S, Yoon YC, Kim JH. T2 mapping of the articular cartilage in the ankle: Correlation to the status of anterior talofibular ligament. *Clinical Radiology*. 2021;68(7):e355–e361. doi:10.1016/j.crad.2013.01.023.

146. Guermazi A, Alizai H, Crema MD, Trattnig S, Regatte RR, Roemer FW. Compositional MRI techniques for evaluation of cartilage degeneration in osteoarthritis. *Osteoarthr Cartil*. 2015;23(10):1639–1653. doi:10.1016/j.joca.2015.05.026.

147. Pfau T, Robillard JJ, Weller R, Jespers K, Eliashar E, WILSON AM. Assessment of mild hindlimb lameness during over ground locomotion using linear discriminant analysis of inertial sensor data. *Equine Veterinary Journal*. 2007;39(5):407–413. doi:10.2746/042516407X185719.

148. Keegan KG, Wilson DA, Kramer J, et al. Comparison of a body-mounted inertial sensor system-based method with subjective evaluation for detection of lameness in horses. *American Journal of Veterinary Research*. 2013;74(1):17–24. doi:10.2460/ajvr.74.1.17.

149. Keegan KG, Kramer J, Yonezawa Y, et al. Assessment of repeatability of a wireless, inertial sensor-based lameness evaluation system for horses. *American Journal of Veterinary Research*. 2011;72(9):1156–1163. doi:10.2460/ajvr.72.9.1156.

150. McCracken MJ, Kramer J, Keegan KG, et al. Comparison of an inertial sensor system of

lameness quantification with subjective lameness evaluation. *Equine Veterinary Journal*. 2012;44(6):652–656. doi:10.1111/j.2042-3306.2012.00571.x.

151. Zumwalt AC, Hamrick M, Schmitt D. Force plate for measuring the ground reaction forces in small animal locomotion. *Journal of Biomechanics*. 2006;39(15):2877–2881. doi:10.1016/j.jbiomech.2005.10.006.

152. McLaughlin RM. Kinetic and kinematic gait analysis in dogs. *Vet Clin North Am Small Anim Pract*. 2001;31(1):193–201. doi:10.1016/S0195-5616(01)50045-5.

153. Gillette RL, Angle TC. Recent developments in canine locomotor analysis: a review. *The Veterinary Journal*. 2008;178(2):165–176. doi:10.1016/j.tvjl.2008.01.009.

154. Keegan KG. Evidence-based lameness detection and quantification. *Vet Clin North Am Equine Pract*. 2007;23(2):403–423. doi:10.1016/j.cveq.2007.04.008.

155. Piel MJ, Kroin JS, van Wijnen AJ, Kc R, Im H-J. Pain assessment in animal models of osteoarthritis. *Gene*. 2014;537(2):184–188. doi:10.1016/j.gene.2013.11.091.

156. Blaker CL, Clarke EC, Little CB. Using mouse models to investigate the pathophysiology, treatment, and prevention of post-traumatic osteoarthritis. *J Orthop Res*. June 2016. doi:10.1002/jor.23343.

157. Neogi T, Guermazi A, Roemer F, et al. Association of Joint Inflammation With Pain Sensitization in Knee Osteoarthritis: The Multicenter Osteoarthritis Study. *Arthritis & Rheumatology*. 2016;68(3):654–661. doi:10.1002/art.39488.

158. Lee AS, Ellman MB, Yan D, et al. A current review of molecular mechanisms regarding osteoarthritis and pain. *Gene*. 2013;527(2):440–447. doi:10.1016/j.gene.2013.05.069.

CHAPTER 3

A PRECLINICAL MODEL TO STUDY ACUTE IMPACT-INDUCED CARTILAGE INJURY AND THE DEVELOPMENT OF EARLY POSTTRAUMATIC ANKLE OSTEOARTHRITIS

Michelle L. Delco[1], Edward D. Bonnevie[2], Lauren DeGenero[1], Peter G. Alexander[3], Rocky S. Tuan[3], Lawrence J. Bonassar[2,4], Lisa A. Fortier[1]

[1]Department of Clinical Sciences, College of Veterinary Medicine, Cornell University, Ithaca, NY

[2]Sibley School of Mechanical and Aerospace Engineering, Cornell University, Ithaca, NY

[3]Department of Orthopaedic Surgery, University of Pittsburgh, Pittsburgh, PA

[4]Meining School of Biomedical Engineering, Cornell University, Ithaca, NY

Abstract

Mechanical injury to articular cartilage causes chondrocyte death and cartilage degeneration in *ex vivo* experimental models. Clinically, ankle (talocrural) joint trauma is known to lead to the development of posttraumatic osteoarthritis (PTOA) in patients. The objective of this study was to develop a single, rapid impact, non-fracture model of talocrural PTOA.

For *ex vivo* model development and validation, osteochondral blocks of the medial trochlea of the equine talus were harvested and the articular surface was impacted over a broad range of stress magnitudes using a custom-built spring loaded impacting device. The mechanical relationship between peak stress and force was determined. Histology and multiphoton microscopy were performed to define the extent of acute cartilage damage. For the *in vivo* cartilage impact model, two cadaveric equine talocrural joints were used to develop the surgical approach. Then, two healthy adult horses were anesthetized and three impacts of varying magnitudes were applied to the left and right talus (n = 4 joints) under arthroscopic guidance. Postoperatively, joint fluid was obtained weekly and analyzed for evidence of inflammation and early degenerative change. Horses were sacrificed at 6 or 12 weeks post operatively and histopathology was performed on each individual impact. One normal horse (2 joints) served as non-operated controls.

Ex vivo impact stress correlated well with force to the 1/3 power as predicted by Hertzian contact mechanics. Joint fluid and histology results were consistent with the development of early PTOA in all injured joints. The severity of focal osteochondral injury correlated to the magnitude of impact delivered ($r^2 = 0.80$, $p = 0.016$).

These studies establish mechanical thresholds for tissue damage and connect mechanical inputs to *in vivo* development of early PTOA-like lesions. Development of an equine talocrural

cartilage impact model, which creates cartilage injury similar to that expected to initiate PTOA in the human ankle, will allow investigation of very early events in PTOA at the cellular and microstructural level *ex vivo* and *in vivo*. This model will also allow preclinical testing of preventative strategies (e.g. exercise modification) and potential disease modifying therapies to minimize progression of PTOA.

Introduction

Osteoarthritis (OA) that develops secondary to a wide variety of joint injury is often grouped into the sub-type of post-traumatic osteoarthritis (PTOA). Common precipitating injuries include high-speed impact trauma to the articular surface, intraarticular fractures, and joint-destabilizing soft-tissue tears. Although the end-stage pathophysiology of PTOA may be similar, there is strong evidence to suggest that the early biological and mechanical events that initiate and perpetuate disease are distinct between different joints, injury types, and patient populations, as discussed in Chapter 2. The ankle is the most commonly injured joint, and up to 90% of ankle OA occurs secondary to joint trauma.[1-5] This is in stark contrast to knee and hip OA, where just 2-10% is attributed to a previous injury.[1,2,6]

The most common injury precipitating end-stage ankle OA is a severe ankle sprain,[7] when rapid ankle inversion causes the distal tibia to impact the medial aspect of the talar dome, often resulting in an osteochondral lesion.[8,9] Ligamentous injuries commonly accompany severe ankle sprains and may result in joint instability, however evidence suggests that the magnitude of the initial cartilage trauma is the most important factor in development of ankle PTOA.

Most PTOA models utilize smaller animal species, and involve creating an osteochondral fragment, intraarticular fracture, or joint destabilization in the knee (stifle) joint. As discussed in Chapter 2, these are useful models, however there are currently no animal models that simulate PTOA of the ankle joint arising from traumatic overloading of the articular surface of the talus, as would be expected during a severe sprain. Therefore, our goal was to develop a large animal ankle model of impact-induced PTOA. Specifically, our objective was to use a minimally invasive surgical approach to deliver a tunable injury to the articular surface of the equine talus,

which progresses to a cartilage lesion of predictable severity and depth, in order to simulate early OA lesions seen in humans.[10]

Specific aims of the *ex vivo* validation portion of the study were to: 1) determine how measurable mechanical inputs relate to the magnitude of acute cartilage injury in this model system, and 2) establish force-stress relationship in order to predict stresses from load cell data obtained during *in vivo* impact. The aims of the *in vivo* portion of the study were to: 1) develop a minimally invasive approach to apply a defined mechanical injury to the equine talus using a hand-held spring-loaded impacting device, and 2) study early disease development in vivo at 6 and 12 weeks post-operatively.

Methods

Ex vivo validation studies

Impactor modification. A spring-loaded impacting device, originally described by Alexander, et al.,[11] and recently modified by Bonnevie, et al.,[12] was further adapted to allow *ex vivo* impact of osteochondral (OC) preparations of the equine talus (**Figure 3.1**). An adjustable vice grip, capable of rotation on 3 axes, was installed below the impactor armature (**Figure S3.1a**). One of 2 hemispherical impacting tips, differing in diameter and radius of curvature, were mounted on the end of the spring-driven missile contained within the device. A load cell (PCBPiezotronics, Depew, NY) mounted in-line between the missile and the impacting tip was used to measure impact force. A linear variable displacement transducer (LVDT; RDP Electronics, Pottstown, PA) was attached to the impacting tip to measure displacement (**Figure 3.1**.)

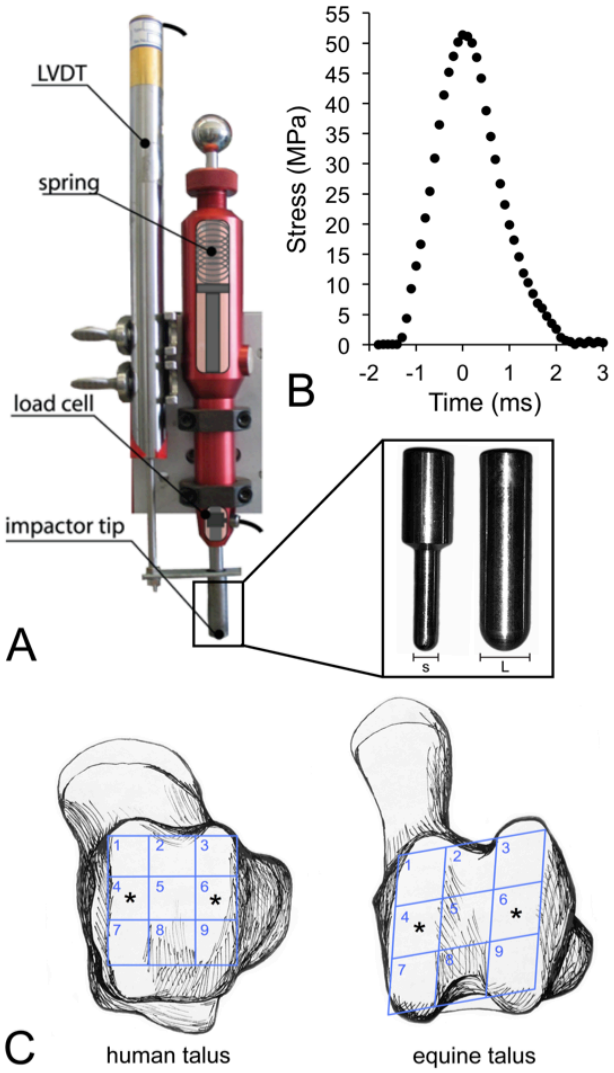

Figure 3.1. *Ex vivo* model development. A) The spring-loaded impacting device was instrumented with an internal load cell to measure force and a linear variable displacement transducer (LVDT) to measure displacement. One of 2 impact tips (s and L; inset). *Modified from Bonnevie, et al., 2015. Reused with permission from SAGE Publications.* B) The impact voltage signal from the load cell was converted to stress, using the contact area of each impact measured on pressure sensitive paper. C) Multiple impacts were applied to each equine talus in areas (*; zones 4 and 6) corresponding to the highest incidence of osteochondral lesions in humans.

Tissue collection and handling. OC blocks comprising the medial and lateral trochlea of the right and left talus were harvested from 6 normal adult horses (ages 2-11 years) immediately following euthanasia, and incubated in phenol red-free MEM supplemented with HEPES (25 mM), penicillin (100 IU/ml), and streptomycin (100 μg/ml). OC blocks were mounted in the adjustable vice grip, and positioned with the articular surface perpendicular to the direction of impact (**Figure S3.1a**). While mounted, samples were kept moist by continuous lavage with phosphate buffered saline (PBS).

Impact and mechanical analysis. The articular surface of the talus was impacted in regions corresponding to the highest incidence of naturally occurring OC lesions in humans,[8] as previously described.[11,12] The purpose of this portion of the study was to determine the relationship between force and stress, to obviate the technical challenges of measuring impact surface area during *in vivo* experiments. Briefly, a total of 180 impacts (6-10 impacts per OC block, spaced approximately 0.5 cm apart) of varying magnitudes were applied to the mid-medial and lateral trochlea of the talus using one of 2 curved impacting tips (**Figure 3.1**). Load cell and LVDT output (voltage) were acquired simultaneously at 50kHz with a custom LabVIEW program (NI, Austin TX). Cartilage thickness (t) was measured by modified needle probe technique[13] on a mechanical testing frame (EnduraTEC ELF3200, EnduraTec, Minnetonka, MN) and validated by manually by cutting and photographing OC blocks in cross-section adjacent to impacts, then measuring thickness on digital images using ImageJ software (Mac OS X version 10.2, Wayen Rasband, U.S. National Institutes of Health, Bethesda, MD, USA; **Figure S3.1c**). LVDT output was converted to displacement (d), then strain was calculated as (d)/(cartilage thickness). Load cell data (voltage) was converted to force (F), then average

peak stress was calculated as (max F)/(contact area of indenter) recorded by pressure sensitive film (FujiFilm Prescale, Tokyo, Japan) and measured using ImageJ (**Figure S3.1b**).

Multiphoton imaging and histology. Impacted OC blocks were incubated in media for approximately 2 hours, then full-thickness cartilage sections containing the impact or control site were cut off the bone and placed in 1 μM sodium fluorescein (AK-FLOUR 25%, Akorn, Inc., Lake Forest, IL) in PBS for 15 minutes to stain dead cells. Samples were then imaged on a multiphoton microscope using a Ti:sapphire laser at 780 nm excitation, as previously described.[14] Images were acquired at the articular surface in the transverse plane (i.e. parallel to the articular surface). Dead cells were quantified using a custom ImageJ macro and extracellular matrix (ECM) microcracks were assessed qualitatively (**Figure S3.1d**). Impacted and control cartilage samples were fixed in 4% paraformaldehyde, then sectioned and stained with hematoxylin and eosin (H&E) and safranin O/fast green to assess structural damage, acute cellular necrosis and proteoglycan content. The purpose of this portion of the study was to determine the range of impact magnitudes to be tested *in vivo*; the goal was to create partial-thickness cartilage pathology, involving approximately 50-75% of the cartilage depth, with cell death and fissures extending into the deep zone, but not involving the calcified cartilage layer.

In vivo model development

Animal subjects. To determine the relationship between impact magnitude and cartilage degradation *in vivo*, two healthy, young adult (3 year old) female horses (n = 4 joints) were operated. Prior to surgery, all TC joints were deemed free of pre-existing OA by 2 board certified equine surgeons on the basis of normal physical examination, gait evaluation, and synovial fluid

analysis. Two joints (1 horse) served as un-operated controls. All animal experiments were approved by Cornell University's Institutional Animal Care and Use Committee.

Surgical technique. The arthroscope was inserted and the joint was inspected for pre-existing pathology. An instrument portal was created half way between the arthroscope portal and the lateral malleolus. The impactor tip was inserted into the joint and positioned perpendicular to the articular surface of the axial aspect of the medial trochlea of the talus. The impactor was held in contact with the articular surface, and the impactor trigger was depressed (**Figure S3.2**). The joint was then flexed several degrees, the spring tension was adjusted to set the impact magnitude, and the impactor spring was compressed. A second impact was delivered ~5 mm distal to the first. This was repeated a third time, so that a total of 3 impact were created along the mid-distal medial trochlea of the talus (**Figure 3.2**) load cell data were recorded and analyzed, as described above.

Postoperative monitoring and synovial fluid analysis. Postoperatively, horses were examined daily for clinical evidence of pain (lameness). Joint effusion was scored on a 4-point scale (**Table S3.1**). Synovial fluid was obtained weekly, starting 1 week postoperatively for 4 weeks, then at 6, 8, and 12 weeks postoperatively. Synovial fluid cytology was evaluated by a board certified veterinary clinical pathologist, and total protein, nucleated cell count, and differential cell counts were measured. Synovial fluid characteristics (viscosity, color, turbidity) reported by the clinical pathologist were combined into a single joint inflammation score (**Table S3.1**). Additional aliquots of synovial fluid were stored at -80°C until further analysis, when synovial fluid biomarkers of early OA (PGE2 and TNFα) were measured on ELISA.[15-17] Cytokine concentration was quantified using commercial ELISA kits (PGE2 ELISA kit, Enzo Life Sciences catalog # ADI-900-001 and Equine TNF alpha ELISA Kit, Thermo Scientific

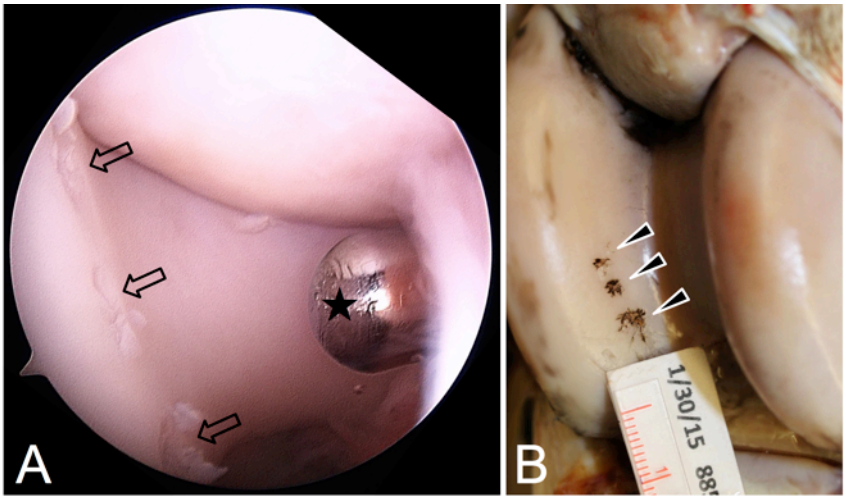

Figure 3.2. Hand-held impactor creates cartilage lesions *in vivo*. A) Intraoperative arthroscopic view of 3 impacts (arrows) of varying magnitude created on the medial trochlea of the left talus in horse 1. The impacting tip (star) is positioned through a standard arthroscopic portal within the joint. B) Post mortem dissection of the same joint; india ink has been applied to the articular surface to mark impact sites (arrow heads).

ESS0017). The assays were completed using undiluted synovial fluid according to manufacturers' directions, and the 96-well plate was read on a spectrophotometric microplate reader (Tecan Safire; Männedorf, Switzerland).

Tissue collection, gross pathology and histopathology

Horses were sacrificed 6 or 12 weeks postoperatively to examine acute stages of PTOA.[17,18] India ink was applied to the articular surface of the medial talus to identify areas of cartilage cracking and fibrillation. Suspect areas of impact (well-circumscribed, circular areas of intense India ink uptake on the axial aspect of the mid-distal aspect of the medial trochlea of the talus) were identified, and this information was cross-referenced with arthroscopic videos obtained during surgery to confirm the location of individual impact sites (**Figure 3.2**). OC blocks containing each of the three impact sites, the opposing articular surface (distal intermediate ridge of the tibia; DIRT) and the un-injured lateral trochlear ridge of the talus (LTR) were harvested, fixed in 4% paraformaldehyde, and decalcified using 20% sodium citrate and 44% formic acid. OC sections were stained with H&E and Safranin O/Fast green. Histology was scored by two independent observers (MLD, LD) blinded to treatment (i.e. injury status and magnitude), based on a 24-point modified OARSI scoring system (**Table S3.2**) and using the 6-point OARSI grading system.[19] Synovial membrane was harvested, processed and stained with H&E and consensus scored (**Table S3.3**) by one experienced observer (MLD) and a board-certified clinical pathologist (ADM) blinded to treatment.

Statistical analysis

The relationship between impact force and impact stress was determined based on Hertz's contact theory,[20] where stress is related to force$^{1/3}$. Linear regression was conducted between these 2 variables. The relationship between OARSI score at 12 weeks post-impact and peak impact stress was determined using linear regression.

Results

Ex vivo

Based on Hertzian contact mechanics, the relationship between impact stress and impact force was determined. As expected, impact stresses for cartilage under impact from a spherical tip correlated well with impact force$^{1/3}$ as predicted by Hertzian contact mechanics[20,21] (**Figure 3.3**). For both the small and large radius impacting tips, the correlations provided $R^2 = 0.71$ and $R^2 = 0.50$, respectively. The increased slope between the small and large radius tips is an effect of contact area, where smaller contact areas provide larger stresses at the same force level.

In vivo

Clinical observations and synovial fluid analysis. No major complications were experienced intra- or post-operatively. Mild to moderate synovial effusion was present in all impacted joints and decreased gradually throughout the study period, with no observable lameness at any time point. Based on synovial fluid analysis and clinical observation, joint inflammation resolved within 2 weeks of impact, but joint inflammation scores did not return to baseline in any experimental joint (**Figure 3.4**), indicating low-grade pathology

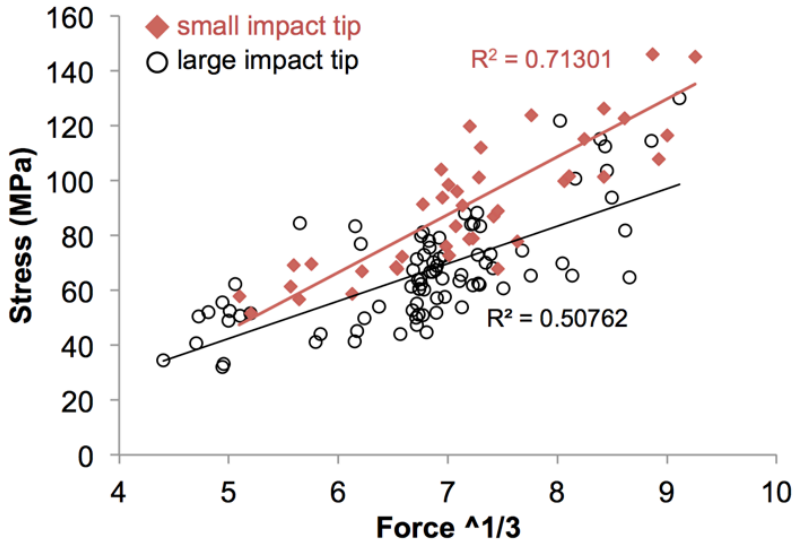

Figure 3.3. Relationship between impact force and stress for the equine talus.

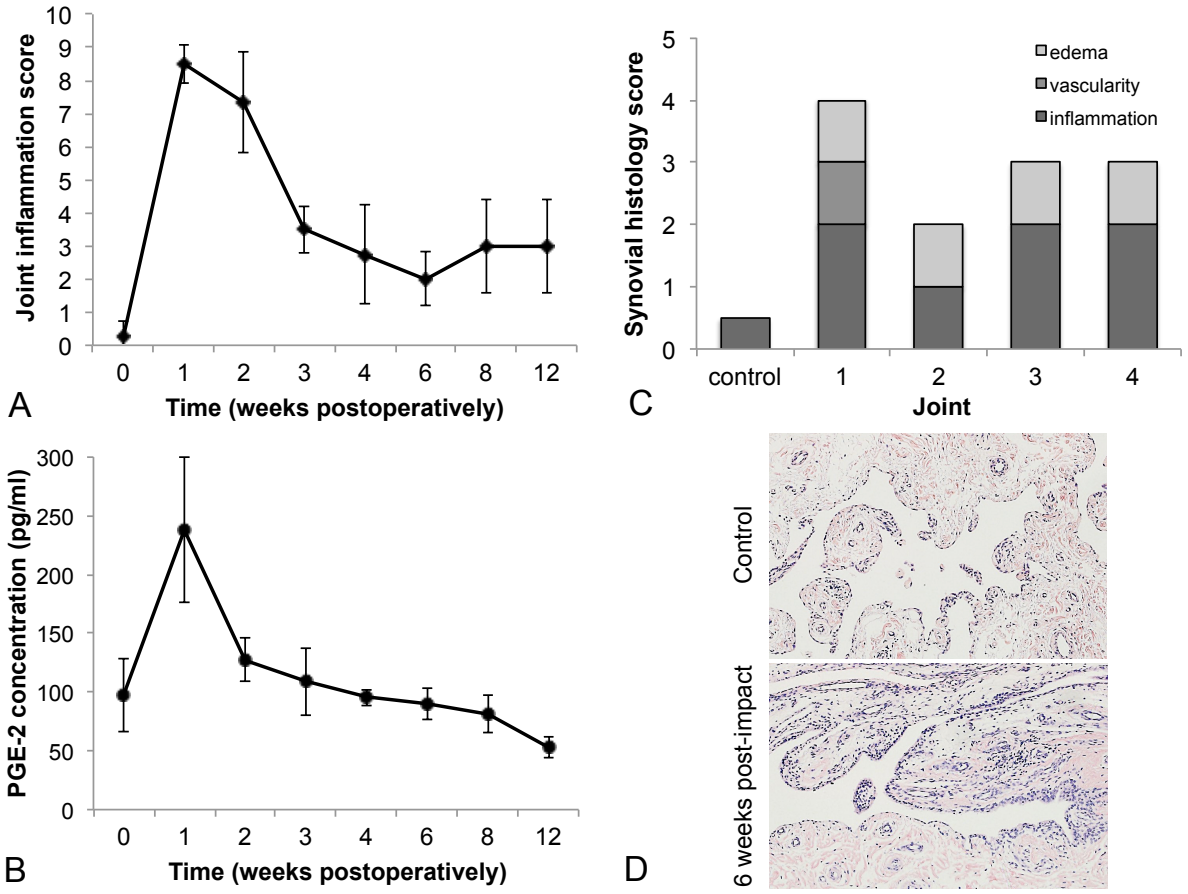

Figure 3.4. Cartilage impact causes joint inflammation. A) Joint inflammation score, a combined measure of synovial fluid changes and clinical joint effusion remains elevated throughout the 12-week study. B) PGE-2 concentrations were increased one week following impact, and returned to baseline levels within 4 weeks. Error bars = ±s.d. C) Synovial histopathology was scored for inflammation, vascularity and subintimal edema, and revealed mild to moderate synovitis at 6 weeks (joints 3 and 4) and 12 weeks (joints 1 and 2) post-impact. Control data represent the average of 2 joints. D) Representative 20x images of synovial sections stained with hematoxylin and eosin from control and injured joints.

throughout the course of the study. PGE-2 increased an average of 2.5 fold (range 1.5-4x) 1 week postoperatively, and returned to baseline by 4 weeks in 3 of the 4 joints (**Figure 3.4**).

Synovial membrane histopathology. Histopathologic examination of the synovial membrane from injured joints indicated mild to moderate inflammation, with or without subintimal edema and/or increased vascularity (**Figure 3.4**). None of the synovium sections showed evidence of subintimal fibrosis or intimal hyperplasia. These changes indicate mild to moderate synovitis at 6 and 12 weeks post-injury, in agreement with synovial fluid analysis results.

Gross and histopathologic osteochondral lesions. At necropsy, all impact sites were grossly identified with the application of India ink. Typically, impacts were easily distinguishable as a cluster of radiating cracks, and in all cases correlated well to images obtained at arthroscopy (**Figure 3.2**). All OC sections from areas of impact showed histopathological evidence of early OA-type lesions (**Figure 3.5**). Changes ranged from mild to severe erosions, cracking/fissuring, hypocellularity, chondrocyte necrosis and clonal expansion of chondrocytes with an average modified OARSI score of 14.8 (s.d. 4.0) out of 24 and a mean OARSI Grade[19] of 3.5 (s.d. 1.1) out of 6 (**Figure 3.5**). At 3 months following injury, OARSI grade for individual impacts correlated with impact magnitude ($r = 0.8953$, $p = 0.016$; **Figure 3.5**).

Discussion

The goal of this work was to develop an *in vivo* large animal model of impact-induced osteochondral injury to study early ankle PTOA. At 6 and 12 weeks after injury, impact sites show histopathologic evidence of moderate to severe OA lesions, and the severity of damage

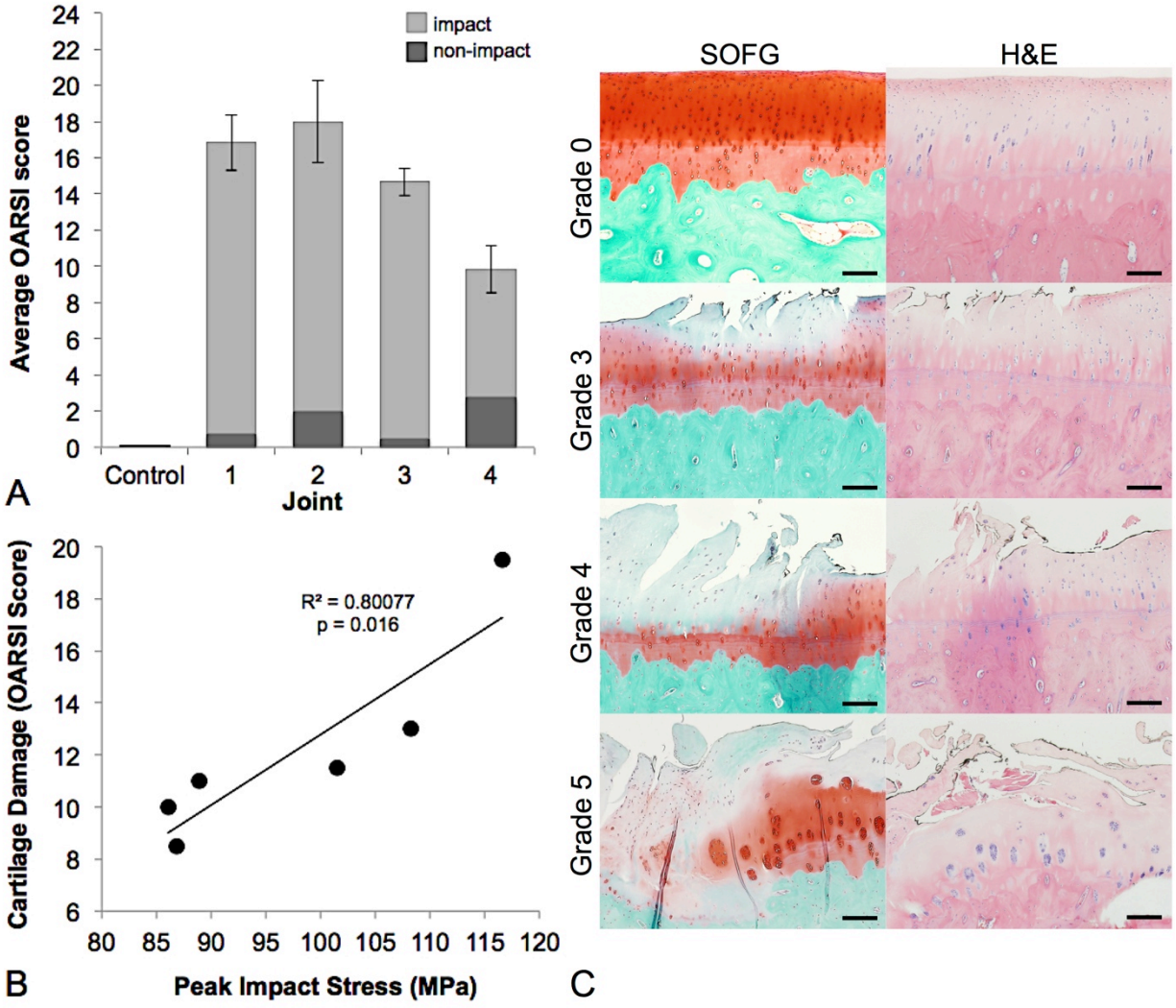

Figure 3.5. Impact causes early OA-like osteochondral lesions and cartilage damage is correlated with impact stress. A) Average OARSI score by experimental joint (1-4) revealed moderate to severe OA at the impact sites (grey) and mild changes in the two non-impacted areas within the experimental joints (black). Error bars = ±s.d. B) OARSI score at 12 weeks correlated with peak impact stress. C) Representative 10x images of osteochondral sections stained with safranin O/fast green (SOFG) and hematoxylin and eosin (H&E) of OARSI grades 0, 3, 4 and 5. Note the persistence of India ink (black) applied at necropsy, marking impacts. Bars = 150µm.

was correlated with impact magnitude. The range of impact magnitudes tested *in vivo* were carefully selected based on extensive *ex vivo* model development, allowing the number of animals used for the *in vivo* portion of the study to be minimized. The impact-induced histopathologic lesions are similar to those observed in clinical cases of posttraumatic osteoarthritis, with lesions ranging in severity from OARSI grade 3-5. In addition to producing focal osteochondral lesions typical of early OA, cartilage injury alone was sufficient to cause joint-wide pathology, evidenced by persistent joint inflammation scores throughout the study period, and synovitis on histopathology. This is a unique feature of our model, in that a minimally invasive surgical approach allowed us to apply articular trauma without damaging supporting ligamentous structures and other surrounding soft tissues.

The horse was selected as the model species of choice for several reasons. First, the horse is the largest available model species with an average weight of 400-500 kg, which provides stringent loading conditions within the joint. Similar to the human ankle, the equine TC joint has a higher GAG content and is stiffer than that of the knee.[22] Equine cartilage is similar in thickness to humans which allows creation of partial-thickness lesions, which is difficult to achieve in similar models using small animal species.[23] In a recent review of preclinical cartilage defect models, the horse was the only species to be placed in group 3 with humans in cluster analysis, indicating that the horse is the only animal model in which defect dimensions relevant to human clinical practice can be produced.[24] Furthermore, the large size of the equine talocrural joint allows the arthroscope and impactor to be positioned within the joint. Arthroscopic visualization ensures appropriate anatomic placement of the impactor tip perpendicular to the articular surface during cartilage injury.

The opportunity for second-look arthroscopy is an important feature of this model. As discussed in Chapter 2, clinical evidence in human patients with ankle injuries suggests that arthroscopic examination of the ankle joint is particularly important in identifying early evidence of PTOA. After severe ankle sprain, early chondral lesions that are difficult or impossible to diagnose on MRI, are often identified on arthroscopy.[25-28]

Limitations of this study include the small number of animals used for the *in vivo* portion of the study and that non-operated controls were used instead of sham-operated controls. Despite low animal numbers, when impacts were analyzed individually, peak impact stress correlated well with the severity of cartilage lesions at 12 weeks. This indicates that the severity of cartilage injury in this model system can be tuned by adjusting both impactor spring tension as well as impact tip geometry. While the scope of this study did not include advanced imaging, MRI is a well validated diagnostic modality to assess the equine TC joint, and future studies will employ MRI for non-invasive longitudinal evaluations of cartilage and subchondral bone changes.[29-32]

Development of an equine talocrural cartilage impact model, which creates cartilage injury similar to that expected to cause PTOA in the human ankle, will allow investigation of the very early events in PTOA pathogenesis at the macroscopic and cellular/microstructural level, as well as longitudinal studies of disease progression. This model will allow preclinical testing of preventative strategies such as exercise modification, targeted drug therapies, regenerative medicine modalities, etc. in a clinically relevant large animal species.

Acknowledgements

The authors thank Shannon Walsh and Meg Goodale for technical and logistical support. We acknowledge and thank Dr. Andrew Miller for his help scoring synovial histopathology. This work was supported by The Harry M. Zweig Memorial Fund for Equine Research and Weill Cornell Medical College Clinical & Translational Science Center Award/National Center for Advancing Translational Sciences (5 UL1 TR000457-09). MD was supported by NIH 5T32OD011000-20.

References

1. Brown TDT, Johnston RCR, Saltzman CLC, Marsh JLJ, Buckwalter JAJ. Posttraumatic osteoarthritis: a first estimate of incidence, prevalence, and burden of disease. *J Orthop Trauma*. 2006;20(10):739–744. doi:10.1097/01.bot.0000246468.80635.ef.

2. Weatherall JM, Mroczek K, McLaurin T, Ding B, Tejwani N. Post-traumatic ankle arthritis. *Bull Hosp Jt Dis (2013)*. 2013;71(1):104–112.

3. Valderrabano V, Horisberger M, Russell I, Dougall H, Hintermann B. Etiology of Ankle Osteoarthritis. *Clin Orthop Relat Res*. 2008;467(7):1800–1806. doi:10.1007/s11999-008-0543-6.

4. Nelson AJ, Collins CL, Yard EE, Fields SK, Comstock RD. Ankle injuries among United States high school sports athletes, 2005-2006. *J Athl Train*. 2007;42(3):381–387.

5. Belmont PJJ, Goodman GP, Waterman B, DeZee K, Burks R, Owens BD. Disease and nonbattle injuries sustained by a U.S. Army Brigade Combat Team during Operation Iraqi Freedom. *Mil Med*. 2010;175(7):469–476.

6. Wilson MG, Michet CJJ, Ilstrup DM, Melton LJ3. Idiopathic symptomatic osteoarthritis of the hip and knee: a population-based incidence study. *Mayo Clin Proc*. 1990;65(9):1214–1221.

7. Gribble PA, Bleakley CM, Caulfield BM, et al. Evidence review for the 2016 International Ankle Consortium consensus statement on the prevalence, impact and long-term consequences of lateral ankle sprains. *Br J Sports Med*. June 2016. doi:10.1136/bjsports-2016-096189.

8. Raikin SM, Elias I, Zoga AC, Morrison WB, Besser MP, Schweitzer ME. Osteochondral Lesions of the Talus: Localization and Morphologic Data from 424 Patients Using a Novel Anatomical Grid Scheme. *Foot Ankle Int*. 2007;28(2):154–161. doi:10.3113/FAI.2007.0154.

9. Klammer G, Maquieira GJ, Spahn S, Vigfusson V, Zanetti M, Espinosa N. Natural history of nonoperatively treated osteochondral lesions of the talus. *Foot & ankle international / American Orthopaedic Foot and Ankle Society [and] Swiss Foot and Ankle Society*. 2015;36(1):24–31. doi:10.1177/1071100714552480.

10. Glasson SS, Chambers MG, van den Berg WB, Little CB. The OARSI histopathology initiative. *Osteoarthr Cartil*. 2010;18(S3):S17–S23. doi:10.1016/j.joca.2010.05.025.

11. Alexander PG, Song Y, Taboas JM, et al. Development of a Spring-Loaded Impact Device to Deliver Injurious Mechanical Impacts to the Articular Cartilage Surface. *Cartilage*. 2012;4(1):52–62. doi:10.1177/1947603512455195.

12. Bonnevie ED, Delco ML, Fortier LA, Alexander PG, Tuan RS, Bonassar LJ.

Characterization of Tissue Response to Impact Loads Delivered Using a Hand-Held Instrument for Studying Articular Cartilage Injury. *Cartilage*. 2015;6(4):226–232. doi:10.1177/1947603515595071.

13. Jurvelin JS, Räsänen T, Kolmonen P, Lyyra T. Comparison of optical, needle probe and ultrasonic techniques for the measurement of articular cartilage thickness. *Journal of Biomechanics*. 1995;28(2):231–235. doi:10.1016/0021-9290(94)00060-H.

14. Novakofski KD, Williams RM, Fortier LA, Mohammed HO, Zipfel WR, Bonassar LJ. cation of cartilage injury using quantitative multiphoton microscopy. *Osteoarthr Cartil*. 2014;22(2):355–362. doi:10.1016/j.joca.2013.10.008.

15. Glaser KE, Sun Q, Wells MT, Nixon AJ. Development of a novel equine whole transcript oligonucleotide GeneChip microarray and its use in gene expression profiling of normal articular-epiphyseal cartilage. *Equine Veterinary Journal*. 2009;41(7):663–670. doi:10.2746/042516409X412381.

16. Kamm JL, Nixon AJ, Witte TH. Cytokine and catabolic enzyme expression in synovium, synovial fluid and articular cartilage of naturally osteoarthritic equine carpi. *Equine Veterinary Journal*. 2010;42(8):693–699. doi:10.1111/j.2042-3306.2010.00140.x.

17. Frisbie DD, Al-Sobayil F, Billinghurst RC, Kawcak CE, McIlwraith CW. Changes in synovial fluid and serum biomarkers with exercise and early osteoarthritis in horses. *Osteoarthritis and Cartilage*. 2008;16(10):1196–1204. doi:10.1016/j.joca.2008.03.008.

18. Ross KA, Williams RM, Schnabel LV, et al. Comparison of Three Methods to Quantify Repair Cartilage Collagen Orientation. *Cartilage*. 2013;4(2):111–120. doi:10.1177/1947603512461440.

19. Pritzker K, Gay S, Jiminez S, et al. Osteoarthritis cartilage histopathology: grading and staging1, 2. *Osteoarthritis and Cartilage*. 2006;14(1):13–29. doi:10.1016/j.joca.2005.07.014.

20. Johnson KL. Contact Mechanics. 1985. Cambridge University Press, UK.

21. Bonnevie ED, Baro VJ, Wang L, Burris DL. Journal of Biomechanics. *Journal of Biomechanics*. 2012;45(6):1036–1041. doi:10.1016/j.jbiomech.2011.12.019.

22. Garcia-Seco E, Wilson DA, Cook JL, Kuroki K, Kreeger JM, Keegan KG. Measurement of Articular Cartilage Stiffness of the Femoropatellar, Tarsocrural, and Metatarsophalangeal Joints in Horses and Comparison with Biochemical Data. *Veterinary Surgery*. 2005;34(6):571–578. doi:10.1111/j.1532-950X.2005.00090.x.

23. Alexander PG, McCarron JA, Levine MJ, et al. An In Vivo Lapine Model for Impact-Induced Injury and Osteoarthritic Degeneration of Articular Cartilage. *Cartilage*. 2012;3(4):323–333. doi:10.1177/1947603512447301.

24. Ahern BJ, Parvizi J, Boston R, Schaer TP. Preclinical animal models in single site

cartilage defect testing: a systematic review. *Osteoarthritis and Cartilage*. 2009;17(6):705–713. doi:10.1016/j.joca.2008.11.008.

25. Sugimoto K, Takakura Y, Okahashi K, Samoto N, Kawate K, Iwai M. Chondral injuries of the ankle with recurrent lateral instability: an arthroscopic study. *J Bone Joint Surg Am*. 2009;91(1):99–106. doi:10.2106/JBJS.G.00087.

26. Gatlin CC, Matheny LM, HO CP, Johnson NS, Clanton TO. Diagnostic accuracy of 3.0 Tesla magnetic resonance imaging for the detection of articular cartilage lesions of the talus. *Foot & ankle international / American Orthopaedic Foot and Ankle Society [and] Swiss Foot and Ankle Society*. 2015;36(3):288–292. doi:10.1177/1071100714553469.

27. Golditz T, Steib S, Pfeifer K, et al. Functional ankle instability as a risk factor for osteoarthritis: using T2-mapping to analyze early cartilage degeneration in the ankle joint of young athletes. *Osteoarthr Cartil*. 2014;22(10):1377–1385. doi:10.1016/j.joca.2014.04.029.

28. O'Loughlin PF, Heyworth BE, Kennedy JG. Current Concepts in the Diagnosis and Treatment of Osteochondral Lesions of the Ankle. *The American Journal of Sports Medicine*. 2010;38(2):392–404. doi:10.1177/0363546509336336.

29. Matzat SJ, van Tiel J, Gold GE, Oei EHG. Quantitative MRI techniques of cartilage composition. *Quant Imaging Med Surg*. 2013;3(3):162–174. doi:10.3978/j.issn.2223-4292.2013.06.04.

30. Koff MF, Shah P, Pownder S, et al. Correlation of meniscal T2* with multiphoton microscopy, and change of articular cartilage T2 in an ovine model of meniscal repair. *Osteoarthritis and Cartilage*. 2013;21(8):1083–1091. doi:10.1016/j.joca.2013.04.020.

31. Latorre R, Arencibia A, Gil F, et al. Correlation of magnetic resonance images with anatomic features of the equine tarsus. *American Journal of Veterinary Research*. 2006;67(5):756–761. doi:10.2460/ajvr.67.5.756.

32. Raes EV, Bergman EHJ, van der Veen H, Vanderperren K, Van der Vekens E, Saunders JH. Comparison of cross-sectional anatomy and computed tomography of the tarsus in horses. *American Journal of Veterinary Research*. 2011;72(9):1209–1221. doi:10.2460/ajvr.72.9.1209.

Supplement 3.1 - *Detailed Methods*

Development of the in vivo surgical approach

Three adult horses, euthanized for reasons other than this study were used to develop the *in vivo* surgical technique. Briefly, two intact left talocrural joints were harvested by transverse cuts through the distal tibia and proximal metatarsus. Large gauge Steinmann pins were driven down the shafts of the long bones to pin one joint in maximum flexion and the other in maximum extension. Skin and soft tissues were removed and margins of maximum articulation of the tibia were marked on the talar joint surface. The pins were removed and the joints were disarticulated. Digital images were obtained and used to lay out the 9-zone grid system, as described for the human talus by Raikin, et al. (**Figure 3.1c**) Two cadaveric limbs were used to develop the arthroscopic approach described in *Surgical technique.*

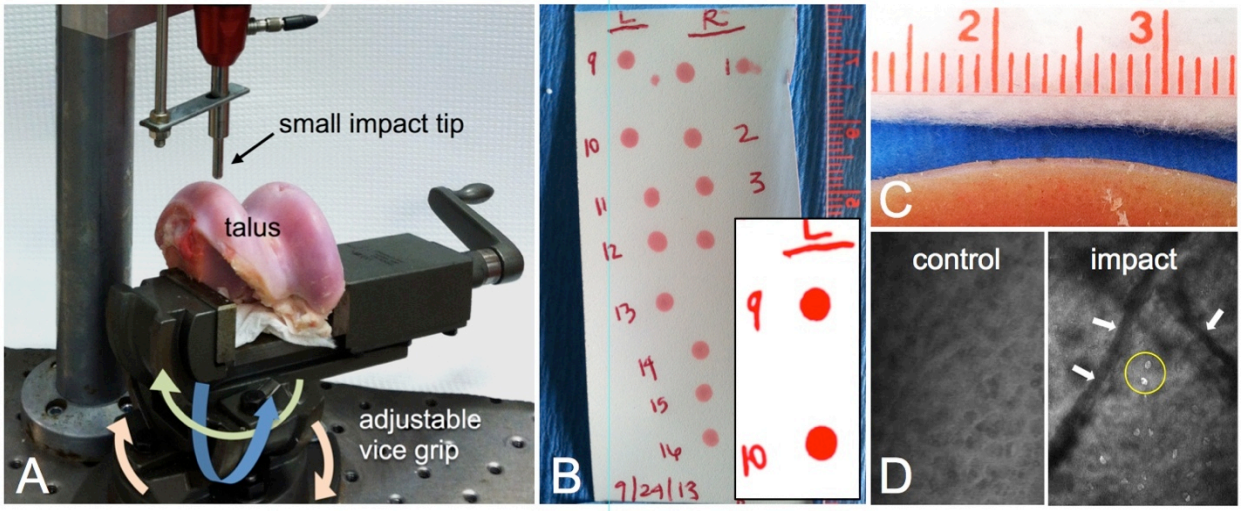

Figure S3.1. *Ex vivo* cartilage impact. A) Impactor mounted to armature, with talar OC block held in a vice grip, which rotates in 3-axis to allowing the impacting tip to be positioned perpendicular to articular surface. B) Impact footprints were recorded using pressure sensitive film and surface area was measured using the ImageJ software masking function (inset). C) Cartilage thickness was measured on cut section adjacent to impact sites using ImageJ software. D) Live multiphoton images (10x) of control and impacted cartilage. Cartilage matrix cracks (arrows) and dead cells (circled) are present after impact.

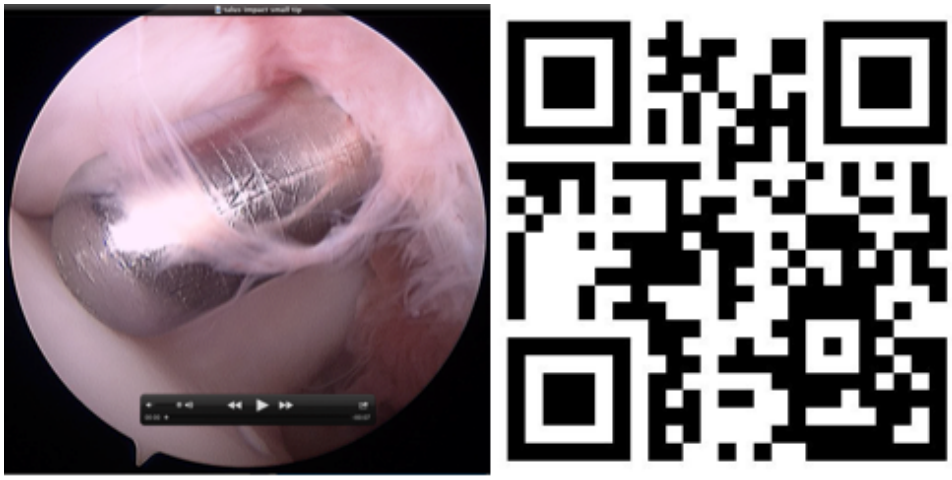

Figure S3.2. **Arthroscopy video of talus impact.** Scan the QR code with a QR code reading app on your smart phone or visit: https://vimeo.com/179513366 and enter the password "impact" to view the video.

Table S3.1. Rubric for joint inflammation score

Analysis	Parameter	Score	Qualifications
Synovial Fluid	Color/clarity/viscosity	0	Normal
		1	Abnormal
	Total Protein	0	<2.5
		1	2.5-4
		2	>4
	Nucleated cell count	0	<1000
		1	1000-9000
		2	>9000
	% Neutrophils on differential cell count	0	0-15%
		1	15-65%
		2	>65%
	Cellular morphology	0	Normal
		1	Abnormal
Clinical Examination	Joint effusion	0	None (Normal)
		1	Mild
		2	Moderate
		3	Severe

Table S3.2. Modified OARSI osteochondral histology scoring for *in vivo* impact model

Analysis	Score	Qualifications
Cartilage Structure (Fibrillation/fissuring of the articular cartilage surface)	0	None (Normal)
	1	Restricted to surface/superficial zone
	2	Fissures/clefts extends into middle zone
	3	Extends to level of deep zone
	4	Extends into the deep zone
	5	Full thickness loss (to calcified cartilage)
Tidemark/subchondral bone remodeling	0	None (Normal)
	1	Duplication of tidemark, advancement of SC bone into calcified cartilage, scalloped margins
	2	Advancement of SC bone through tidemark(s)
	3	Complete disruption/disorganization of tidemark, SC bone
Chondrocyte necrosis (Necrotic cells near the articular surface per 20X objective)	0	Normal
	1	1 necrotic cell
	2	1-2 necrotic cells
	3	2-3 necrotic cells
	4	3-4 necrotic cells
Focal cell loss (Area of acellularity per 20x field)	0	Normal
	1	10-20%
	2	20-30%
	3	40-50%
	4	>50%
Cluster (complex chondrone) **formation**	0	None
	1	2 chondrocytes
	2	2-3 chondrocytes
	3	3-4 chondrocytes
	4	>4 chondrocytes
Loss of GAG staining (on SOFG)	0	Normal
	1	<25% loss
	2	25-50%
	3	50-75%
	4	>75%

Table S3.3. Synovial membrane histopathology scoring for *in vivo* impact model

Analysis	Score	Qualifications
Inflammatory cell infiltration	0	None
	1	Mild presence in 25%
	2	Moderate presence in 25-50%
	3	Marked presence in >50%
Vascularity (Number of vessels)	0	Normal
	1	Mild increase in focal areas
	2	Moderate increase up to 50%
	3	Marked increase in >50%
Intimal hyperplasia	0	None
	1	Villi with 2-4 rows intimal cells
	2	Villi with 4-5 row
	3	Villi with >5 rows
Subintimal edema	0	None
	1	Mild edema in 25%
	2	Moderate edema in 25-50%
	3	Marked edema in >50%
Subintimal fibrosis	0	Normal
	1	Mild increase in 25%
	2	Moderate increase in 25-50%
	3	Marked increase in >50%

CHAPTER 4

MITOCHONDRIAL DYSFUNCTION IS AN ACUTE RESPONSE OF ARTICULAR CHONDROCYTES TO MECHANICAL INJURY

Michelle L. Delco, DVM[1], Edward D. Bonnevie[2,] Lawrence J. Bonassar, PhD[2,3],

Lisa A. Fortier, DVM, PhD[1]

[1]Department of Clinical Sciences, College of Veterinary Medicine, Cornell University, Ithaca, NY

[2]Sibley School of Mechanical and Aerospace Engineering, Cornell University, Ithaca, NY

[3]Meinig School of Biomedical Engineering, Cornell University, Ithaca, NY

Manuscript in review, Journal of Orthopedic Research.

Abstract

Mitochondrial (MT) dysfunction is known to occur in chondrocytes isolated from end-stage osteoarthritis (OA) patients, but the role of MT dysfunction in the initiation and early pathogenesis of post-traumatic OA (PTOA) remains unclear. The objective of this study was to investigate chondrocyte MT function immediately following mechanical injury in cartilage, and to determine if the response to injury differed between a weight bearing region (medial femoral condyle; MFC) and a non-weight bearing region (distal patellofemoral groove; PFG) of the same joint. Cartilage was harvested from the MFC and PFG of 10 neonatal bovids, and subjected to injurious compression at varying magnitudes (5-17MPa, 5-34GPa/sec) using a rapid single-impact model. Chondrocyte MT respiratory function, MT membrane polarity, chondrocyte viability and cell membrane damage were assessed *in situ.* Cartilage impact resulted MT depolarization and impaired MT respiratory function within 2 hours of injury. Cartilage from a non-weight bearing region of the joint (PFG) was more sensitive to impact-induced MT dysfunction and chondrocyte death than cartilage from a weight-bearing surface (MFC). Our findings suggest that MT dysfunction is an acute response of chondrocytes to cartilage injury, and that MT may play a key mechanobiological role in the initiation and early pathogenesis of PTOA. Clinical significance: Direct therapeutic targeting of MT function in the early post-injury time frame may provide a strategy to block perpetuation of tissue damage and prevent the development of PTOA.

Introduction

Despite decades of evidence establishing a link between mechanical injury to cartilage and post-traumatic osteoarthritis (PTOA),[1,2] no effective therapies exist to prevent or slow progression of the disease.[3] A sizeable body of research has focused on the molecular, cellular, and structural changes occurring in the days to weeks following cartilage injury. However, mounting evidence suggests that interventions must target the earliest pathologic events in order to modify the disease course.[4,5] Therefore, an improved understanding of the acute (within hours) events after cartilage injury is necessary to develop novel preventative therapies.

Mitochondria (MT) are subcellular organelles that drive tissue development, repair, and aging.[6] In addition to their role in cellular ATP production by oxidative phosphorylation, MT act as intracellular mechanotransducers via strain-mediated release of reactive oxygen species (ROS), which function in normal cell signaling.[7,8] When MT dysfunction, cellular energy production declines and ROS are produced in excess, leading to degradation of lipid membranes, accumulation of DNA damage, initiation of catabolic signaling cascades, and cell death.[9] Apoptosis is triggered when cytochrome C dissociates from the inner MT membrane and activates the caspase cascade in the cytosol.[10]

Bioenergetic failure, cumulative oxidative stress, and MT-mediated apoptosis are implicated in the pathogenesis of many complex degenerative diseases,[11] and substantial evidence supports a role for MT dysfunction in the chronic stages of osteoarthritis (OA).[12-14] In chondrocytes isolated from patients with end-stage OA, MT dysfunction is associated with later-stage pathologic events including upregulation of matrix metalloproteinase-1, -3 and -13, decreased synthesis of collagen and proteoglycans, and pathologic calcification of cartilage.[15,16] Additionally, MT dysfunction and oxidative stress were recently linked to chronic overloading of

chondrocytes.[17] Several studies provide indirect evidence that MT play a central mechanobiological role in impact-induced chondrocyte death. For example, MT-derived ROS contribute to chondrocyte death after cartilage injury,[18] and antioxidants prevent impact-induced cell death.[19,20] Furthermore, inhibition of calcium signaling and activation of the caspase cascade after cartilage injury can prevent impact-induced chondrocyte death.[21] These findings suggest a causal link between MT-dysfunction and PTOA pathogenesis, however, a significant knowledge gap remains in identifying the relationship between mechanical injury, *in situ* chondrocyte MT respiratory function, and cell death immediately after impact injury.

The objective of this study was to investigate chondrocyte MT function *in situ* immediately following cartilage impact injury using a real-time microscale respirometry assay modified for explanted cartilage. Our hypothesis was that MT dysfunction is an acute response of chondrocytes to mechanical injury. Furthermore, we hypothesized that a joint surface adapted to withstand predominantly compressive loads during weight-bearing (the MFC) would be less sensitive to impact-induced cell death and MT dysfunction than a non-weight-bearing region within the same joint.

Methods

Cartilage Harvest and Mechanical Injury

Healthy bovids (n = 10; 1-3 days of age) were obtained from a livestock auction and humanely euthanized in accordance with AVMA guidelines.[22] Within 12 hours of sacrifice, full thickness cartilage explants were harvested from both the left and right knee joints, using an 8mm biopsy punch (**Figure 4.1a**). Explants were rinsed in phosphate-buffered saline (PBS), trimmed to a uniform thickness of 3mm from the articular surface using a custom jig, and placed

in cartilage explant media (phenol-free DMEM containing FBS 10%, HEPES 0.025ml/ml, penicillin 100U/mL and streptomycin 100U/mL). All animal experiments were approved by Cornell University's Institutional Animal Care and Use Committee.

Explants were subjected to a single, rapid impact injury using a validated model, as previously described, or served as un-injured controls.[23] Briefly, explants were positioned in a well containing media under the plane-ended tip of a spring-loaded impacting device.[23,24] Impact magnitude was adjusted by setting the deflection of the impactor's internal spring. During impact, force was measured at 50 kHz by an in-line load cell (PCB Piezotronics, Depew, NY) and displacement was measured by a linear variable differential transducer (LVDT; RDP Electronics, Pottstown PA) attached to the impactor tip. Voltages from the load cell and LVDT were recorded simultaneously with a custom LabVIEW program (NI, Austin TX) and mechanical parameters for each impact were calculated as previously described.[23]

Characterization of In Situ Chondrocyte Mitochondrial Respiratory Function Immediately Following Cartilage Injury

The goal of the first set of experiments was to determine the effect of acute mechanical injury on chondrocyte mitochondrial function. Microrespirometry has previously been used to investigate respiratory function of cultured chondrocytes,[17,25] but has not been applied to chondrocytes *in situ*. Studying chondrocytes within their native extracellular matrix minimizes alterations in the mechanobiological environment and shortens the time frame between injury and observation. Therefore, based on previously described modifications of this technique for

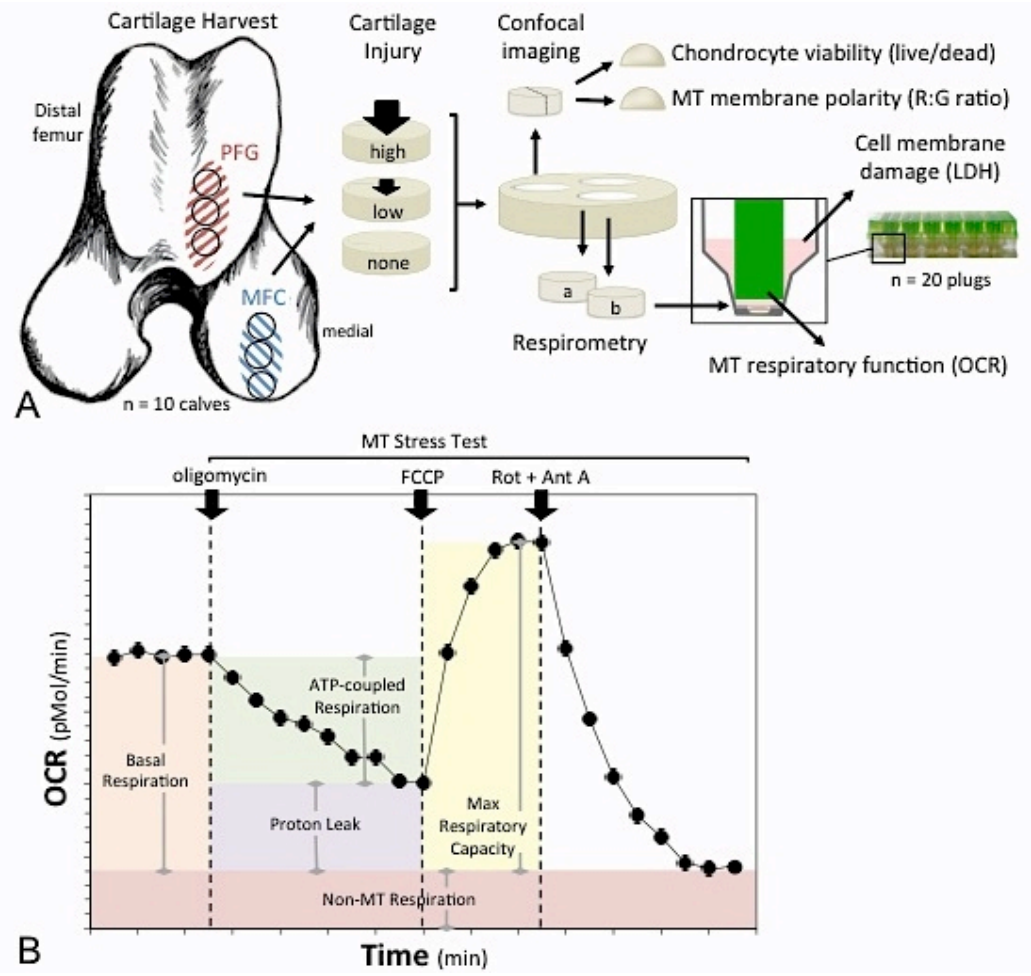

Figure 4.1. Experimental design and methods. A) Cartilage explants were harvested from the medial femoral condyle (MFC) for the first set of experiments, and from 2 sites for the second set of experiments; the MFC and the distal patellofemoral groove (PFG). One explant from each region was impacted at a higher impact magnitude, one was impacted at a lower magnitude, and one served as an un-impacted control. Explants were then divided for use in several assays; chondrocyte viability was quantified using live/dead staining, mitochondrial (MT) membrane polarity was determined as red to green fluorescent intensity (R:G) ratio on confocal imaging and MT respiratory function was assessed via microrespirometry. Cell membrane damage was assessed by measuring lactate dehydrogenase (LDH) activity in cartilage conditioned media. B) MT respiratory function was quantified by measuring oxygen consumption rate (OCR) over time. After basal OCR was determined, a MT stress test was performed by sequential addition of 1) oligomycin, an ATP synthase inhibitor 2) FCCP, a proton circuit uncoupler 3) rotenone (Rot) and antimycin A (Ant A), inhibitors of MT complexes I and III. Parameters of respiratory control were calculated as depicted by the shaded areas under the curve.

use in whole tissues[26,27] and after assay optimization (**Supplement 4.1**, *Detailed Methods*), real-time microscale respirometry was used to measure chondrocyte MT respiratory function in explanted cartilage, as follows. Explants (n = 65 total) from the medial femoral condyle (MFC) were harvested and impacted over a broad range of injury magnitudes (M1-M4; 5-17MPa, 5-34GPa/sec; Table 1), as described above. This range was selected based on preliminary trials (160 explants, 8 trials) and previous work[23] to determine the stress and stress rate thresholds associated with cell death and extracellular matrix damage in this system. The goal was to apply a range of injury magnitudes, from minimal cell death (M1) to cell death without surface cracking (M2) to subcritial damage (i.e. impacts that produced surface fissuring but not full thickness defects; M3 and M4, **Table 4.1**).

Following impact, two cartilage disks (3mm diameter x 500um thickness from the articular surface) were prepared (**Supplement 4.1**) and immediately loaded into a randomly assigned well of a 24-well tissue capture microplate (Seahorse Biosciences, Billerica, MA) containing assay media (bicarbonate-free DMEM supplemented with 2.5mM glucose, 2mM L-glutamine, 2 mM pyruvate, and 1% FBS). Following a calibration cycle, glycolysis and oxidative phosphorylation were quantified every 8 minutes for a minimum of 225 minutes by measuring extracellular acidification (ECAR) and oxygen consumption rates (OCR) within each well, respectively using an XF24 Extracellular Flux Analyzer (Seahorse Biosciences). After basal respiration was measured for at least 40 minutes, a MT stress test was performed according to standard protocols, as previously described.[9,25,28] Briefly, OCR was measured in response to the automated sequential addition of 1) oligomycin (1.5 uM), an ATP synthase inhibitor 2) carbonyl cyanide-4-(trifluoromethoxy) phenylhydrazone (FCCP; 1.0 uM), a proton circuit uncoupler 3) a

Table 4.1. Mechanical parameters of impact by experimental group

Experimental Group	Impact Magnitude	
	Mean Peak Stress; MPa (+/- s.d.)	Mean Peak Stress Rate; GPa/sec (+/- s.d.)
Control	n/a	n/a
M1	5.6 (0.4)	6.7 (1.3)
M2	7.5 (0.4)	9.3 (1.5)
M3	14.1 (0.7)	28.1 (1.8)
M4	16.2 (0.7)	32.0 (1.6)

combination of rotenone (0.5 uM) + antimycin A (1.0 uM), inhibitors of MT complexes I and III, respectively (Seahorse Biosciences).

The remainder of each explant was used to determine chondrocyte density and viability, as described below, in order to normalize respirometry data to viable cell number on an individual explant basis (**Supplement 4.1**). Data were normalized to viable cell number by dividing OCRs measured in each well containing a single cartilage plug, by the number of viable cells in that well. MT functional indices were calculated as previously described[9,25] and visually represented in **Figure 1b**, using OCR values as follows: basal OCR (bOCR) = initial OCR – nonMT respiration (NMR); maximal (uncoupled) respiration (mOCR) = FCCP stimulated OCR – NMR; spare respiratory capacity (SCR) = (uncoupled respiration – NMR) – (bOCR – NMR); Proton leak = (oOCR– NMR).

Chondrocyte Viability and Cell Membrane Damage Assays

In order to determine cell density and quantify chondrocyte viability, cartilage was placed in PBS containing calcein AM (2uM) and ethidium homodimer (1uM) for 30 minutes at 37°C in the dark, to stain live and dead cells, respectively. Explants were then rinsed in PBS and imaged on a Leika SP5 confocal microscope. Digital z-stacked images were acquired in two channel sequential scans (488/498-544 and 514/563-663 nm excitation/emission, respectively) using a modified 3D scanning protocol consisting of 10 z-stacked 512x512 pixel (387.5µm x 387.5µm) images spaced 10um apart in the z plane at 20x magnification. The number of live, dead, and total cells in each image was quantified using a custom ImageJ macro (**Supplement 4.1**). The explant volume and chondrocyte density were calculated for each explant and used to normalize respirometry data to viable cell number (**Supplement 4.1**).

As a measure of cell membrane damage, lactate dehydrogenase (LDH) activity was assayed in cartilage-conditioned media from each well of the XF assay plate, according to manufacturer's instructions (Sigma-Aldrich, St. Louis, MO). Briefly, equal volumes of cartilage-conditioned media and kit reagent were added to a 96-well plate and absorbance was measured at 450nm in 5-minute intervals by a spectrophotometric microplate reader (Tecan Safire; Männedorf, Switzerland). To established a post-impact LDH release time-course and validate the use of media obtained from the XF assay plates following microrespirometry assays, cartilage explants (n = 16) were impacted at the magnitudes described above (M1-M4: **Table 4.1**), and incubated for 24 hours in cartilage explant media. LDH assay was performed on cartilage-conditioned media at 1, 5, 7 and 24 hours after impact.

Comparison of chondrocyte response to injury between two locations within the same joint

The goal of the second set of experiments was to compare MT response to injury between a weight bearing and non-weight bearing surface within the same joint. Explants were harvested from the medial femoral condyle (MFC) and distal patellofemoral groove (PFG), as described above (n = 40 total). The MFC is the main weight-bearing surface of the knee, while the distal PFG is a non-weight bearing articular surface. Three explants were harvested from two locations within each joint. One explant from each area was subjected to one of 3 impact treatments; lower magnitude (M1; 5.6 ±0.4 MPa mean peak stress, 6.7 ±1.3 GPa/sec mean peak stress rate), higher magnitude impact (M2; 7.5 ±0.4 MPa, 9.3 ±1.5 GPa/sec) or non-impacted control. Microrespirometry was performed (n = 8/group) and data was normalized as described above. Impact magnitudes (M1 and M2) were chosen based on preliminary data, which revealed that

impact above ~8MPa peak stress (~11GPa/sec peak stress rate) in the PFG resulted in extensive cell death, preventing comparisons to the MFC (**Figure S4.1**).

Mitochondrial Membrane Polarity Assay

The functional integrity of the inner MT membrane was assessed *in situ* using confocal imaging of fluorescent MT probes. Following impact and sectioning, samples (n = 40) were placed in PBS containing tetramethylrhodamine methyl ester perchlorate (TMRM;10nM, Molecular Probes), MitoTracker Green (MTrG; 200nM, Molecular Probes, Eugene, OR), and Hoechst 33342 (1ug/ml, Molecular Probes) for 40 minutes and protected from light. TMRM is a polarity-sensitive MT probe, and red fluorescence indicates active transport of the dye across a polarized (functional) MT membrane. MTrG is a polarity-insensitive MT probe, which stains all MT regardless of MT membrane potential. Hoechst acts as a nuclear counterstain, and preferentially stains cells with compromised plasma membranes. After staining, explants were rinsed in PBS and imaged on a Leica SP5 confocal microscope. Images were acquired and analyzed as described above (for live/dead staining), with the exception that 1024x1024 pixel (775μm x775μm) images were acquired in three channel sequential scans (405/411-497, 488/498-544 and 561/569-611 nm excitation/emission, respectively) spaced 5um in the z-plane at 20x magnification and red:green florescent intensity (R:G) ratios for each image were determined using a custom ImageJ macro (**Supplement 4.1**). Macros for each imaging channel were optimized and image-wide analysis of R:G ratio was validated by manual ROI selection of individual cells at higher (40x) magnification for control and impacted explants.

Statistical Analysis

The response variables bOCR and mOCR were analyzed using a linear mixed effects model with fixed effects of treatment group and site (MFC or PFG) and random effect of trial (animal) and limb (left or right). The unit of study was a cartilage explant. The relationship between impact magnitude (stress and stress rate) and chondrocyte death was analyzed using a linear regression model. A one-way ANOVA was used to compare response variables between treatment groups. Post-hoc pairwise comparisons between treatment groups were performed using Tukey's HSD method to control for multiple comparisons. Residual analyses were performed on log-transformed data to ensure the assumptions of normality and homogeneous variance were met. Differences were considered statistically significant when $p < 0.05$. All statistical analyses were performed using JMP Pro Version 11.0 (SAS Inc.) software.

Results

Chondrocyte respiration after cartilage injury

Mitochondrial respiratory function in MFC cartilage was assessed by measuring oxygen consumption rate (OCR) in the acute phase (from 2-6 hours) after injury. Representative curves for OCR are shown in **Figure 4.2a**, and demonstrate differences in respiratory function between low impacted, high impacted and control cartilage. MT respiration declines with increasing injury magnitude, revealing acute impact-induced MT dysfunction (**Figure 4.2**); There was a significant effect of treatment (impact) group on bOCR ($F_{4,56} = 5.4135$, $p = 0.0009$) and mOCR ($F_{4,56} = 3.0572$, p 0.026). Cartilage injury resulted in a 20-32% decrease in bOCR in explants from impact groups M2 - M4 (**Figure 4.2b**), and a 26-44% decrease in mOCR in groups M3 and M4 compared to un-impacted controls (**Figure 4.2c**). Parameters of respiratory control

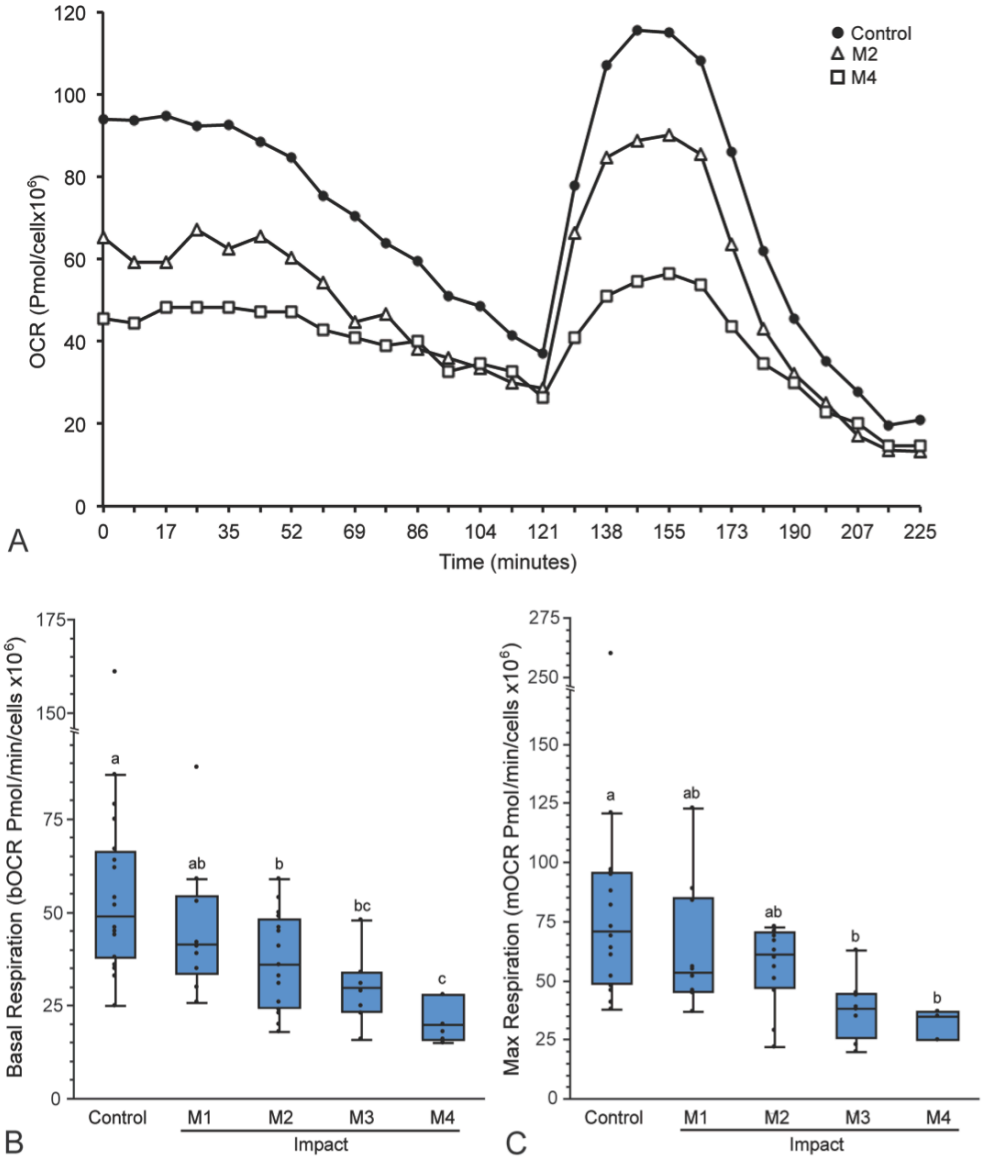

Figure 4.2. Respirometry reveals acute impact-induced mitochondrial (MT) dysfunction. Cartilage from the medial femoral condyle was impacted at various magnitudes (M1-M4) and MT respiration was quantified by measuring oxygen consumption rate (OCR), then normalizing data to live cell number for each explant. A) Representative curves for OCR versus time for control, low impact (M2) and high impact (M4) groups demonstrate differences in MT respiratory function between groups. Note that oligomycin-inhibited respiration does not reach steady state (121 minutes), but Rot+AA inhibited respiration does (225 minutes.) B) Baseline OCR (bOCR) and C) maximum respiration (mOCR) decreased with increasing impact magnitude (M1-M4). Groups that do not share a letter are significantly different at $p < 0.05$. Error bars = ±s.d.

calculated using oligomycin-inhibited OCR (oOCR) could not be reliably determined because steady state OCR following oligomycin treatment was not reached in the majority of samples (**Figure 4.2a**). Injury had no effect on ECAR ($p = 0.66$).

Chondrocyte death in MFC cartilage was positively correlated with impact magnitude (**Figure S4.1**), with the strongest correlation associated with peak impact stress ($r^2 = 0.70$, $p<0.0001$). A significant increase in cell death was observed above 7MPa peak stress, establishing a threshold for acute chondrocyte death in this model system. Cell membrane damage was assessed in cartilage-conditioned media obtained from wells following the respirometry assay, and revealed 2-3 fold increase in LDH activity for explants impacted at higher peak stresses (M3, M4) compared to lower impacts (M1, M2) and controls (**Figure S4.2a**). Based on the time-course experiment, LDH activity peaked at approximately 5 hours following cartilage injury at all impact magnitudes (**Figure S4.2b**).

Comparison of Chondrocyte Response to Injury in MFC versus PFG cartilage

Similar to MFC explants, chondrocyte death in PFG explants was positively correlated with peak impact stress ($r^2 = 0.79$, $p<0.001$; **Figure S4.1**). However, chondrocytes from PFG cartilage, a non-weight-bearing articular surface, were more sensitive than the MFC to impact-induced cell death; PFG explants experienced an approximately 2-fold and 5-fold increase in cell death over controls at the lower (M1) and higher (M2) impact magnitudes, respectively (**Figure 4.3**). At lower impact magnitudes (M1), MFC viability was not affected.

Cartilage from the PFG was more sensitive to impact-induced MT respiratory dysfunction (**Figure 4.4**). The basal oxygen consumption rate of viable PFG chondrocytes was significantly lower in groups impacted at the lowest (M1) and higher (M2) magnitudes compared

to un-injured control cartilage, whereas in MFC cartilage, bOCR was only affected at the higher impact magnitude (M2). Relative MT membrane potential (MT polarity) was used to assess the functional integrity of the inner MT membrane by calculating the R:G ratio, which represents the ratio of polarized to depolarized MT within each explant. In uninjured controls, MT polarity was similar in MFC and PFG cartilage. MT polarity was significantly decreased in both the lower (M1) and higher (M2) impacted explants from the PFG. Over this range of impact magnitudes, no statistically significant differences were detected between control and impacted samples from the MFC (**Figure 4.5**).

Discussion

The goal of this work was to investigate the role of mitochondria in the very early response of cartilage to mechanical injury. The most important findings of this study were that MT dysfunction is an acute response of chondrocytes to cartilage trauma, and that the response of chondrocytes to injury differs based on location within a single joint.

Although several lines of investigation have supported the assumption that MT participate in catabolic events immediately following cartilage injury,[21,29,30] and microscale respirometry has recently been used to assess MT function in cultured chondrocytes,[17,25] this is the first report of assessing *in situ* chondrocyte MT respiratory function in the acute time frame following cartilage trauma. This distinction is important for several reasons. First, chondrocyte phenotype and gene expression change significantly when cells are isolated from the native extracellular matrix and cultured in monolayer.[31-33] In one study, MT metabolism and MT biogenesis were drastically altered in both primary cultured (i.e. non-passaged) and first-passage

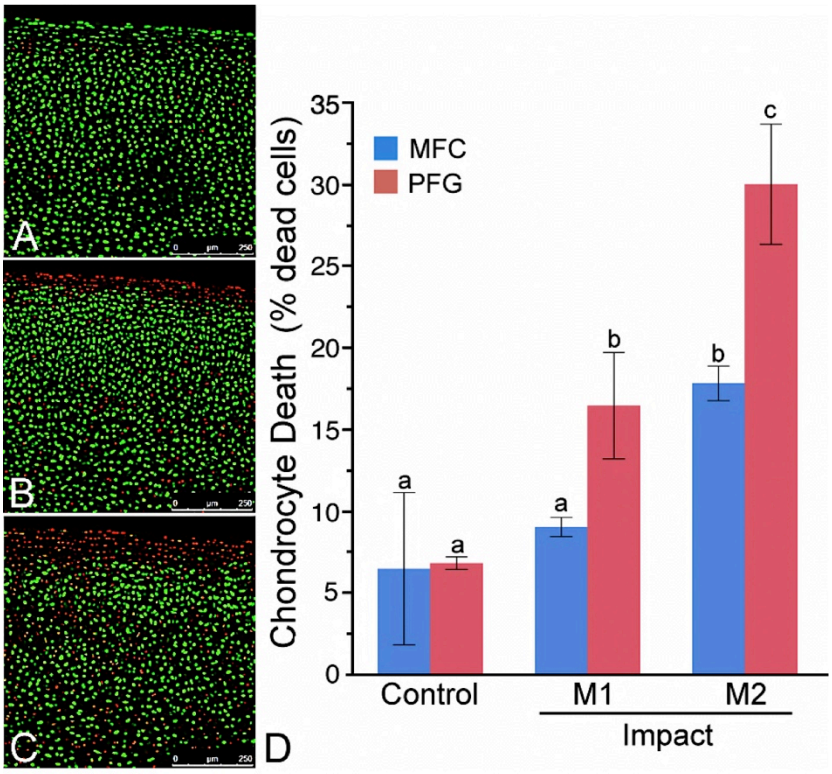

Figure 4.3. Impact-induced chondrocyte death differs by location within the joint.

A-C) Representative images of PFG cartilage stained for live cells (green) with calcein AM and dead cells (red) with ethidium homodimer and imaged in cross-section using confocal microscopy. A) Un-impacted control cartilage had less dead (red) staining than B) lower impacted (M1) and C) higher impacted (M2) PFG explants. D) Chondrocytes from the patellofemoral groove (PFG) were more sensitive to impact-induced cell death than the medial femoral condyle (MFC). At lower impact magnitudes (M1) MFC viability was not affected. Groups that do not share a letter are significantly different at $p < 0.05$. Error bars = ±s.d.

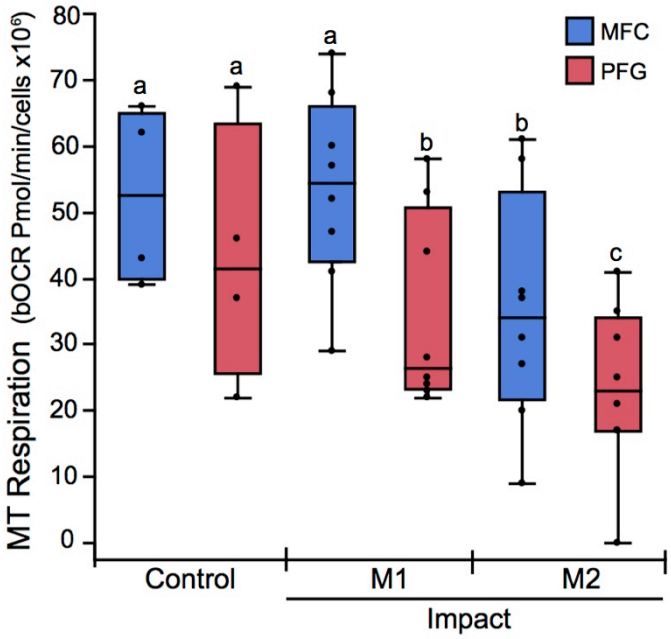

Figure 4.4. The patellofemoral groove (PFG) is more sensitive to impact-induced MT respiratory dysfunction than the medial femoral condyle (MFC). The basal oxygen consumption rate (bOCR) of viable chondrocytes was significantly lower in PFG cartilage (red box and whisker plots) impacted at the lowest (M1) and higher (M2) magnitudes compared to un-injured control cartilage, whereas in MFC cartilage (blue box and whisker plots), bOCR is only affected at the higher impact magnitude (M2). Groups that do not share a letter are significantly different at $p<0.05$. Error bars = ±s.d.

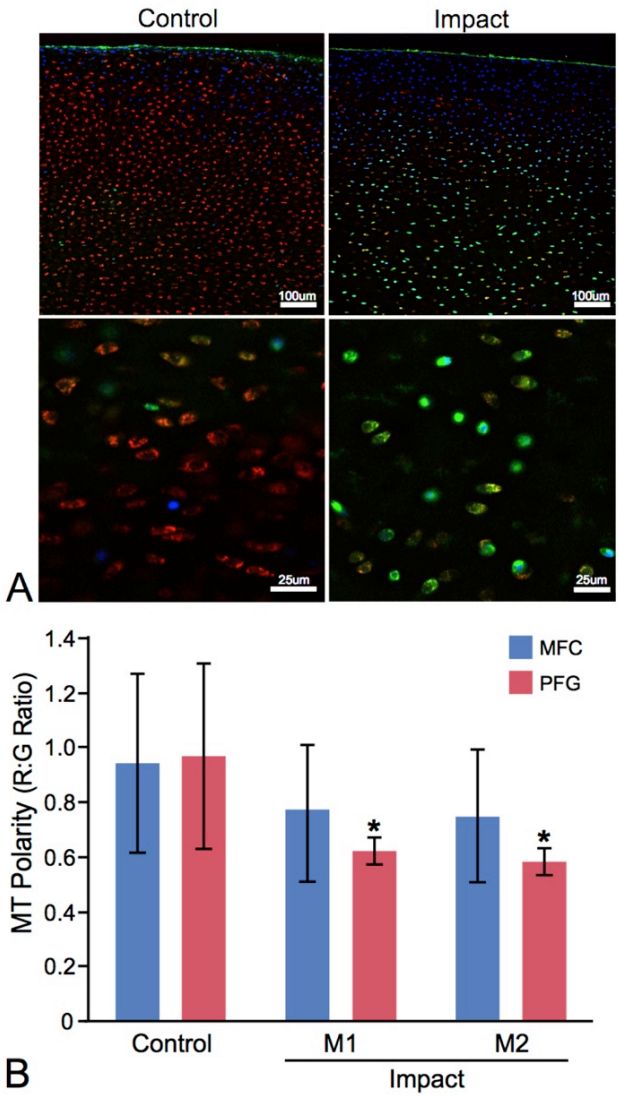

Figure 4.5. The patellofemoral groove (PFG) is more sensitive to impact-induced MT depolarization than the medial femoral condyle (MFC). A) Representative confocal images of control and impacted (M2) PFG explants stained for MT polarity at low (top) and high (bottom) magnification. Cartilage is stained with Mitotracker Green (green; all MT), tetramethylrhodamine methyl ester perchlorate (red; polarized/functional MT), and Hoechst 33342 (blue; nuclear counterstain, higher affinity for cells with compromised cell membranes). Red:green fluorescent intensity ratios were calculated on an image-wide basis using multiple low magnification z -stacks for each explant (top) using a custom ImageJ macro. This technique was validated on a single-cell basis by manually drawing ROIs around single cells at higher magnification (bottom). B) MT depolarization occurred in PFG cartilage from both the lower (M1) and higher impact (M2) groups compared to PFG controls. Significant differences were not detected between impact groups from the MFC. Asterisks denote a significant difference compared to control at $p < 0.05$. Error bars = ±s.d.

chondrocytes.[34] Secondly, accurate modeling of mechanical trauma to cartilage requires the native ECM. Finally, our primary objective was to investigate MT function within hours of mechanical injury, and the time required to isolate and perform primary chondrocyte culture is incompatible with this goal.

Recent evidence suggests that the main determinant for the development of PTOA is the magnitude of the initial cartilage/subchondral bone injury.[1] A challenge in the field of early PTOA research has been to establish thresholds for mechanical injury in vitro and correlate these to the development of disease. Recently, our group fully characterized the mechanics of *an in vivo* impactor system and correlated impact magnitude (stress and stress rate) with structural damage *in vitro*.[23] A threshold for superficial ECM cracking was established above a peak stress of 13 MPa. In the present study, the same impact system was used to determine the relationship between impact magnitude and tissue damage (i.e., chondrocyte death and cell membrane damage) in the acute phase after cartilage impact. That study revealed cell death was correlated to impact stress above a threshold of 7 MPa in MFC cartilage. In the current study, MT respiration in viable cells declined with increasing injury magnitude. This suggests a population of unhealthy but viable chondrocytes undergoing impact-induced MT dysfunction. This sub-population of dysfunctional cells may represent a target for therapeutics that would protect MT function, prevent cell death, and block perpetuation of tissue damage. To more specifically investigate this hypothesis, present studies are focused on improving spatial and temporal resolution of MT dysfunction in whole cartilage in the peracute (minutes to hours) time frame after injury and following the fate of depolarized cells for days to weeks after impact.

Our finding that MT dysfunction occurs independent of cell death is in agreement with recent work by Coleman et al,[17] which demonstrated MT dysfunction and oxidative stress after

one week in chronically overloaded cartilage. The loading regimen consisted of load-controlled cyclic compression at 0.25 MPa (physiologic loading) or 1 MPa (supra-physiologic) amplitude and 0.5 Hz frequency for 3 hours once daily for one week. Slow load rise times resulted in stress rates in the MPa/sec range. In that study, no differences were observed in chondrocyte viability or mechanical behavior of the tissue between the physiologically loaded and overloaded chondrocytes after 7 days. Furthermore, no differences in MT function or oxidation status were observed between groups after one day. Therefore, their model may aptly be described as chronic, moderate overloading.

In contrast, the current study was designed to more closely model acute cartilage trauma, and utilized an energy-controlled spring-loaded device to deliver a single rapid impact, with impact times in the millisecond range and stress rates in the GPa/sec range. In addition to distinct mechanobiology in these 2 systems, Coleman *et al.* models the early chronic time frame, with MT function assessed 1-2 weeks after start of loading, whereas the aim of this study was to assess the acute responses of chondrocytes after injury. This is an important distinction, because the subcellular mechanisms occurring within these time frames are likely different. Chronic MT dysfunction, as occurs in aging, can encompass many cellular processes including chronic oxidative stress, altered mitochondrial dynamics (MT biogenesis, turnover, and plasticity), metabolic reprogramming, and inflammation through a complex network of signaling pathways, while acute mitochondrial dysfunction occurs following traumatic injury before transcriptional changes can occur.[35,36] Examples of disease processes mediated by acute MT dysfunction include ischemia reperfusion injury after acute myocardial infarction (MI), neuronal damage following traumatic brain injury (TBI), and here we propose PTOA.[37] Clinical MI and TBI research focuses on potentially treatable events in the early phase following injury. In this acute

phase, MT participate in both the perpetuation of tissue damage, as well as protective mechanisms. For example, following injury, rapid calcium buffering occurs, whereby Ca^{++} flows into the cytosol due to changes in cell membrane permeability and is rapidly sequestered within MT. This process leads to MT swelling within 10 minutes of TBI. MT swelling is reversible if cell repair mechanisms remain intact and the MT transition pore (MTP) does not open.[38] Opening of the MTP results in further osmotic swelling of the MT, complete uncoupling of oxidative phosphorylation, rupture of the MT membrane and subsequent cell death. Calcium signaling is known to be involved in chondrocyte death after injury,[21] and our data supports impaired efficiency of the ETC after cartilage injury, consistent with acute swelling of the MT.

Our findings suggest that chondrocytes of the MFC are less sensitive to impact-induced cell death and MT dysfunction than those of the PFG. The MFC and PFG sites were selected because the cartilage in these locations is subjected to distinct physiological loading regimens. As the major weight-bearing surface of the knee, the MFC is exposed to the highest compressive and shear strains, and is a common site for focal cartilage lesions within the knee.[39] In contrast, the inferior aspect of the PFG is a non-weight bearing articular surface and is often used as a donor harvest site for cartilage autograft procedures.[40] The inferior PFG articulates with the patella alone, and only when the knee is in maximal flexion, so it experiences relatively low compressive and shear forces.[41] It therefore stands to reason that chondrocytes in these regions are adapted to respond differently to injurious loading. Recently, post-impact chondrocyte viability was found to differ between joints,[42] but to our knowledge, this is the first report of regional differences in impact-induced cellular responses within the same joint. Differing thresholds for MT dysfunction and cell death could be the result of distinct chondrocyte populations and/or site-specific structural variations in the ECM of these regions. Regardless, our

findings suggest that there are differences in tissue-scale mechanotransduction between weight bearing and non-weight bearing regions within a joint. This is particularly interesting related to MT function, as MT act as mechanotransducers in other tissues, converting stress and strain experienced by the tissue to chemical signals in the form of ROS.[7,18,43] Clinically, this finding may have important implications for osteochondral grafting procedures, because a more thorough understanding of the mechanisms underlying local differences in mechanotransduction may inform selection of optimal autograft and allograft harvest sites.

When interpreting the results of this study, it should be noted that all experiments were performed at 21% O_2 concentration, which is considered relative hyperoxia for cartilage.[44] There is considerable disagreement in the literature regarding the effect of O_2 concentration on chondrocyte metabolism.[45-48] Most studies have investigated this question in isolated chondrocytes, after days or weeks in culture. One group assessed the OCR of freshly harvested cartilage (1mm cubes) from young mature (18-24 month old) bovids and found that at O_2 concentrations between 5 and 21%, OCR was relatively constant at ~10 nM/10^6 cells/hour,[47] a value comparable to the bOCR values measured for un-injured cartilage in the present study. Furthermore, OCR in cultured chondrocytes was found to be independent of O_2 and glucose concentration in short term (48 hour) culture.[46] Therefore, the caveat of relative hyperoxia is unlikely to have bearing on our finding of acute impact-induced MT dysfunction.

A limitation of the current work is the use of immature cartilage. Previous work has shown that young bovine cartilage is more metabolically active and more sensitive to injury-induced apoptosis than mature cartilage.[49,50] Although the magnitudes differ between young and mature tissue, chondrocytes respond to injurious mechanical loading with increased cell death, intracellular ROS, increased catabolism and a decrease in anabolic activity, regardless of donor

age. The rationale for selecting young cartilage for this proof of concept study is that chondrocyte density in young cartilage is approximately twofold higher in the first 1mm of depth from the articular surface than adult cartilage, maximizing our ability to measure impact-induced changes in OCR *in situ*, over a broad range of impact magnitudes.[51] Further studies are warranted investigate the effect of tissue maturity on the acute response of chondrocytes to injury, as well as the specific mechanisms of acute impact-induced chondrocyte MT dysfunction.

In summary, this study demonstrates that MT dysfunction is an acute response of chondrocytes to cartilage impact and is the first report of adapting microrespirometry to study the subcellular mechanisms of impact-induced chondrocyte MT dysfunction *in situ*. Our results reveal impact-induced decline in basal OCR and maximum respiratory capacity, which suggests inhibition of the MT electron transport chain (ETC). This finding is consistent with the known phenomenon of MT membrane swelling after injury, which causes unfolding of the cristae leading to decreased efficiency of the ETC.[9] Cartilage from the weight-bearing surface of the distal femur (MFC) is more resistant to impact-induced MT dysfunction and cell death than that of a non-weight bearing surface (PFG). This suggests regional differences between weight bearing and non-weight bearing articular surfaces, either due to structural differences of the ECM or cellular response to injury and/or differences in mechanotransduction. Our findings suggest that direct targeting of MT respiratory function in the acute stages after cartilage injury may represent a viable therapeutic strategy in the prevention of PTOA.

Acknowledgements

The authors thank Hussni Mohammed and Lynn Johnson for statistical consulting. We also thank and Meg Goodale and Becky Hicks for technical and logistical support. This work was supported by Weill Cornell Medical College Clinical & Translational Science Center Award/National Center for Advancing Translational Sciences (5 UL1 TR000457-09) and The Harry M. Zweig Memorial Fund for Equine Research. MD was supported by NIH 5T32OD011000-20. Funding sources did not participate in any aspect of this study.

References

1. Buckwalter JA. The role of mechanical forces in the initiation and progression of osteoarthritis. *HSS Jrnl*. 2012;8(1):37–38. doi:10.1007/s11420-011-9251-y.

2. Kramer WC, Hendricks KJ, Wang J. Pathogenetic mechanisms of posttraumatic osteoarthritis: opportunities for early intervention. *Int J Clin Exp Med*. 2011;4(4):285–298.

3. Cheng DS, Visco CJ. Pharmaceutical therapy for osteoarthritis. *PM&R*. 2012;4(5):S82–S88.

4. Anderson DD, Chubinskaya S, Guilak F, et al. Post-traumatic osteoarthritis: improved understanding and opportunities for early intervention. *J Orthop Res*. 2011;29(6):802–809. doi:10.1002/jor.21359.

5. Chubinskaya S, Wimmer MA. Key Pathways to Prevent Posttraumatic Arthritis for Future Molecule-Based Therapy. *Cartilage*. 2013;4(3 Suppl):13S–21S. doi:10.1177/1947603513487457.

6. Pagano G, Talamanca AA, Castello G, et al. Oxidative stress and mitochondrial dysfunction across broad-ranging pathologies: toward mitochondria-targeted clinical strategies. *Oxid Med Cell Longev*. 2014;2014:541230. doi:10.1155/2014/541230.

7. Ali MH, Pearlstein DP, Mathieu CE, Schumacker PT. Mitochondrial requirement for endothelial responses to cyclic strain: implications for mechanotransduction. *Am J Physiol Lung Cell Mol Physiol*. 2004;287(3):L486–L496. doi:10.1152/ajplung.00389.2003.

8. Finkel T. Signal transduction by reactive oxygen species. *The Journal of Cell Biology*. 2011;194(1):7–15. doi:10.1038/nature09663.

9. Brand MD, Nicholls DG. Assessing mitochondrial dysfunction in cells. *Biochem J*. 2011;435(2):297–312. doi:10.1042/BJ20110162.

10. Lee H-C, Wei Y-H. Mitochondrial biogenesis and mitochondrial DNA maintenance of mammalian cells under oxidative stress. *The International Journal of Biochemistry & Cell Biology*. 2005;37(4):822–834. doi:10.1016/j.biocel.2004.09.010.

11. Dai D-F, Chiao YA, Marcinek DJ, Szeto HH, Rabinovitch PS. Mitochondrial oxidative stress in aging and healthspan. *Longev Healthspan*. 2014;3:6. doi:10.1186/2046-2395-3-6.

12. Blanco FJ, Rego I, Ruiz-Romero C. The role of mitochondria in osteoarthritis. *Nat Rev Rheumatol*. 2011;7(3):161–169. doi:10.1038/nrrheum.2010.213.

13. Maneiro E, Martín MA, de Andres MC, et al. Mitochondrial respiratory activity is altered in osteoarthritic human articular chondrocytes. *Arthritis & Rheumatism*. 2003;48(3):700–708. doi:10.1002/art.10837.

14. Ruiz-Romero C, Calamia V, Mateos J, et al. Mitochondrial dysregulation of osteoarthritic human articular chondrocytes analyzed by proteomics: a decrease in mitochondrial superoxide dismutase points to a redox imbalance. *Mol Cell Proteomics*. 2009;8(1):172–189. doi:10.1074/mcp.M800292-MCP200.

15. Johnson K, Jung A, Murphy A, Andreyev A, Dykens J, Terkeltaub R. Mitochondrial oxidative

phosphorylation is a downstream regulator of nitric oxide effects on chondrocyte matrix synthesis and mineralization. *Arthritis & Rheumatism*. 2001;43(7):1560–1570. doi:10.1002/1529-0131(200007)43:7<1560::AID-ANR21>3.0.CO;2-S.

16. Cillero-Pastor B, Rego-Pérez I, Oreiro N, Fernandez-Lopez C, Blanco FJ. Mitochondrial respiratory chain dysfunction modulates metalloproteases -1, -3 and -13 in human normal chondrocytes in culture. *BMC Musculoskelet Disord*. 2013;14:235–235. doi:10.1186/1471-2474-14-235.

17. Coleman MC, Ramakrishnan PS, Brouillette MJ, Martin JA. Injurious Loading of Articular Cartilage Compromises Chondrocyte Respiratory Function. *Arthritis & Rheumatology*. September 2015:n/a–n/a. doi:10.1002/art.39460.

18. Brouillette MJ, Ramakrishnan PS, Wagner VM, et al. Strain-dependent oxidant release in articular cartilage originates from mitochondria. *Biomech Model Mechanobiol*. 2014;13(3):565–572. doi:10.1007/s10237-013-0518-8.

19. Martin JA, McCabe D, Walter M, Buckwalter JA, McKinley TO. N-acetylcysteine inhibits post-impact chondrocyte death in osteochondral explants. *J Bone Joint Surg Am*. 2009;91(8):1890–1897. doi:10.2106/JBJS.H.00545.

20. Garrido CP, Hakimiyan AA, Rappoport L, Oegema TR, Wimmer MA, Chubinskaya S. Anti-apoptotic treatments prevent cartilage degradation after acute trauma to human ankle cartilage. *Osteoarthritis and Cartilage*. 2009;17(9):1244–1251. doi:10.1016/j.joca.2009.03.007.

21. Huser CAM, Davies ME. Calcium signaling leads to mitochondrial depolarization in impact-induced chondrocyte death in equine articular cartilage explants. *Arthritis & Rheumatism*. 2007;56(7):2322–2334. doi:10.1002/art.22717.

22. Leary S, Underwood W, Anthony R, Cartner S, Corey D. AVMA guidelines for the euthanasia of animals: 2013 edition. 2013.

23. Bonnevie ED, Delco ML, Fortier LA, Alexander PG, Tuan RS, Bonassar LJ. Characterization of Tissue Response to Impact Loads Delivered Using a Hand-Held Instrument for Studying Articular Cartilage Injury. *Cartilage*. 2015;6(4):226–232. doi:10.1177/1947603515595071.

24. Alexander PG, Song Y, Taboas JM, et al. Development of a Spring-Loaded Impact Device to Deliver Injurious Mechanical Impacts to the Articular Cartilage Surface. *Cartilage*. 2012;4(1):52–62. doi:10.1177/1947603512455195.

25. Gavriilidis C, Miwa S, Zglinicki von T, Taylor RW, Young DA. Mitochondrial dysfunction in osteoarthritis is associated with down-regulation of superoxide dismutase 2. *Arthritis & Rheumatism*. 2013;65(2):378–387. doi:10.1002/art.37782.

26. Stackley KD, Beeson CC, Rahn JJ, Chan SSL. Bioenergetic Profiling of Zebrafish Embryonic Development. Kowaltowski AJ, ed. *PLoS ONE*. 2011;6(9):e25652. doi:10.1371/journal.pone.0025652.t002.

27. Schuh RA, Clerc P, Hwang H, et al. Adaptation of microplate-based respirometry for hippocampal slices and analysis of respiratory capacity. McKenna MC, Schousboe A, eds. *J Neurosci Res*. 2011;89(12):1979–1988. doi:10.1002/jnr.22650.

28. Goetz JE, Coleman MC, Fredericks DC, et al. Time-dependent loss of mitochondrial function precedes progressive histologic cartilage degeneration in a rabbit meniscal destabilization model. *J Orthop Res*. June 2016. doi:10.1002/jor.23327.

29. Goodwin W, McCabe D, Sauter E, et al. Rotenone prevents impact-induced chondrocyte death. *J Orthop Res*. 2010:n/a–n/a. doi:10.1002/jor.21091.

30. Huser CAM, Peacock M, Davies ME. Inhibition of caspase-9 reduces chondrocyte apoptosis and proteoglycan loss following mechanical trauma. *Osteoarthritis and Cartilage*. 2006;14(10):1002–1010. doi:10.1016/j.joca.2006.03.012.

31. Diaz-Romero J, Gaillard JP, Grogan SP, Nesic D, Trub T, Mainil-Varlet P. Immunophenotypic analysis of human articular chondrocytes: changes in surface markers associated with cell expansion in monolayer culture. *J Cell Physiol*. 2005;202(3):731–742. doi:10.1002/jcp.20164.

32. Schnabel M, Marlovits S, Eckhoff G, et al. Dedifferentiation-associated changes in morphology and gene expression in primary human articular chondrocytes in cell culture. *Osteoarthr Cartil*. 2002;10(1):62–70. doi:10.1053/joca.2001.0482.

33. Benya PD, Shaffer JD. Dedifferentiated chondrocytes reexpress the differentiated collagen phenotype when cultured in agarose gels. *Cell*. 1982;30(1):215–224.

34. Champagne AM, Benel L, Ronot X, Mignotte F, Adolphe M, Mounolou JC. Rhodamine 123 uptake and mitochondrial DNA content in rabbit articular chondrocytes evolve differently upon transfer from cartilage to culture conditions. *Exp Cell Res*. 1987;171(2):404–410.

35. Olsen RKJ, Cornelius N, Gregersen N. Redox signalling and mitochondrial stress responses; lessons from inborn errors of metabolism. *J Inherit Metab Dis*. 2015;38(4):703–719. doi:10.1007/s10545-015-9861-5.

36. Soubannier V, McBride HM. Positioning mitochondrial plasticity within cellular signaling cascades. *Biochim Biophys Acta*. 2009;1793(1):154–170. doi:10.1016/j.bbamcr.2008.07.008.

37. Mazzeo AT, Beat A, Singh A, Bullock MR. Experimental Neurology. *Experimental Neurology*. 2009;218(2):363–370. doi:10.1016/j.expneurol.2009.05.026.

38. Sullivan PGEA. Cyclosporin A Attenuates Acute Mitochondrial Dysfunction Following Traumatic Brain Injury. October 1999:1–9.

39. Curl WW, Krome J, Gordon ES, Rushing J, Smith BP, Poehling GG. Cartilage injuries: a review of 31,516 knee arthroscopies. *Arthroscopy*. 1997;13(4):456–460.

40. Cole BJ, Gomoll AH. *Biologic Joint Reconstruction: Alternatives to Arthroplasty*. Slack Incorporated; 2009.

41. Madeti BK, Chalamalasetti SR, Bolla Pragada SKSSR. Biomechanics of knee joint — A review. *Front Mech Eng*. 2015;10(2):176–186. doi:10.1007/s11465-014-0306-x.

42. Novakofski KD, Berg LC, Bronzini I, et al. Joint-dependent response to impact and implications for post-traumatic osteoarthritis. *Osteoarthritis and Cartilage*. 2015;23(7):1130–1137. doi:10.1016/j.joca.2015.02.023.

43. Szafranski JD, Grodzinsky AJ, Burger E, Gaschen V, Hung H-H, Hunziker EB. Chondrocyte mechanotransduction: effects of compression on deformation of intracellular organelles and relevance to cellular biosynthesis. *Osteoarthr Cartil*. 2004;12(12):937–946. doi:10.1016/j.joca.2004.08.004.

44. Rajpurohit R, Koch CJ, Tao ZL, Teixeira CM, Shapiro IM. Adaptation of chondrocytes to low oxygen tension: Relationship between hypoxia and cellular metabolism. *J Cell Physiol*. 1996;168(2):424–432. doi:10.1002/(SICI)1097-4652

45. Ströbel S, Loparic M, Wendt D, et al. Anabolic and catabolic responses of human articular chondrocytes to varying oxygen percentages. *Arthritis Research & Therapy*. 2010;12(2):R34–R34. doi:10.1186/ar2942.

46. Schneider N, Mouithys-Mickalad A, Lejeune J-P, et al. Oxygen consumption of equine articular chondrocytes: Influence of applied oxygen tension and glucose concentration during culture. *Cell Biol Int*. 2007;31(9):878–886. doi:10.1016/j.cellbi.2007.02.002.

47. Zhou S, Cui Z, Urban JPG. Factors influencing the oxygen concentration gradient from the synovial surface of articular cartilage to the cartilage-bone interface: A modeling study. *Arthritis & Rheumatism*. 2004;50(12):3915–3924. doi:10.1002/art.20675.

48. Grimshaw MJ, Mason RM. Bovine articular chondrocyte function in vitro depends upon oxygen tension. *Osteoarthr Cartil*. 2000;8(5):386–392. doi:10.1053/joca.1999.0314.

49. Kurz B, Lemke A, Kehn M, et al. Influence of tissue maturation and antioxidants on the apoptotic response of articular cartilage after injurious compression. *Arthritis & Rheumatism*. 2004;50(1):123–130. doi:10.1002/art.11438.

50. Farnsworth NL, Antunez LR, Bryant SJ. Influence of chondrocyte maturation on acute response to impact injury in PEG hydrogels. *Journal of Biomechanics*. 2012;45(15):2556–2563. doi:10.1016/j.jbiomech.2012.07.035.

51. Jadin KD. Depth-varying Density and Organization of Chondrocytes in Immature and Mature Bovine Articular Cartilage Assessed by 3D Imaging and Analysis. *Journal of Histochemistry and Cytochemistry*. 2005;53(9):1109–1119. doi:10.1369/jhc.4A6511.2005.

Supplement 4.1 - *Detailed methods*

Microscale Respirometry

Each well of a specialized XF24 islet capture microplate (Seahorse Biosciences) was pre-loaded with assay media (bicarbonate-free DMEM supplemented with 2.5mM glucose, 2mM L-glutamine, 2 mM pyruvate, and 1% FBS.) The XF sensor cartridge is equipped with 4 injection ports per well, which allow automated addition of drugs during the experiment. Approximately one hour prior to experimentation, three of the four injection ports were preloaded with MT inhibitors to perform a MT stress test. Concentrations for MT inhibitors were determined by preliminary dose response optimization assays. The sensor cartridge was allowed to equilibrate in a 0%-CO_2 incubator prior to being loaded into the XF24 analyzer for calibration.

Cartilage slices were prepared as follows; immediately following cartilage injury, a 3mm biopsy punch was used to harvest 2 cylindrical plugs from each explant. These plugs were then trimmed to 500um thickness from the articular surface using a custom jig cartilage using a custom cutting jig and tissue slicer blade (Thomas Scientific, Swedesboro, NJ). Cartilage was kept hydrated, each cut was performed with a new and lubricated instrument, and handling of the tissue was strictly minimized. Cartilage slices (n = 20 per assay; 3mm diameter by 500μm thick) were loaded into the islet capture plate, articular surface facing up, then the capture screens were snapped in place to retain the cartilage at the bottom of each well. Four wells containing media only served as background control wells. The plate was equilibrated in a 0%-CO_2 incubator for one hour and then loaded into a Seahorse XF24 analyzer for analysis. The time between cartilage impact and start of the assay was a mean of 154 minutes (range 143-167).

Image analysis

Digital image analysis was carried out using ImageJ software (Mac OS X version 10.2, Wayen Rasband, U.S. National Institutes of Health, Bethesda, MD, USA; website: http://rsb.info.nih.gov/ij/download.html) with macros customized for each imaging channel. Key parameters including pixel intensity threshold and max/min particle size were optimized based on manual counts of a minimum of 5 z-stacks obtained from both control and impacted explants. Following optimization, all images were digitally analyzed using the same macro as follows: Each individual image in a stack was thresholded based on mean pixel intensity of that image, then individual particles were identified and counted based on particle size. A mean value (e.g. # of dead cells) for each stack was calculated by averaging the values for all 10 images in that stack and excluding any image outside one standard deviation of the mean. This was done to minimize any potential artifact from the cut surface in the superficial slices and/or differential changes in signal intensity between channels based on imaging depth in the deep slices, and resulted in exclusion of approximately one image per stack (range 0-2). At least two stacks were acquired per explant (mean 3, range 2-4), and final reported values are the mean for all stacks acquired of that explant.

Normalization of respirometry data

Calculation of cell density: For each image, the imaging field was set at 512pixels (775um) wide, and the depth of imaged tissue from articular surface to the bottom of the imaging field was measured digitally using the ImageJ software measuring tool, with the average depth of 700(±22.8)μm. The volume of tissue imaged was calculated as the width x average depth x 10μm slices. This resulted in an average calculated chondrocyte density of 0.22×10^6 cells/mm^3, which

is in excellent agreement with Jadin, et al., who used more sophisticated technique (3D image analysis) to measure cell density in fetal and calf MFC. They estimated density of 0.3 $x10^6$ cells/mm^3 at the articular surface and $0.15x10^6$ cells/mm^3 at a depth of 0.5mm from the articular surface.[51]

Calculation of explant volume: Following completion of the XF assay, explant discs were bisected, placed cut-surface down on a glass cover slip and imaged using an inverted light microscope. Digital images were obtained and the volume of each explant was calculated using ImageJ software by 2 methods; 1) the diameter of each explant was measured using the line measuring tool, 6-8 thickness (height) measurements were obtained at 90° to the diameter measurement, then the volume of the cylinder was calculated as = π $(diameter/2)^2$ x mean thickness, and 2) cross-sectional area of each hemi-cylinder was measured using the tracing tool, then the volume of the explant was calculated as = π * $radius^2$ (area of cut surface/diameter). Values for individual explant volume were obtained by averaging the tissue volume obtained using both methods of calculation.

Supplementary Figures

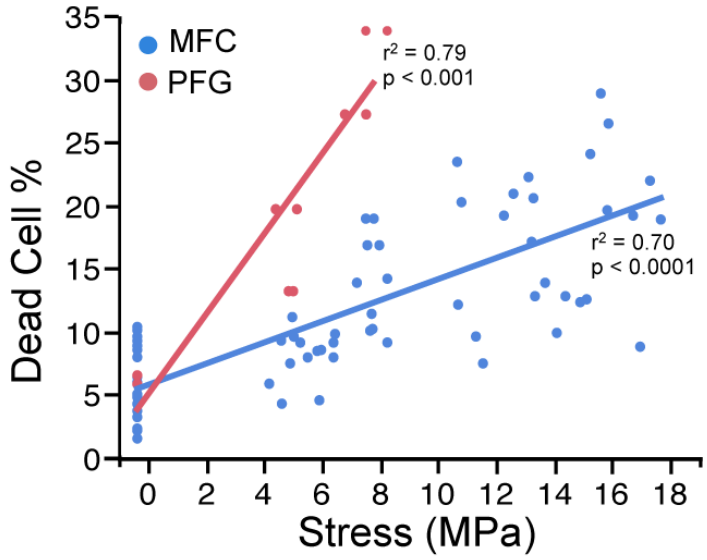

Figure S4.1. Chondrocyte death is correlated with impact magnitude. Cell death was positively correlated with peak impact stress for both the MFC and PFG (PFG $r^2 = 0.79$, $p<0.001$; MFC $r^2 = 0.70$, $p<0.0001$). Data presented is for all impacts performed throughout this study.

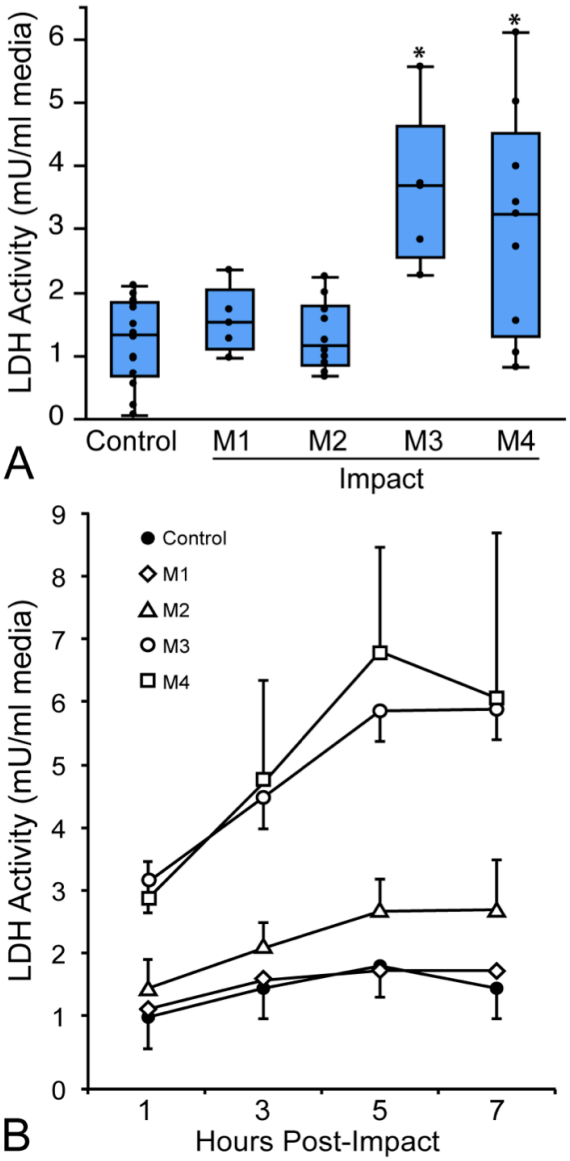

Figure S4.2. Cartilage impact results in cell membrane damage. Cell membrane damage was quantified in cartilage explants from the medial femoral condyle by performing lactate dehydrogenase (LDH) activity assay on cartilage-conditioned media following respirometry assay. A) Cell damage was increased in explants impacted at higher magnitudes (M3 and M4) compared to un-impacted controls; Asterisks denote significant increase compared to controls at $p < 0.05$. B) LDH activity in cartilage conditioned media peaks at approximately 5-7 hours after impact. Error bars = ±s.d.

CHAPTER 5

MITOPROTECTION AS A NEW STRATEGY TO PREVENT CHONDROCYTE DEATH AND CARTILAGE DEGENERATION FOLLOWING INJURY

Michelle L. Delco, DVM[1], Edward D. Bonnevie[2], Hazel S. Szeto, MD, PhD[3], Lawrence J. Bonassar, PhD[2,4], Lisa A. Fortier, DVM, PhD[1]

[1]Department of Clinical Sciences, College of Veterinary Medicine, Cornell University, Ithaca, NY

[2]Sibley School of Mechanical and Aerospace Engineering, Cornell University, Ithaca, NY

[3]Department of Pharmacology, Weill Cornell Medical College, New York, NY

[4]Meining School of Biomedical Engineering, Cornell University, Ithaca, NY

Abstract

Objective: No disease modifying osteoarthritis (OA) drugs are available to prevent posttraumatic osteoarthritis (PTOA), and mounting evidence suggests that intervention must occur shortly after injury to slow or halt disease progression. Mitochondrial (MT) dysfunction plays a central role in aging and mediates the pathogenesis of many complex, degenerative diseases including syndromes that develop secondary to traumatic injury. MT dysfunction is well documented in the later stages of OA, and recent evidence indicates that MT dysfunction is a peracute (within minutes to hours) response of cartilage to mechanical injury. A novel class of MT-targeted peptide antioxidants has been found to have preclinical efficacy in treating several diseases by targeting and stabilizing the MT-specific phospholipid, cardiolipin. The effect of these peptides on cartilage have not previously been investigated. The goal of this study was to investigate targeted mitoprotection as a strategy to prevent chondrocyte death and cartilage degeneration after injury.

Methods: Cartilage was harvested from the knee joints of 6 neonatal bovids. Cartilage explants were subjected to single, rapid impact (24.0 ±1.4 MPa peak stress; 53.8 ±5.3 GPa/s peak stress rate) using a subcritical damage model. Explants (n = 7/group) were treated with SS-31 (1uM) immediately after injury (T0), one hour following injury (T1), or 6 hours after injury (T6), and then cultured for 7 days. Cartilage conditioned media was sampled at 0, 1, and 6 hours, then every 24 hours after injury for up to 7 days. Explants were stained with calcein AM and ethidium homodimer to quantify live and dead chondrocytes, respectively at 1 and 7 days after injury using confocal microscopy. Live, dead, and total cell numbers were quantified in z-stacked digital images using a custom ImageJ macro. To quantify cell membrane damage, cartilage conditioned media was analyzed using a colorimetric lactate dehydrogenase (LDH) activity

assay, and cumulative cell membrane damage over the 7-day incubation period was determined for each explant. Cartilage matrix degradation was quantified by measuring GAG loss into the media via DMMB assay.

Results: SS-31 treatment at 0, 1, or 6 hours after impact significantly reduced chondrocyte death at 24 hours ($P < 0.001$), resulting in chondrocyte viability similar to that of un-injured controls. This effect was sustained for up to a week in culture, with chondrocyte viability in all groups similar on day 1 and 7 after injury. SS-31 prevented impact-induced apoptosis at 1 day ($p = 0.007$) and 7 days ($p = 0.04$) after cartilage injury. Cumulative cell membrane damage over the 7 days following injury was 2-fold lower in treated than untreated cartilage. Impact-induced GAG loss was decreased by ~30% in explants treated with SS-31 ($p = 0.002$).

Conclusions: This study is the first investigation of targeted mitoprotective therapy in cartilage. Our data demonstrate that SS-31 prevents chondrocyte death, cell membrane damage, and cartilage matrix degradation after cartilage injury. These results suggest that even when treatment is delayed by up to 6 hours after injury, mitoprotection may be a useful strategy in the prevention of PTOA.

Introduction

Bioenergetic failure, cumulative oxidative stress, and MT-mediated apoptosis are implicated in the pathogenesis of a wide variety of degenerative diseases, including neurodegenerative diseases, metabolic disorders and syndromes initiated by trauma.[1-3] A significant body of evidence suggests that MT dysfunction occurs in the later stages of osteoarthritis (OA), and MT-associated disease pathways are linked to chronic OA changes including decreased synthesis of extracellular matrix proteins, pathologic calcification of cartilage and upregulation of catabolic cytokines including MMP 1, 3, and 13.[4-13] One notable study demonstrating MT respiratory dysfunction in chondrocytes isolated from OA patients, with lower spare respiratory capacity and higher proton leak compared to healthy chondrocytes.[5] They also demonstrated that OA cartilage has higher levels of oxidative damage to lipid membranes, and that these changes are associated with depletion of the MT-specific antioxidant superoxide dismutase-2 (SOD_2).

Increasing experimental evidence also suggests that MT dysfunction plays a role in the pathogenesis of early OA. Redox imbalance and apoptosis are prominent features of early PTOA, and ROS are well established early mediators of the disease.[6,9-13] MT-derived ROS have also been linked to chondrocyte death after cartilage injury.[14,15] In an *in vitro* model of chronic, moderate cartilage overloading, MT respiratory function and ATP production declined and oxidative stress occurred after one week.[16] Several recent studies have also identified MT dysfunction in experimental models of early-chronic post-traumatic POTA. For example, chondrocyte respiratory function was found to be reduced 4 weeks after surgical destabilization of the medial meniscus (DMM) in rabbits.[17] In mice, MT superoxide overproduction and SOD_2 down regulation occurred in knee cartilage 2 weeks after DMM.[7] The same group demonstrated

accelerated cartilage destruction in aged (12 month) chondrocyte-specific SOD_2-knockout mice (SOD-2 cKO). Chondrocytes isolated from young SOD-2 cKOs displayed MT depolarization, decreased MT respiratory function and swollen MT, with disrupted cristae structure on electron microscopy. They went on to show that proteoglycan content was decreased and extracellular matrix metabolism was impaired by down regulation of anabolic genes and upregulation of catabolic genes, including MMP-13. These findings indicate that MT respiratory dysfunction and redox imbalance due to overproduction of ROS by MT and/or deficient MT-antioxidant defenses very likely play an important role in the early pathogenesis of OA.

Evidence for the central role of MT dysfunction in OA has led to interest in developing clinical therapies that target MT-associated pathways. For example, many groups have found free radical scavengers such as N-acetyl cysteine and vitamin C, to be protective in animal models of PTOA, however antioxidants have not provided benefit in clinical OA patients.[4,7,18,19] This may be due to their inability to penetrate cell membranes and reach the MT, where ROS are generated.[20,21] Caspase inhibitors, including synthetic inhibitors of caspase 3 and 9, prevent MT-mediated cell death by preventing activation of the caspase cascade and apoptosis *in vitro*, but have not been tested clinically.[18,22] These promising drugs act on MT-associated pathways of cell death and cartilage degradation but target downstream consequences of MT dysfunction. Ideally, to prevent the initiation and progression of PTOA, interventions would be target the very earliest disease pathomechanisms.[23] Therefore, the concept of targeting MT directly is attractive, however no mitoprotective therapies have been investigated as potential disease modifying OA drugs.

A novel class of MT-targeted peptide antioxidant drugs, Szeto-Schiller (SS) peptides are currently being developed as mitoprotective therapeutics.[21] SS peptides are water soluble, cell-

permeable, and concentrate over 1000 fold in the inner MT membrane. One member of this class, SS-31 prevents MT dysfunction, improve MT bioenergetics, reduce MT ROS generation, inhibits MT depolarization and prevents caspase-3 activation in addition to directly scavenging ROS.[1,21] SS-31 exerts all of these effects through its specific interaction with the MT-specific phospholipid, cardiolipin (CL).[24,25]

Cardiolipin is exclusively expressed on the inner MT membrane, and comprises ~10% of its content.[26] The conical structure of CL promotes curvature of the inner MT membrane and formation of cristae structure. Curvature of the inner MT membrane and CL rafts allow electron transport chain proteins to form supercomplexes, and anchors the non-integral/soluble cytochrome C to the inner MT membrane. By arranging and maintaining the electron transport chain proteins in close proximity, CL improves the efficiency of electron transfer, optimizing ATP production and reducing ROS generation. CL also modulates the opposing actions of cytochrome C, which can either execute the rate-limiting step of oxidative phosphorylation, or dissociate from the inner MT membrane and trigger apoptosis.[27] During MT stress, peroxidation of CL results in loss of cristae structure, a decline in ATP production and dissociation of cytochrome C form the inner MT membrane, setting the stage for apoptosis. SS-31 selectively binds and protects cardiolipin from oxidation, thereby preserving MT cristae structure, promoting electron transfer and inhibiting ROS production.[25]

SS-31 is currently in stage II clinical trials for the treatment of several MT-mediated diseases including acute coronary syndrome, renal failure, MT myopathy and diabetic retinopathy.[25,28] SS-31 has not previously been studied in cartilage. The goals of this study were to test mitoprotection as a strategy to prevent PTOA, and investigate the therapeutic window for treatment after injury. Specifically, we tested if SS-31 can prevent impact-induced chondrocyte

death and cartilage degeneration, and if mitoprotective efficacy is affected by the time of administration after impact.

Methods

Tissue harvest

Full thickness cartilage explants were harvested from the knee joints (n = 12 joints) of healthy bovids (n = 6 animals, 1-3 days of age) within 48 hours of sacrifice using an 8mm biopsy punch. Specimens were rinsed in phosphate-buffered saline (PBS), trimmed to a uniform thickness of 3mm from the articular surface using a custom jig, and placed in cartilage explant media (phenol free DMEM containing 1% FBS, HEPES 0.025ml/ml, penicillin 100U/mL, streptomycin 100U/mL and .1g/L glucose). Experiments were approved by Cornell University's Institutional Animal Care and Use Committee.

Rapid impact injury model

Explants were subjected to injury using validated rapid-impact model, or served as un-impacted controls, as previously described.[29] Briefly, explants were positioned in a well containing PBS under the plane-ended tip of a spring-loaded impacting device.[30,31] The impactor was used to deliver a single, rapid cycle of unconfined axial compression (24.0 ±1.4 MPa peak stress; 53.8 ±5.3 GPa/s peak stress rate). Impact force was measured at 50 kHz by a load cell (PCBPiezotronics, Depew, NY) attached to the impactor tip. Voltage from the load cell was recorded with a custom LabVIEW program (NI, Austin TX). The impact magnitude was adjusted by setting the deflection of the impactor's internal spring and mechanical parameters for each impact were calculated as previously described.[29]

SS-31 treatment

Following injury, explants were cut perpendicular to the articular surface into 2 hemicylinders using a custom cutting jig to ensure uniform geometry. Cartilage was kept moist at all times and each cut was performed with a fresh (unused) and lubricated cutting instrument. Handling of the experimental tissues was strictly minimized at each step. Explants were placed directly into an individual well of a 24-well untreated tissue culture plate containing a known volume (1.5ml) of cartilage explant media. Cartilage hemicylinders were randomly assigned to one of 8 treatment groups (n = 7/group, **Figure 5.1**). Injured (I) and uninjured control (C) explants in the non-treated groups (IT_X, CT_X) were placed into wells containing only media. Explants in the time zero treatment groups (IT_0, CT_0) were placed directly into media containing SS-31 (1μM). Explants in the one-hour treatment groups (IT_1, CT_1), were placed into media, and SS-31 (1μM) was added to the wells 1 hour after impact. In the final groups (IT_6, CT_6), SS-31 was added 6 hours after impact (**Figure 5.1**). Explants were maintained under standard tissue culture conditions (36°C and 21% O_2) for 7 days. Medium was sampled at 1, 6, and 24 hours, and at 3, 5, and 7 days after impact, and stored at -80°C until biochemical assays were performed. Culture media was replaced with fresh media (no SS-31) after 24 hours, then every other day for the duration of the experiment. After imaging was complete on day 7, cartilage explants were lyophilized and weighed for normalization of LDH and DMMB data.

Chondrocyte viability

At 1 or 7 days, cartilage was rinsed three times, then placed in PBS containing calcein AM (2uM) and ethidium homodimer (1uM) for 30 minutes at 37°C in the dark, to stain live and

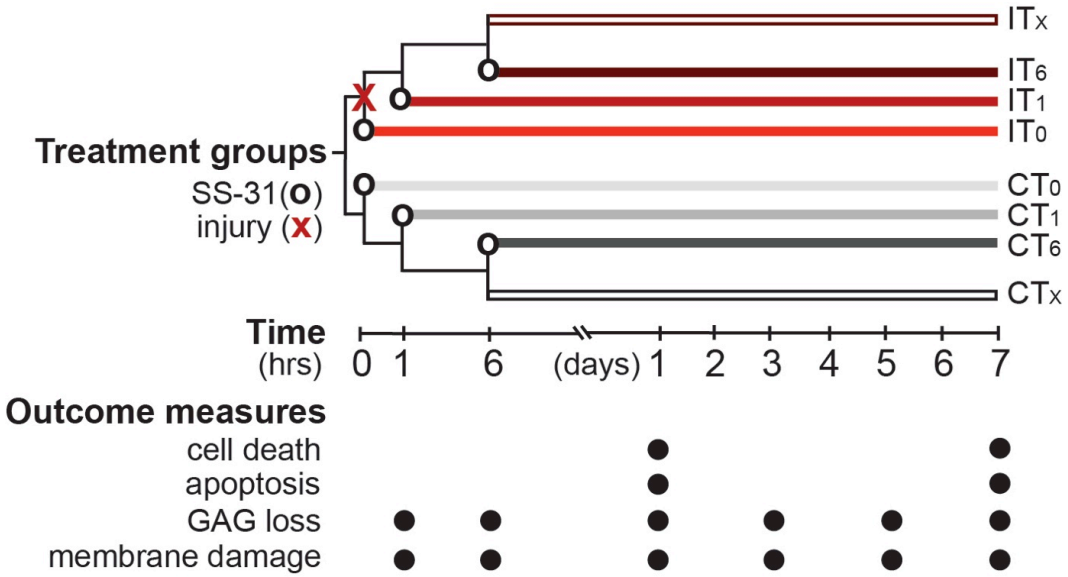

Figure 5.1. Study design. Half the cartilage explants were impacted (**X**) at time 0. Injured groups (I; red bars) and non-injured groups (C; grey bars) were then treated (**O**) with SS-31 (1μM) at time zero (T_0), 1 hour after injury (T_1), 6 hours after injury (T_6), or left untreated (T_X). Explants were imaged on day 1 or 7 for cell death or apoptosis, and cartilage conditioned medium was collected at 1 hour, 6 hours and 1, 3, 5 and 7 days after injury to assess cartilage matrix degeneration (GAG loss) and cell membrane damage.

dead cells, respectively. Explants were then rinsed in PBS and imaged on a Leika SP5 confocal microscope. Digital z-stacked images were acquired in two channel sequential scans (green; 488/498-544 and red; 514/563-663 nm excitation/emission, respectively) using a modified 3D scanning protocol consisting of 10 z-stacked 512x512 pixel (387.5µm x387.5µm) images spaced 10um apart in the z plane at 10x magnification.

The number of live, dead, and total cells in each image was quantified using a custom ImageJ (Mac OS X version 10.2, Wayen Rasband, U.S. National Institutes of Health, Bethesda, MD) macro. Pixel intensity threshold, max/min particle size, and particle circularity were optimized for each imaging channel based on manual counts of a minimum of 5 z-stacks obtained from control and impacted explants. Following optimization, all images were digitally analyzed using the same macro as follows: red and green channels for each image were thresholded based on mean pixel intensity of that image, then individual particles were identified and counted based on particle size and circularity. For each image, the % of dead cells was calculated as the number of dead cells counted in the red channel divided by the total number of cells (live + dead) counted in both channels. To minimize artifact from cell death occurring at the cut surface, the average % dead cell for all images in a z-stack was calculated, and any individual image with a value outside one standard deviation from the mean was excluded from analysis. This resulted in few images being excluded (mean 1 image per stack, range 0-2). The final reported values for live, dead and total cells were calculated as the mean of a minimum of 3 z-stacks obtained for each explant.

Apoptosis (activated caspase staining)

At 1 or 7 days cartilage was rinsed with PBS three times, then placed in PBS containing CellEvent Caspase 3/7 (Molecular Probes, Eugene, OR) to stain for activated caspase activity. Explants were imaged in on a Leika SP5 confocal microscope. Digital z-stacked images were acquired in two channel sequential scans (488/498-544 excitation/emission, respectively to image apoptotic cells and reflectance to highlight collagen in the extracellular matrix) using a modified 3D scanning protocol consisting of 10 z-stacked 512x512 pixel (387.5μm x387.5μm) images spaced 10um apart in the z plane at 10x magnification. The number of caspase-positive cells per field were counted using a custom ImageJ macro, as described above and expressed as the number of apoptotic cells per mm^2.

Cell membrane damage

Imaging studies were validated with biochemical assays performed on cartilage-conditioned media. As a measure of cell membrane damage, the release of lactate dehydrogenase (LDH) from cartilage explants into culture media was quantified using an LDH activity assay (Sigma-Aldrich) that detects NADH, which is reduced from NAD by LDH. The assay was executed per the manufacturer's instructions. Briefly, equal volumes of cartilage conditioned media and kit reagent were added to a 96-well assay plate (Corning, Corning, NY) and absorbance was measured at 450nm in 5-minute intervals by a spectrophotometric microplate reader (Tecan Safire; Männedorf, Switzerland). Using a standard curve generated by dilutions of NADH, LDH activity was calculated following subtraction of background media values and expressed as milliunits of LDH per ml of cartilage conditioned media.

Cartilage GAG loss

To determine if SS-31 could provide structural protection after impact injury, the loss of glycosaminoglycan (GAG) was determined by routine 1,9-dimethyl-methylene blue dye binding (DMMB) assay, as previously described.[32] Briefly, media samples were digested using papain (Sigma Aldrich, St. Louis, MO) 0.25 mg/ml at 65°C for 4 hours. A standard curve was prepared using chondroitin-4-sulfate (Sigma Aldrich). Equal volumes of sample and DMMB dye (Sigma Aldrich) were mixed in a 96-well plate. Total GAG content was read fluorometrically, and expressed as the total GAG released into cartilage conditioned media over the culture period per μg dry weight of cartilage.

Statistical analysis

Data were analyzed using a linear mixed effects model, with a random effect of trial and fixed effects of injury (I, C), treatment time (T_X, T_0, T_1, T_6), and response time, including all interactions. Comparisons between groups were performed using Tukey's HSD method. Residual analyses were performed to ensure the assumptions of normality and homogeneous variance were met. Differences were considered statistically significant when $p \leq 0.05$. All statistical analyses were performed using JMP Pro Version 11.0 (SAS Inc.) software.

Results

Chondrocyte death and apoptosis

Cartilage impact resulted in a roughly 3-fold increase in the amount of cell death at 1 day post-injury (**Figure 5.2a**). At 1 day, SS-31 potently reduced cell death in all injured treatment

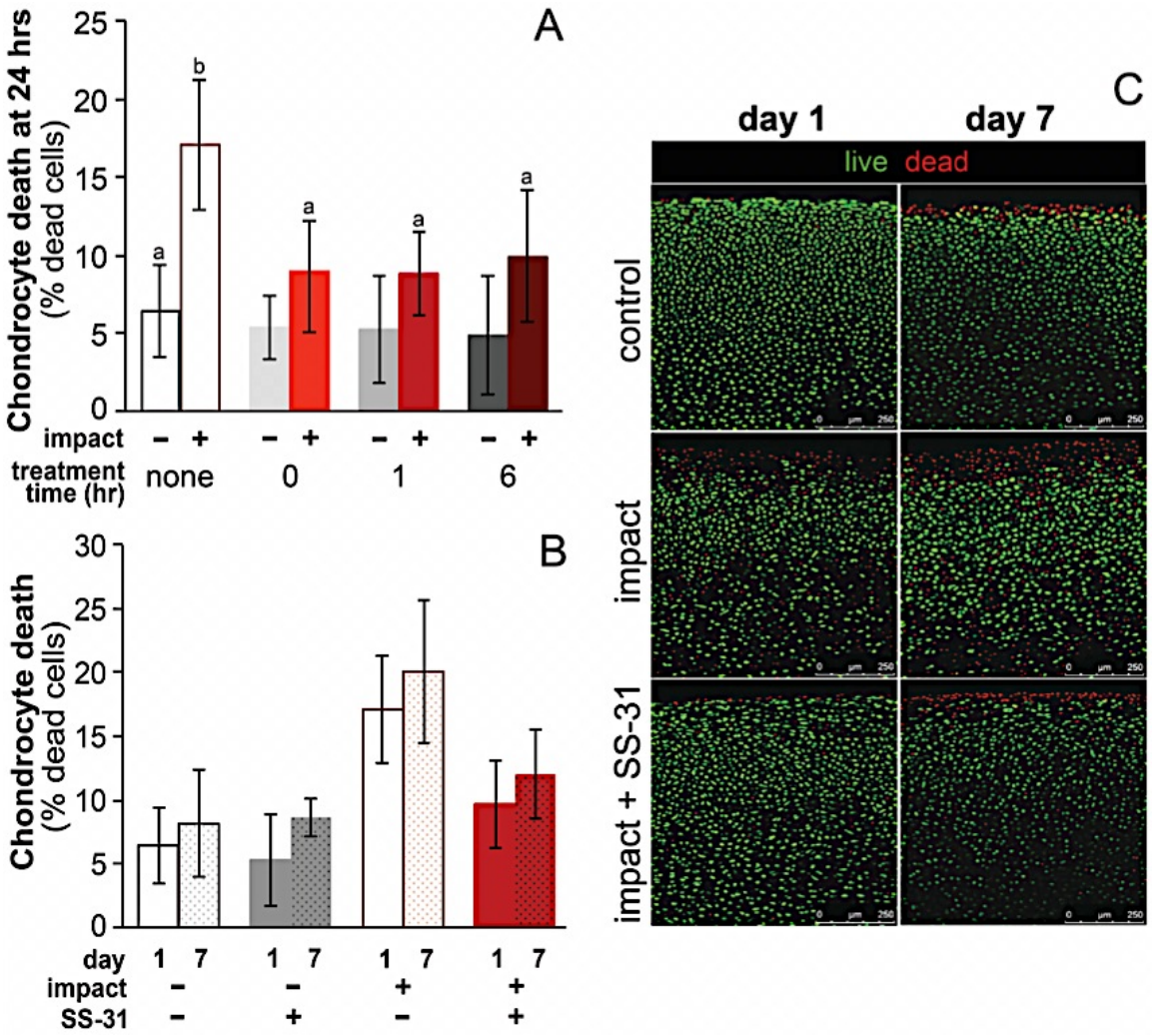

Figure 5.2. SS-31 prevents impact-induced chondrocyte death at day 1 and day 7.

A) Chondrocyte death (% dead cells) in injured explants treated with SS-31 at 0, 1, or 6 hours was equivalent to uninjured controls. Timing of treatment did not affect chondrocyte viability. B) SS-31 was effective at preventing chondrocyte death on day 1 and 7 post-impact. C) Representative confocal images of uninjured (control), injured (impact) and injured, treated (impact + SS-31) cartilage on day 1 and 7. Explants are stained for live and dead cells with calcein AM (green) and ethidium homodimer (red), respectively. Groups that do not share a letter are significantly different at $p \leq 0.05$. Error bars = ±s.d.

groups (IT_0; $p = 0.0007$, IT_1; $p < 0.0001$, IT_6; $p = 0.0003$); this equates to over 50% reduction in impact-induced chondrocyte death in treated versus untreated explants (IT_X). In all injury + treatment groups, chondrocyte viability was similar to un-injured controls (CT_X; $p = 0.16$). Cell death also did not differ between injury groups treated at 0, 1, or 6 hours, indicating no effect of treatment time ($p = 0.93$). When chondrocyte viability was assessed on day 7, the same trends were present; SS-31 prevented impact-induced cell death to a similar degree, regardless of whether treatment was applied immediately following, at 1 hour or at 6 hours after impact (**Figure 5.2**). Note that since no effect of treatment time was detected on day 1 or day 7, groups T_0, T_1 and T_6 were collapsed and represented as a single treatment group in Figures 5.2b – 5.4. Cell death was not significantly different on day 1 and day 7 in uninjured, non-treated (CT_X) explants ($p = 0.98$), indicating baseline chondrocyte viability was maintained for the 7-day culture period (**Figure 5.2**).

Activated caspase 3/7 staining of injured explants on day 1 and 7 revealed an increase in the number of apoptotic cells throughout the depth of the cartilage (**Figure 5.3**). SS-31 prevented impact-induced apoptosis at 1 day ($p = 0.007$) and 7 days ($p = 0.04$) after cartilage injury. There was a trend toward fewer apoptotic cells on day 7 than day 1 in all groups, most notably in injured, treated explants but this difference did not reach statistical significance ($p = 0.07$).

Cell membrane damage and cartilage GAG loss

Cumulative cell membrane damage, quantified by LDH activity in cartilage conditioned media over the 7 days following injury, was approximately twofold lower after injury in treated than untreated cartilage ($p = 0.0005$, **Figure 5.4**). SS-31 also appears to have a protective effect

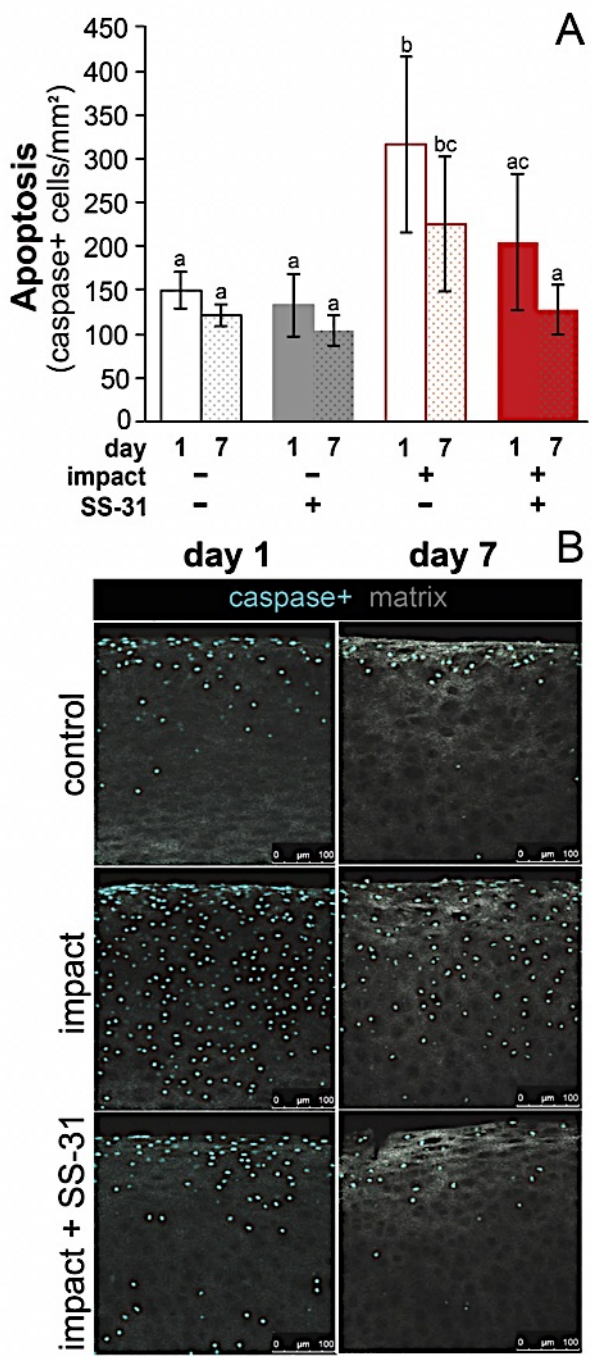

Figure 5.3. SS-31 prevents impact-induced apoptosis. A) Apoptosis in injured explants treated with SS-31 was equivalent to uninjured controls at day 1 and 7. B) Representative confocal images of uninjured (control), injured (impact) and injured, treated (impact + SS-31) cartilage on day 1 and 7. Explants are stained for activated caspase 3 and 7 (caspase+) and imaged using reflectance to highlight collagen in the extracellular matrix (matrix.) Groups that do not share a letter are significantly different at $p \leq 0.05$. Error bars = ±s.d.

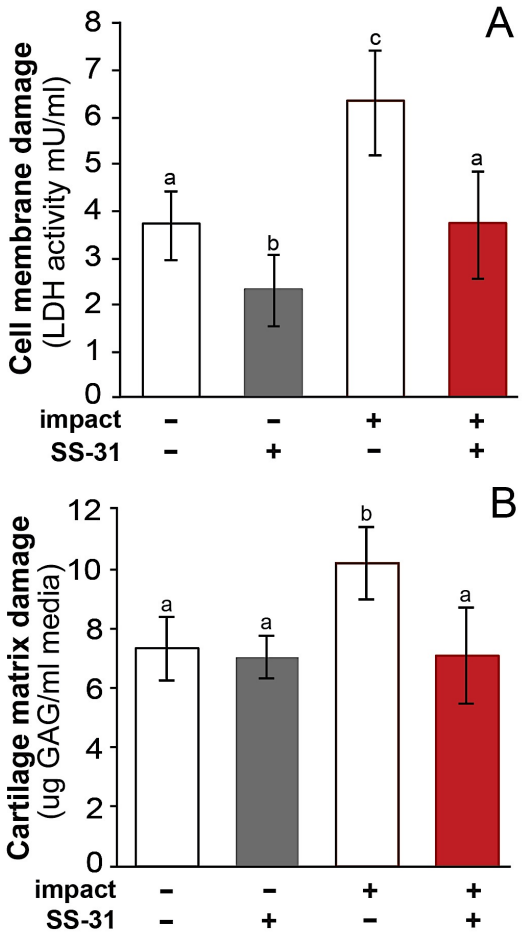

Figure 5.4. SS-31 prevents impact-induced chondrocyte membrane damage and cartilage matrix degradation. A) LDH activity in the media of injured, treated groups is lower than injured, untreated explants, and similar to uninjured controls. SS-31 also appears to have a protective effect against cell membrane damage in treated controls ($p = 0.05$). B) Cumulative GAG loss into the media on days 3-7 was increased in injured, untreated explants compared to uninjured controls. GAG loss was similar in injured, treated and control groups. Groups that do not share a letter are significantly different at $p \leq 0.05$. Error bars = ±s.d.

against cell membrane damage in uninjured controls; uninjured, treated samples had a lower cumulative LDH than untreated controls ($p = 0.05$). Impact-induced GAG loss was decreased by ~30% in explants treated with SS-31 ($p = 0.002$, **Figure 5.4**).

Discussion

The purpose of this study was to investigate the effects of mitoprotection on chondrocyte death and matrix degradation after cartilage injury. To investigate the possible clinical relevance of SS-31 as a "point-of-injury" therapy to prevent cartilage degeneration if administered in the acute stages following cartilage trauma, a time course experiment was performed. This study demonstrates that SS-31 prevents injury-induced chondrocyte death, apoptosis, cell membrane damage, and matrix degradation. Even when treatment was delayed by up to 6 hours after injury, mitoprotective therapy may be a useful strategy in the prevention of PTOA.

Somewhat surprisingly, no detectable effect of treatment time was observed in this study. Previous in vitro work indicates that cell death staining peaks at 2-3 hours following impact,[33] MT respiratory dysfunction occurs within 2 hours of impact (Chapter 4) and MT depolarization occurs within minutes of impact (un-published data, in progress). Further evidence suggests that following injury, a subset of chondrocytes experience MT-dysfunction but remain viable for an indeterminate amount of time. We therefore hypothesized that SS-31 would act to stabilize this subpopulation of cells and prevent MT-mediated cell death in the earliest treatment groups (T_0, T_1) more effectively than the T_6 group. There are several possible explanations for why no effect of treatment time was detected. First, the outcome measure of cell death (i.e. % dead cells quantified by live/dead cell staining at 1 and 7 days post-impact) measures non-specific cell death and may not be sensitive enough to detect small differences in treatment time groups.

Although calceinAM/ethidium homodimer (EtHD) staining is a commonly used to quantify chondrocyte viability, EtHD is actually an indicator of plasma membrane integrity because it gains access to the cytosol through permeabilized cell membranes, and fluoresces when bound to nucleic acids.[34] Therefore, EtHD–positive staining may identify cells at any point along a continuum between potentially rescuable cell membrane damage and death. Activated caspase 3/7 staining is a more specific measure of cells committed to apoptotic cell death, and detection of caspase activation should exclude the population of cells that presumably rupture immediately upon impact, cells with damaged cell membranes that remain viable, and cells undergoing necrotic cell death. In the current study, the outcome measure of apoptosis by treatment time sample size was low (n = 4), and individual group data were not presented. Ongoing experiments to increase statistical power, and methods to normalize the number of caspase-positive cells by total cell number rather than cartilage volume, may reveal significant differences in apoptosis between T_0, T_1 and T_6 groups. One would expect that further delaying treatment (e.g. 12 hours after impact) would reveal an effect of treatment time, and further studies are underway to identify this temporal threshold.

Although unexpected, our finding of equivalent mitoprotective efficacy with treatment delayed up to 6 hours is supported by other studies. MT-mediated cell death evolves over a slower time scale than necrotic cell death (days versus hours, respectively).[13,33,35-38] The pathway of MT-mediated cell death by apoptosis is initiated when cytochrome C (CytC) dissociates from the inner MT membrane and Bcl-2 proteins cause permeabilization of the outer MT membrane, allowing Cyt C to other MT proteins to leak into the cytosol. CytC initiates oligomerization of APAF-1, recruitment and dimerization of caspase-9 and formation of the apoptosome. Activated caspase-9 cleaves caspase-3 and -7 and these activated ‘executioner’ caspases commit the cell to

death by apoptosis. Evidence suggest these events, from MT permeabilization to caspase 3/7 activation are rapid, occurring over ~10 minutes.[39] However, the events leading up to MT permeabilization may be more gradual. In injured cartilage, delayed MT depolarization has been linked to cumulative oxidative stress as well as accumulation of specific ROS, namely NO.[13,35,40,41] Time course studies of progressive apoptosis in cartilage have been investigated by several methods, and suggest that chondrocyte apoptosis may be initiated around 6 hours and sustained for up to 7 days post-injury.[35,36,38] Therefore, it is reasonable that mitoprotection initiated at 6 hours may be sufficient to rescue cells undergoing impact induced MT-dysfunction but not yet committed to programmed cell death. Ideally, to further define the therapeutic window for mitoprotective therapy after cartilage injury, additional time-points would be investigated.

GAG release into cartilage-conditioned media is a well established indicator of cartilage injury.[38,42] In the present study we found that GAG loss was significantly increased in injury groups versus controls starting on day 3 post-injury. This is different than the findings of Patwari, et al. and others who found that GAG loss was increased in injury groups compared to controls between days 1 and 3 post-injury, but not after day 3.[42] The reason for this difference is unclear, however, is likely related to the different loading regimens employed. Patwari used a displacement controlled mechanical testing frame to deliver unconfined compression to 50% strain, while our spring-loaded impactor delivered an energy-controlled cycle of compression. The most significant difference is the rate of loading; although peak stresses in both studies were very similar (23 MPa versus 24 MPa), load in the current study was delivered over 1-2 milliseconds (~54GPa/s peak stress rate) versus 0.1-0.2 seconds by Patwari. This is important because immediate and non-sustained GAG loss, as seen in other models, suggests that the cause

is mechanical disruption of matrix rather than to cell-mediated enzymatic degradation.[42] This is supported by the finding that incubation of cartilage with protein synthesis inhibitors did not effect GAG release after injury. A lag time in injury-induced GAG release in the present study, and inhibition of GAG release by SS-31 suggests that mitoprotection prevents injury-induced cartilage matrix degradation.

This was designed as a proof-of-concept study to support the strategy of mitoprotection after cartilage injury. We therefore focused on the time-dependence of SS-31 treatment, but did not investigate dose-response. The dose 1μM was chosen based on preliminary experiments, however a full dose-response study would be useful to optimize the protective effects of this drug. *Ex vivo* studies of SS-31 peptides in other tissues suggest this drug may be effective at nanomolar concentrations. It is clinically important to note that SS-31 has no effect on normal cells and no cytotoxic or mitotoxic effects have been observed in studies at concentrations exceeding 100uM *ex vivo*, up to 10mg/kg in vivo animal models, and up to 0.25 mg kg^{-1} h^{-1} over 4 hours in human safety studies.[21]

A concern with any cartilage-targeted osteoarthritic drug is question of diffusion through the avascular, highly charged cartilage matrix. Owing to their unique chemical structure, SS peptides are extremely water soluble, while able to freely diffuse (translocate) across lipid membranes by a phenomenon known as transcellular transport.[43] This results in a volume of distribution similar to blood volume, and no accumulation in lipid, further limiting concerns for toxicity.

In summary, this study demonstrates that mitoprotection with SS-31 prevents chondrocyte death and cartilage matrix degradation, even when treatment is delayed up to 6 hours after cartilage injury. The unique properties of this class of drugs confer their ability to

provide structural protection to MT cristae by specifically interacting with cardiolipin, thereby preventing MT dysfunction.[25] Our data suggest that SS-31 has the potential to be the first effective disease modifying osteoarthritis drug.

Acknowledgements

The authors thank Lynn Johnson for statistical consulting. We thank Alexis Gale, Meg Goodale and Becky Hicks for help executing assays and for technical support. This work was supported by Weill Cornell Medical College Clinical & Translational Science Center Award/National Center for Advancing Translational Sciences (5 UL1 TR000457-09) and The Harry M. Zweig Memorial Fund for Equine Research. MD was supported by NIH 5T32OD011000-20.

References

1. Powers SK, Hudson MB, Nelson WB, et al. Mitochondria-targeted antioxidants protect against mechanical ventilation-induced diaphragm weakness. *Crit Care Med*. 2011;39(7):1749–1759. doi:10.1097/CCM.0b013e3182190b62.

2. Dai D-F, Chiao YA, Marcinek DJ, Szeto HH, Rabinovitch PS. Mitochondrial oxidative stress in aging and healthspan. *Longev Healthspan*. 2014;3:6. doi:10.1186/2046-2395-3-6.

3. Kim J-A, Wei Y, Sowers JR. Role of mitochondrial dysfunction in insulin resistance. *Circulation Research*. 2008;102(4):401–414. doi:10.1161/CIRCRESAHA.107.165472.

4. Kurz B, Lemke A, Kehn M, et al. Influence of tissue maturation and antioxidants on the apoptotic response of articular cartilage after injurious compression. *Arthritis & Rheumatism*. 2004;50(1):123–130. doi:10.1002/art.11438.

5. Gavriilidis C, Miwa S, Zglinicki von T, Taylor RW, Young DA. Mitochondrial dysfunction in osteoarthritis is associated with down-regulation of superoxide dismutase 2. *Arthritis & Rheumatism*. 2013;65(2):378–387. doi:10.1002/art.37782.

6. Ruiz-Romero C, Calamia V, Mateos J, et al. Mitochondrial dysregulation of osteoarthritic human articular chondrocytes analyzed by proteomics: a decrease in mitochondrial superoxide dismutase points to a redox imbalance. *Mol Cell Proteomics*. 2009;8(1):172–189. doi:10.1074/mcp.M800292-MCP200.

7. Koike M, Nojiri H, Ozawa Y, et al. Mechanical overloading causes mitochondrial superoxide andSOD2 imbalance in chondrocytes resulting in cartilage degeneration. *Nature Publishing Group*. June 2015:1–16. doi:10.1038/srep11722.

8. Blanco FJ, Rego I, Ruiz-Romero C. The role of mitochondria in osteoarthritis. *Nat Rev Rheumatol*. 2011;7(3):161–169. doi:10.1038/nrrheum.2010.213.

9. Del Carlo M, Loeser R. Cell death in osteoarthritis. *Curr Rheumatol Rep*. 2008;10(1):37–42. doi:10.1007/s11926-008-0007-8.

10. Maneiro E, Martín MA, de Andres MC, et al. Mitochondrial respiratory activity is altered in osteoarthritic human articular chondrocytes. *Arthritis & Rheumatism*. 2003;48(3):700–708. doi:10.1002/art.10837.

11. Johnson EO, Charchandi A, Babis GC, Soucacos PN. Apoptosis in osteoarthritis: morphology, mechanisms, and potential means for therapeutic intervention. *J Surg Orthop Adv*. 2008;17(3):147–152.

12. Terkeltaub R, Johnson K, Murphy A, Ghosh S. Invited review: the mitochondrion in osteoarthritis. *Mitochondrion*. 2002;1(4):301–319. doi:10.1016/S1567-7249(01)00037-X.

13. Lotz M, Hashimoto S, Kühn K. Mechanisms of chondrocyte apoptosis. *Osteoarthr Cartil*.

1999;7(4):389–391. doi:10.1053/joca.1998.0220.

14. Brouillette MJ, Ramakrishnan PS, Wagner VM, et al. Strain-dependent oxidant release in articular cartilage originates from mitochondria. *Biomech Model Mechanobiol*. 2014;13(3):565–572. doi:10.1007/s10237-013-0518-8.

15. Sauter E, Buckwalter JA, McKinley TO, Martin JA. Cytoskeletal dissolution blocks oxidant release and cell death in injured cartilage. *J Orthop Res*. 2012;30(4):593–598. doi:10.1002/jor.21552.

16. Coleman MC, Ramakrishnan PS, Brouillette MJ, Martin JA. Injurious Loading of Articular Cartilage Compromises Chondrocyte Respiratory Function. *Arthritis & Rheumatology*. September 2015:n/a–n/a. doi:10.1002/art.39460.

17. Goetz JE, Coleman MC, Fredericks DC, et al. Time-dependent loss of mitochondrial function precedes progressive histologic cartilage degeneration in a rabbit meniscal destabilization model. *J Orthop Res*. June 2016. doi:10.1002/jor.23327.

18. Chubinskaya S, Wimmer MA. Key Pathways to Prevent Posttraumatic Arthritis for Future Molecule-Based Therapy. *Cartilage*. 2013;4(3 Suppl):13S–21S. doi:10.1177/1947603513487457.

19. Martin JA, McCabe D, Walter M, Buckwalter JA, McKinley TO. N-acetylcysteine inhibits post-impact chondrocyte death in osteochondral explants. *J Bone Joint Surg Am*. 2009;91(8):1890–1897. doi:10.2106/JBJS.H.00545.

20. Halliwell B. The antioxidant paradox: less paradoxical now? *Br J Clin Pharmacol*. 2013;75(3):637–644. doi:10.1111/j.1365-2125.2012.04272.x.

21. Szeto HH, Schiller PW. Novel therapies targeting inner mitochondrial membrane--from discovery to clinical development. *Pharm Res*. 2011;28(11):2669–2679. doi:10.1007/s11095-011-0476-8.

22. Garrido CP, Hakimiyan AA, Rappoport L, Oegema TR, Wimmer MA, Chubinskaya S. Anti-apoptotic treatments prevent cartilage degradation after acute trauma to human ankle cartilage. *Osteoarthritis and Cartilage*. 2009;17(9):1244–1251. doi:10.1016/j.joca.2009.03.007.

23. Anderson DD, Chubinskaya S, Guilak F, et al. Post-traumatic osteoarthritis: improved understanding and opportunities for early intervention. *J Orthop Res*. 2011;29(6):802–809. doi:10.1002/jor.21359.

24. Birk AV, Liu S, Soong Y, et al. The Mitochondrial-Targeted Compound SS-31 Re-Energizes Ischemic Mitochondria by Interacting with Cardiolipin. *Journal of the American Society of Nephrology*. 2013;24(8):1250–1261. doi:10.1681/ASN.2012121216.

25. Szeto HH. First-in-class cardiolipin-protective compound as a therapeutic agent to restore mitochondrial bioenergetics. *Br J Pharmacol*. 2014;171(8):2029–2050.

doi:10.1111/bph.2014.171.issue-8.

26. Osman C, Voelker DR, Langer T. Making heads or tails of phospholipids in mitochondria. *The Journal of Cell Biology*. 2011;192(1):7–16. doi:10.1002/yea.320110602.

27. Birk AV, Chao WM, Liu S, Soong Y, Szeto HH. Biochimica et Biophysica Acta. *BBA - Bioenergetics*. 2015;1847(10):1075–1084. doi:10.1016/j.bbabio.2015.06.006.

28. Szeto HH, Birk AV. Serendipity and the Discovery of Novel Compounds that Restore Mitochondrial Plasticity. *Clin Pharmacol Ther*. September 2014. doi:10.1038/clpt.2014.174.

29. Bonnevie ED, Delco ML, Fortier LA, Alexander PG, Tuan RS, Bonassar LJ. Characterization of Tissue Response to Impact Loads Delivered Using a Hand-Held Instrument for Studying Articular Cartilage Injury. *Cartilage*. 2015;6(4):226–232. doi:10.1177/1947603515595071.

30. Alexander PG, Song Y, Taboas JM, et al. Development of a Spring-Loaded Impact Device to Deliver Injurious Mechanical Impacts to the Articular Cartilage Surface. *Cartilage*. 2012;4(1):52–62. doi:10.1177/1947603512455195.

31. Alexander PG, McCarron JA, Levine MJ, et al. An In Vivo Lapine Model for Impact-Induced Injury and Osteoarthritic Degeneration of Articular Cartilage. *Cartilage*. 2012;3(4):323–333. doi:10.1177/1947603512447301.

32. Fortier LA, Motta T, Greenwald RA, Divers TJ, Mayr KG. Synoviocytes are more sensitive than cartilage to the effects of minocycline and doxycycline on IL-1alpha and MMP-13-induced catabolic gene responses. *J Orthop Res*. 2010;28(4):522–528. doi:10.1002/jor.21006.

33. Bartell LR, Fortier LA, Bonassar LJ, Cohen I. Measuring microscale strain fields in articular cartilage during rapid impact reveals thresholds for chondrocyte death and a protective role for the superficial layer. *Journal of Biomechanics*. 2015;48(12):3440–3446. doi:10.1016/j.jbiomech.2015.05.035.

34. Kaplan LD. The analysis of articular cartilage after thermal exposure: “Is red really dead?.” *Arthroscopy: The Journal of Arthroscopic & Related Surgery*. 2003;19(3):310–313. doi:10.1053/jars.2003.50087.

35. Kühn K, D’Lima DD, Hashimoto S, Lotz M. Cell death in cartilage. *Osteoarthritis and Cartilage*. 2004;12(1):1–16. doi:10.1016/j.joca.2003.09.015.

36. Grogan SP, Aklin B, Frenz M, Brunner T, Schaffner T, Mainil-Varlet P. In vitro model for the study of necrosis and apoptosis in native cartilage. *J Pathol*. 2002;198(1):5–13. doi:10.1002/path.1169.

37. Green DM, Noble PC, Ahuero JS, Birdsall HH. Cellular events leading to chondrocyte death after cartilage impact injury. *Arthritis & Rheumatism*. 2006;54(5):1509–1517.

doi:10.1002/art.21812.

38. D'lima D. Human chondrocyte apoptosis in response to mechanical injury. *Osteoarthritis and Cartilage*. 2001;9(8):712–719. doi:10.1053/joca.2001.0468.

39. Green DR. Apoptotic Pathways: Ten Minutes to Dead. *Cell*. 2005;121(5):671–674. doi:10.1016/j.cell.2005.05.019.

40. Vaillancourt F, Fahmi H, Shi Q, et al. 4-Hydroxynonenal induces apoptosis in human osteoarthritic chondrocytes: the protective role of glutathione-S-transferase. *Arthritis Research & Therapy*. 2008;10(5):R107. doi:10.1186/ar2503.

41. Taskiran D, Stefanovic-Racic M, Georgescu H, Evans C. Nitric oxide mediates suppression of cartilage proteoglycan synthesis by interleukin-1. *Biochemical and Biophysical Research Communications*. 1994;200(1):142–148.

42. Patwari P, Cook MN, DiMicco MA, et al. Proteoglycan degradation after injurious compression of bovine and human articular cartilage in vitro: interaction with exogenous cytokines. *Arthritis & Rheumatism*. 2003;48(5):1292–1301. doi:10.1002/art.10892.

43. Zhao K. Transcellular Transport of a Highly Polar 3+ Net Charge Opioid Tetrapeptide. *Journal of Pharmacology and Experimental Therapeutics*. 2003;304(1):425–432. doi:10.1124/jpet.102.040147.

CHAPTER 6

GENERAL DISCUSSION

Thesis summary and significance

The goal of this thesis was to investigate mitochondrial dysfunction as a potential therapeutic target to prevent PTOA. Although a large body of evidence supports MT dysfunction in the early-chronic and late stages of OA, this work is the first to directly assess MT respiratory function *in situ* within hours of impact injury, and link these findings with indicators of cartilage degeneration.[1,2] We confirmed that MT respiratory dysfunction is an acute response of chondrocytes to injury. This forms the basis of our rationale to investigate mitoprotection as a point-of-care therapy to prevent PTOA after joint injury. This strategy is used in other diseases of MT dysfunction mediated by acute mechanical trauma and ischemia-reperfusion injury, for example traumatic brain injury and myocardial infarction, respectively. The concept is to limit ongoing tissue damage following the initial insult. Although not directly assessed in this body of work, SS-31 also holds promise in the treatment of established disease, and our findings have potential implications in age-related/idiopathic OA.[3-5]

Future directions

Basic science/mechanistic questions

Mechanisms of MT-related mechanotransduction in chondrocytes. Based on our work and others, it is clear that MT participate in the acute transduction of mechanical forces into cellular signaling within chondrocytes, but the exact mechanisms remain unclear.[6-9] A more

nuanced understanding of these acute-phase pathways may have important implications for the development of drug therapies as well as orthopedic regenerative medicine and tissue engineering applications.

The extent to which, and the conditions under which acute MT mechanotransduction participates in, or is mediated by soluble and/or physical/structural elements is an evolving area of investigation. Both soluble factors such as Ca^{2+}, ROS, and fibronectin fragments, as well as physical/structural elements are known to play important roles mechanotransduction pathways connecting cartilage injury to the down-stream catabolic signaling cascades responsible for irreversible cartilage degeneration.[10-14] For example, studies have implicated Ca^{2+} signaling as a primary mechanism underlying MT dysfunction in articular chondrocytes[15] and the role of ROS has been discussed throughout this thesis. Integrin signaling is involved in both soluble and structural mechanotransduction. Fragments of ECM proteins, most prominently fibronectin fragments, can bind to integrin receptors and initiate intracellular MAP kinase pathways mediated catabolic signaling.[14] In addition to integrins, many transmembrane cell surface receptors are known to transduce physical and chemical stimuli to the chondrocyte including cytokine receptors, toll-like receptors and others. For example, binding of ECM type II collagen to the receptor tyrosine kinase discoidin domain receptor (DDR) 2 activates the RAS/RAF/MEK/extracellular-regulated kinase (ERK) signaling independent of integrin and cytokine signaling, and leads to upregulation of MMP-13, the major type II collagen-degrading collagenase considered a marker for OA progression.[14]

Other physical/structural components of chondrocyte mechanotransduction include structural components of the ECM, namely type II collagen, the pericellular matrix (PCM), made up of collagen VI, fibromodulin, and matrilin, and the chondrocyte actin/myosin/intermediate

filament cytoskeleton.[16-19] The PCM plays an important role at the interface between mechanical signals and gene expression in response to compression[20] and the mechanical properties of the PCM can play a protective role by modulating local chondrocyte strain during compression.[21] Mechanical forces influence chondrocyte cytoskeletal organization and cytoskeletal components are known to play a central role in the transduction of mechanical stimuli to biochemical responses.[22,23] For example, mechanical loading causes differential deformations of organelles[24] and actin microfilaments and microtubules act to transfer strain to intracellular organelles, including the MT.[25] Direct links between these ECM-PCM-chondrocyte cytoskeletal proteins to the MT have not been well investigated in cartilage, but some evidence exists in other tissues. MT are tethered to the cytoskeleton yet are highly mobile, and evidence suggests MT use cytoskeletal proteins as tracks to move along during intracellular transport.[26] At the same time, cytoskeletal proteins influence MT dynamics (fission/fusion), shape and function in other tissues, and recent evidence suggests crosstalk between receptors that control MT organization, movement and apoptosis.[26] The mechanisms by which local mechanical forces and physical deformations of the ECM, PCM and the cytoskeleton influence chondrocyte MT function and the initiation of PTOA are questions that our group is just beginning to explore. For example, recent work by Bonnevie, et al. (*Bonnevie ED, 2016 Doctoral thesis*) suggests that chondrocyte MT depolarization is correlated with local shear strain during cartilage sliding. Furthermore, this work connects MT depolarization and chondrocyte apoptosis with increased frictional coefficients due to inadequate cartilage lubrication.

Finally, interesting research implicates the primary cilium in chondrocyte mechanosensing,[27-30] however very little information is available regarding interaction between this organelle and the MT network. In light of the current work that supports a role for MT as

acute mechanotransducers in chondrocytes, the possible physical and biochemical relationships between these organelles are intriguing and warrant investigation.

Detailed tracking of cell fate - timing and mechanisms of impact-induced chondrocyte death. Our research suggests that immediately after cartilage injury, there are at least three distinct population of chondrocytes: 1) dead cells, 2) cells that are alive and functioning normally, and 3) viable cells with MT dysfunction. What is unknown is the fate of cells in group 3. Presumably, they can either go on to die by non-specific, necrotic, or apoptotic cell death, recover and re-enter group 2, or continue to survive and remain dysfunctional, thereby contributing to ongoing tissue damage. Our ongoing studies include a more detailed investigation of the spatial and temporal distribution of MT dysfunction and cell fate after mechanical injury will provide useful insights into the mechanisms of impact-induced chondrocyte death and the critical window for mitoprotective therapy after joint injury.

Mechanism of chondroprotection by SS-peptides. Our findings indicate that targeted mitoprotective therapy prevents cell death and cartilage degeneration, however the mechanism has not been investigated in this work. Because chondrocyte metabolism is significantly different from more energy-expensive tissues such as skeletal muscle, improved bioenergetics may not be the primary means of chondroprotection by SS-31 observed in our work. Instead, the beneficial effects of SS-31 may be due to its role in reduced ROS generation and free radical scavenging. Several methods could be used to investigate this theory. Repeating the studies performed in chapter 5 with SS-20 would provide useful mechanistic insight, because SS-20 acts by a very similar mechanism as SS-31, but lacks the ability to scavenge free radicals. Transmission electron microscopy studies are in progress to evaluate the efficacy of SS-31 to protect chondrocyte MT christae structure after injury. Microrespirometry studies similar to those

performed in Chapter 4 could provide information about the effect of SS peptides on chondrocyte bioenergetic function after injury. Finally, the development of a reliable and practical assay for the immediate detection of ROS/redox imbalance/oxidative damage to lipid membranes in whole cartilage would be very useful, but to date, efforts have been unrewarding.[31,32]

Preclinical and clinical testing of mitoprotection to prevent and treat osteoarthritis

Preclinical testing of SS-31 in animal models of PTOA. Surgical destabilization (e.g., DMM) and non-invasive destabilization models of knee of PTOA in mice are well validated, relatively inexpensive, and have been used as screening tools to test many putative PTOA therapies. Limitations of these models were discussed in Chapter 2, nevertheless, a mouse study is a practical first-step to investigate the efficacy of SS-31 to prevent PTOA. Our group has work in progress to develop a method of non-invasive anterior cruciate ligament rupture in the mouse, which will be used to evaluate the efficacy of SS-31 in prevention of PTOA secondary to joint destabilization.

For the reasons outlined in Chapter 2, the next logical step, in conjunction with small animal model studies, is to test the preclinical efficacy of SS-31 in our equine model of impact-induced talocrural PTOA. Plans to further develop and validate this model include: 1) *In vivo* confocal/multiphoton cartilage imaging. Our group, in collaboration with the Cornell Imaging Core, has been working to develop an arthroscopically adapted microscope. This technology would allow us to study cellular events immediately following cartilage injury, and connect them directly with disease development in vivo. Much of the preliminary work has already been completed. Horses will undergo arthroscopic surgery, as described in Chapter 3. Following

cartilage injury, the impactor will be swapped with an aiming device, to accept an arthroscopically adapted multiphoton microscope. Sodium fluorescein will be added to the arthroscopic fluid to stain dead cells, and TMRM will be used to image MT function *in vivo*. Cartilage will be imaged for cell death, matrix cracks and MT depolarization *in vivo* for up to 4 hours. Horses will be treated with SS-31 intraarticularly, and development of PTOA will be assessed as described in Chapter 3; 2) Additional synovial fluid biomarkers of early OA that have been validated in equine PTOA models will be assessed on ELISA;[33,34] 3) Evaluation of OA- and MT-related gene expression profiles in cartilage and synovium; 4) Clinical (antemortem) and research (postmortem) grade MRI. Collaborators at the musculoskeletal MRI unit at Hospital for Special Surgery/Weill Cornell Medical College, will perform 3T MRI evaluation of the joint after euthanasia, and cartilage will be studied using quantitative T2 MRI mapping, as previously reported.[35,36] Fast spin echo sequences will be used to image the articular cartilage and surrounding soft tissues. Short tau inversion recovery and spectral fat suppression will be used to detect subchondral bone pathology. Quantitative pulse sequences will be used to assess collagen orientation and proteoglycan content.

Clinical testing of mitoprotection to prevent PTOA in veterinary patients. Veterinary orthopedic patients represent a high-risk population for development of naturally occurring PTOA. The two species that are athletic and prone to PTOA are horses and dogs. In dogs, the most common cause of lameness and the most common surgically treated orthopedic injury is rupture of the cranial cruciate ligament (CCL).[37] Most dogs diagnosed with CCL rupture display radiographic signs of OA, which often progresses despite surgical intervention.[38-40] It is therefore feasible to design a prospective, randomized clinical trial to test the efficacy of SS-31 to prevent radiographic progression of PTOA in dogs presenting for the surgical treatment of acute CCL

ruptures. Treatment could commence immediately upon diagnosis, or at the time of surgery. This would require collaboration with small animal orthopedic surgeons who perform high volumes of this procedure.

Similarly in equine patients, several candidate patient populations at risk for developing PTOA exist, including racehorses presenting for surgical repair of condylar fractures, and arthroscopic removal of osteochondral fragments of the metacarpo/metatarsophalangeal and carpal joints. Pharmacokinetic studies would be required in individual species.

Clinical trial of SS-31 in human patients. Ultimately, the goal is to test mitoprotection in human patients at risk for PTOA after joint trauma. Specific patient populations would need to be identified in order to test the point-of-care strategy. This would require large numbers of individuals at risk for a specific subset of joint injury, with a point of access to immediate medical care. One such population is members of the armed services. In deployed military personnel, ankle sprains are the most common non-combat injury with over 15% incidence in ~4000 soldiers evaluated by a doctor.[41] In military cadets, a total of 614 new ankle sprains occurred during 10,511 person-years at risk, resulting in an overall IR of 58.4 per 1000 person-years.[42] Each year, 17,000 trainees attend the U.S. Army Airborne School at Fort Benning, GA and make ~200,000 parachuting jumps. In this population, ankle injures occur at a rate of 3-6 per 1000 parachute jumps. These statistics indicate that members of the armed services are at least 5 times higher risk for ankle injury than the general population.[43-45] Other at-risk populations are athletes involved in high school, college and professional level sports including basketball, soccer, football and rugby.[46,47] An alternative to the point-of-injury strategy would be to recruit patients being evaluated by orthopedic surgeons for specific acute orthopedic injuries with a high

risk of developing PTOA. This might include severe ankle sprains, intraarticular fractures or anterior cruciate ligament or meniscal tears of the knee.

Conclusion

Largely thanks to advances in biomedical research, expected lifespan has roughly doubled over the past 175 years, however expected years with mobility-related disability also continues to increase.[48] In addition to the enormous financial burden imposed by direct costs associated with treating osteoarthritis, the indirect costs of OA are nearly impossible to fully quantify.[49,50] Going forward, an urgent goal for the biomedical community is to improve healthy (disability-free) lifespan. With OA being the leading cause of chronic disability, developing an FDA approved disease-modifying OA therapy is an immediate priority. To realize this ultimate goal, future work will continue to require a multi-disciplinary approach with biologists, engineers, pharmacologists, veterinarians and human clinicians working together to better understand the role of MT in OA, and pursue MT-targeted therapies.

References

1. Blanco FJ, Rego I, Ruiz-Romero C. The role of mitochondria in osteoarthritis. *Nat Rev Rheumatol*. 2011;7(3):161–169. doi:10.1038/nrrheum.2010.213.

2. Terkeltaub R, Johnson K, Murphy A, Ghosh S. Invited review: the mitochondrion in osteoarthritis. *Mitochondrion*. 2002;1(4):301–319. doi:10.1016/S1567-7249(01)00037-X.

3. Szeto HH, Liu S, Soong Y, Alam N, Prusky GT, Seshan SV. Protection of mitochondria prevents high-fat diet-induced glomerulopathy and proximal tubular injury. *Kidney Int*. 2016;90(5):997–1011. doi:10.1016/j.kint.2016.06.013.

4. Loeser RF, Collins JA, Diekman BO. Ageing and the pathogenesis of osteoarthritis. *Nature Publishing Group*. May 2016:1–9. doi:10.1038/nrrheum.2016.65.

5. Szeto HH. First-in-class cardiolipin-protective compound as a therapeutic agent to restore mitochondrial bioenergetics. *Br J Pharmacol*. 2014;171(8):2029–2050. doi:10.1111/bph.2014.171.issue-8.

6. Brouillette MJ, Ramakrishnan PS, Wagner VM, et al. Strain-dependent oxidant release in articular cartilage originates from mitochondria. *Biomech Model Mechanobiol*. 2014;13(3):565–572. doi:10.1007/s10237-013-0518-8.

7. Ingber D. Mechanobiology and diseases of mechanotransduction. *Ann Med*. 2003;35(8):564–577. doi:10.1080/07853890310016333.

8. Sauter E, Buckwalter JA, McKinley TO, Martin JA. Cytoskeletal dissolution blocks oxidant release and cell death in injured cartilage. *J Orthop Res*. 2012;30(4):593–598. doi:10.1002/jor.21552.

9. Bonnevie ED, Delco ML, Jasty N, et al. Chondrocyte death and mitochondrial dysfunction are mediated by cartilage friction and shear strain. *Osteoarthr Cartil*. 2016;24, Supplement 1 IS -:S46EP–.

10. Levin A. Intercellular signaling as a cause of cell death in cyclically impacted cartilage explants. *Osteoarthritis and Cartilage*. 2001;9(8):702–711. doi:10.1053/joca.2001.0467.

11. Kurz B, Lemke AK, Fay J, Pufe T, Grodzinsky AJ, Schünke M. Pathomechanisms of cartilage destruction by mechanical injury. *Annals of Anatomy - Anatomischer Anzeiger*. 2005;187(5-6):473–485. doi:10.1016/j.aanat.2005.07.003.

12. Anderson DD, Chubinskaya S, Guilak F, et al. Post-traumatic osteoarthritis: improved understanding and opportunities for early intervention. *J Orthop Res*. 2011;29(6):802–809. doi:10.1002/jor.21359.

13. Goldring MB. Articular Cartilage Degradation in Osteoarthritis. *HSS Jrnl*. 2012;8(1):7–9. doi:10.1007/s11420-011-9250-z.

14. Goldring MB. Chondrogenesis, chondrocyte differentiation, and articular cartilage metabolism in health and osteoarthritis. *Therapeutic Advances in Musculoskeletal Disease*. 2012;4(4):269–285. doi:10.1177/1759720X12448454.

15. Huser CAM, Davies ME. Calcium signaling leads to mitochondrial depolarization in impact-induced chondrocyte death in equine articular cartilage explants. *Arthritis & Rheumatism*. 2007;56(7):2322–2334. doi:10.1002/art.22717.

16. Dang Y, Cole AA, Homandberg GA. Comparison of the catabolic effects of fibronectin fragments in human knee and ankle cartilages. *Osteoarthr Cartil*. 2003;11(7):538–547.

17. Orazizadeh M, Cartlidge C, Wright MO, et al. Mechanical responses and integrin associated protein expression by human ankle chondrocytes. *Biorheology*. 2006;43(3-4):249–258.

18. Parker E, Vessillier S, Pingguan-Murphy B, Abas W, Bader DL, Chowdhury TT. Low oxygen tension increased fibronectin fragment induced catabolic activities--response prevented with biomechanical signals. *Arthritis Research & Therapy*. 2013;15(5):R163. doi:10.1186/ar4346.

19. Ding L, Heying E, Nicholson N, et al. Mechanical impact induces cartilage degradation via mitogen activated protein kinases. *Osteoarthritis and Cartilage*. 2010;18(11):1509–1517. doi:10.1016/j.joca.2010.08.014.

20. Wang QG, Magnay JL, Nguyen B, et al. Gene expression profiles of dynamically compressed single chondrocytes and chondrons. *Biochemical and Biophysical Research Communications*. 2009;379(3):738–742. doi:10.1016/j.bbrc.2008.12.111.

21. Choi JB, Youn I, Cao L, et al. Zonal changes in the three-dimensional morphology of the chondron under compression: The relationship among cellular, pericellular, and extracellular deformation in articular cartilage. *Journal of Biomechanics*. 2007;40(12):2596–2603. doi:10.1016/j.jbiomech.2007.01.009.

22. Blain EJ. Involvement of the cytoskeletal elements in articular cartilage homeostasis and pathology. *International Journal of Experimental Pathology*. 2009;90(1):1–15. doi:10.1111/j.1365-2613.2008.00625.x.

23. Grodzinsky AJ, Levenston ME, Jin M, Frank EH. Cartilage tissue remodeling in response to mechanical forces. *Annu Rev Biomed Eng*. 2000;2:691–713. doi:10.1146/annurev.bioeng.2.1.691.

24. Szafranski JD, Grodzinsky AJ, Burger E, Gaschen V, Hung H-H, Hunziker EB. Chondrocyte mechanotransduction: effects of compression on deformation of intracellular organelles and relevance to cellular biosynthesis. *Osteoarthr Cartil*. 2004;12(12):937–946. doi:10.1016/j.joca.2004.08.004.

25. Ohashi T, Hagiwara M, Bader DL, Knight MM. Intracellular mechanics and mechanotransduction associated with chondrocyte deformation during pipette aspiration.

Biorheology. 2006;43(3-4):201–214.

26. Anesti V, Scorrano L. The relationship between mitochondrial shape and function and the cytoskeleton. *Biochimica et Biophysica Acta (BBA) - Bioenergetics*. 2006;1757(5-6):692–699. doi:10.1016/j.bbabio.2006.04.013.

27. Whitfield JF. The solitary (primary) cilium–A mechanosensory toggle switch in bone and cartilage cells. *Cellular Signalling*. 2008;20(6):1019–1024. doi:10.1016/j.cellsig.2007.12.001.

28. Farnum CE, Wilsman NJ. Orientation of Primary Cilia of Articular Chondrocytes in Three-Dimensional Space. *Anat Rec*. 2011;294(3):533–549. doi:10.1002/ar.21330.

29. Donnelly E, Williams R, Farnum C. The Primary Cilium of Connective Tissue Cells: Imaging by Multiphoton Microscopy. *Anat Rec*. 2008;291(9):1062–1073. doi:10.1002/ar.20665.

30. Ruhlen R, Marberry K. The chondrocyte primary cilium. *Osteoarthr Cartil*. 2014;22(8):1071–1076. doi:10.1016/j.joca.2014.05.011.

31. Kundu K, Knight SF, Willett N, Lee S, Taylor WR, Murthy N. Hydrocyanines: A Class of Fluorescent Sensors That Can Image Reactive Oxygen Species in Cell Culture, Tissue, and In Vivo. *Angew Chem Int Ed*. 2009;48(2):299–303. doi:10.1002/anie.200804851.

32. Kalyanaraman B, Darley-Usmar V, Davies KJA, et al. Measuring reactive oxygen and nitrogen species with fluorescent probes: challenges and limitations. *Free Radic Biol Med*. 2012;52(1):1–6. doi:10.1016/j.freeradbiomed.2011.09.030.

33. Kamm JL, Nixon AJ, Witte TH. Cytokine and catabolic enzyme expression in synovium, synovial fluid and articular cartilage of naturally osteoarthritic equine carpi. *Equine Veterinary Journal*. 2010;42(8):693–699. doi:10.1111/j.2042-3306.2010.00140.x.

34. Frisbie DD, Al-Sobayil F, Billinghurst RC, Kawcak CE, McIlwraith CW. Changes in synovial fluid and serum biomarkers with exercise and early osteoarthritis in horses. *Osteoarthritis and Cartilage*. 2008;16(10):1196–1204. doi:10.1016/j.joca.2008.03.008.

35. Koff MF, Shah P, Pownder S, et al. Correlation of meniscal T2* with multiphoton microscopy, and change of articular cartilage T2 in an ovine model of meniscal repair. *Osteoarthritis and Cartilage*. 2013;21(8):1083–1091. doi:10.1016/j.joca.2013.04.020.

36. Potter HG, Koff MF. MR Imaging Tools to Assess Cartilage and Joint Structures. *HSS Jrnl*. 2012;8(1):29–32. doi:10.1007/s11420-011-9241-0.

37. Wilke VL, Robinson DA, Evans RB, Rothschild MF, Conzemius MG. Estimate of the annual economic impact of treatment of cranial cruciate ligament injury in dogs in the United States. *J Am Vet Med Assoc*. 2005;227(10):1604–1607.

38. Hurley CR, Hammer DL, Shott S. Progression of radiographic evidence of osteoarthritis following tibial plateau leveling osteotomy in dogs with cranial cruciate ligament rupture: 295 cases (2001-2005). *J Am Vet Med Assoc*. 2007;230(11):1674–1679. doi:10.2460/javma.230.11.1674.

39. DeLuke AM, Allen DA, Wilson ER, et al. Comparison of radiographic osteoarthritis scores in dogs less than 24 months or greater than 24 months following tibial plateau leveling osteotomy. *Can Vet J*. 2012;53(10):1095–1099.

40. ls SHM, inen HKH, rkman AKH-B, Laitinen-Vapaavuori OM. Long-term functional outcome after surgical repair of cranial cruciate ligament disease in dogs. November 2014:1–11. doi:10.1186/s12917-014-0266-8.

41. Belmont PJJ, Goodman GP, Waterman B, DeZee K, Burks R, Owens BD. Disease and nonbattle injuries sustained by a U.S. Army Brigade Combat Team during Operation Iraqi Freedom. *Mil Med*. 2010;175(7):469–476.

42. Waterman BR, Belmont PJ, Cameron KL, DeBerardino TM, Owens BD. Epidemiology of Ankle Sprain at the United States Military Academy. *The American Journal of Sports Medicine*. 2010;38(4):797–803. doi:10.1177/0363546509350757.

43. Knapik JJ, Spiess A, Swedler DI, Grier TL, Darakjy SS, Jones BH. Systematic Review of the ParachuteAnkle Brace. *AMEPRE*. 2010;38(S):S182–S188. doi:10.1016/j.amepre.2009.10.012.

44. Wallace RF, Wahi MM, Hill OT, Kay AB. Rates of ankle and foot injuries in active-duty U.S. Army soldiers, 2000-2006. *Mil Med*. 2011;176(3):283–290.

45. Cameron KL, Owens BD, DeBerardino TM. Incidence of ankle sprains among active-duty members of the United States Armed Services from 1998 through 2006. *J Athl Train*. 2010;45(1):29–38. doi:10.4085/1062-6050-45.1.29.

46. Nelson AJ, Collins CL, Yard EE, Fields SK, Comstock RD. Ankle injuries among United States high school sports athletes, 2005-2006. *J Athl Train*. 2007;42(3):381–387.

47. McKay GD, Goldie PA, Payne WR, Oakes BW. Ankle injuries in basketball: injury rate and risk factors. *Br J Sports Med*. 2001;35(2):103–108.

48. Christensen K, Doblhammer G, Rau R, Vaupel JW. Ageing populations: the challenges ahead. *The Lancet*. 2009;374(9696):1196–1208. doi:10.1016/S0140-6736(09)61460-4.

49. Ma VY, Chan L, Carruthers KJ. Incidence, Prevalence, Costs, and Impact on Disability of Common Conditions Requiring Rehabilitation in the United States: Stroke, Spinal Cord Injury, Traumatic Brain Injury, Multiple Sclerosis, Osteoarthritis, Rheumatoid Arthritis, Limb Loss, and Back Pain. *Archives of Physical Medicine and Rehabilitation*. 2014;95(5):986–995.e1. doi:10.1016/j.apmr.2013.10.032.

50. Yelin E, Murphy L, Cisternas MG, Foreman AJ, Pasta DJ, Helmick CG. Medical care expenditures and earnings losses among persons with arthritis and other rheumatic conditions in 2003, and comparisons with 1997. *Arthritis & Rheumatism*. 2007;56(5):1397–1407. doi:10.1002/art.22565.